REPORT NO.
UCB/EERC-83/20
MAY 1988
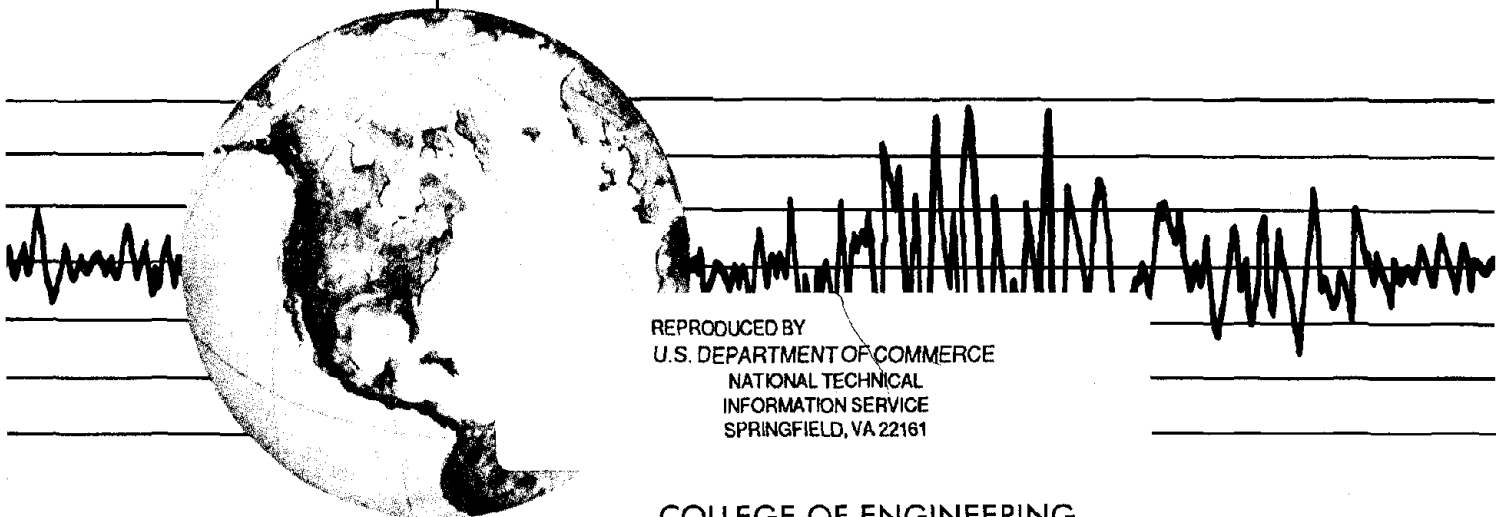
EARTHQUAKE ENGINEERING RESEARCH CENTER

CORRELATION OF ANALYTICAL AND EXPERIMENTAL RESPONSES OF LARGE-PANEL PRECAST BUILDING SYSTEMS

by

M. G. OLIVA
R. W. CLOUGH
M. VELKOV
P. GAVRILOVIC

Report to the National Science Foundation

COLLEGE OF ENGINEERING

UNIVERSITY OF CALIFORNIA AT BERKELEY

CORRELATION OF ANALYTICAL AND EXPERIMENTAL RESPONSES

OF LARGE-PANEL PRECAST BUILDING SYSTEMS

by

M. G. Oliva

R. W. Clough

M. Velkov

P. Gavrilović

ABSTRACT

This report presents an analytical and experimental correlation of large-panel precast building system performance on the basis of experimental studies of three-storey models by means of shaking table and pseudostatic tests. The experimental shaking table tests were performed at the Earthquake Simulation Laboratory of the University of California at Berkeley, while the pseudostatic ones were carried out at the Institute of Earthquake Engineering and Engineering Seismology, Skopje, Yugoslavia.

The study of the correlation between the two types of experimental studies as well as with analytical investigations is part of a joint US - Yugoslav project on the seismic response of high-rise residential buildings, involving cooperative research between the Earthquake Engineering Research Center of the University of California at Berkeley and the Institute of Earthquake Engineering and Engineering Seismology of the University "Kiril and Metodij", Skopje, Yugoslavia.

The investigations of the response of large-panel building structures have been carried out with models of a large-panel system produced by the RAD Construction Company, Belgrade.

ACKNOWLEDGEMENTS

TABLE OF CONTENTS

LIST OF TABLES

LIST OF FIGURES

1. INTRODUCTION

1.1. Background of the Research

The long range research project "Experimental and Theoretical Investigations of the Seismic Stability of the Precast Large Panel System RAD - Yugoslavia" has been carried out to substantiate the seismic stability of prefabricated systems, in response to the need for extensive application of the large panel system RAD - Yugoslavia for multistorey structures in regions having seismic events of different intensities. The project has been carried out by the following participating organizations: (1) RAD Construction Company of Belgrade; (2) Institute of Earthquake Engineering and Engineering Seismology (IZIIS) of the University "Kiril and Metodij", Skopje; (3) Civil Engineering Faculty of the Institute of Materials and Structures in Belgrade, and (4) Earthquake Engineering Research Center (EERC) of the University of California at Berkeley.

To achieve the goals of the research program, the project has involved analysis of existing large panel structural buildings and their joint systems, not only from the viewpoint of their bearing and deformability capacity but also from that of their production and assemblage technology. The system has been improved by introducing a closed type of joint. Modifications to the joint system as well as other necessary structural modifications have been made on the basis of a complete analysis of the structure and the joint system. These structural elements and joints have been utilized in a number of projects of different types and composition in order to show their multi-purpose character and their application in a variety of conditions requiring solution of modern urban design and architectural problems.

The research project described in this report is one phase of a continuing

cooperative research program in earthquake engineering between the Institute of Earthquake Engineering and Engineering Seismology (IZIIS) of the University "Kiril and Metodij", Skopje, Yugoslavia and the Earthquake Engineering Research Center (EERC) of the University of California at Berkeley, California, U.S.A. In 1975, previous activities were extended with the principal thrust of the cooperative research directed towards "Seismic Stability of High-Rise Residential Buildings Constructed as Precast Monolithic Reinforced Concrete Systems".

This investigation is an integrated research project using the structural test facilities and computers of both EERC and IZIIS. The test specimens were contributed by and produced by the RAD Construction Company of Belgrade, Yugoslavia. The RAD Company supplied one-third scale model concrete panels, typical of their high-rise building system, to both EERC and IZIIS and similar full-scale panels to IZIIS. The reduced scale panels were assembled into three different types of three-storey assemblages, representing portions of high-rise buildings. The resulting specimens were tested on the shaking table at EERC, and at IZIIS by a pseudo-static test method; both tests are described in detail in separate reports, see References 1 and 2. In this final joint report, a summary of the investigation is given with special emphasis on the correlation between the shaking table test results and those obtained during the pseudostatic tests. Also, conclusions are drawn from the experimental and analytical studies on the stability of the system as a whole.

1.2. Objectives

The disastrous effects of the Second World War caused tremendous economic difficulties in almost all European countries. Reconstruction of structures of vital importance was performed immediately after the war in order to

reestablish their economies, while the construction of residential buildings began later on. Under such conditions, the classical methods of construction were unable to satisfy the increased demand. The need for expanded construction capacity led to the application of prefabricated elements (columns, beams) in the construction of residential buildings; subsequently, large-panel systems appeared having a thoroughly prefabricated structural system which is assembled at the construction site, the elements being produced industrially.

The large panels are surface concrete elements, which are applied as either horizontal or vertical, bearing or non-bearing components. The structural system is made up of vertical panel walls interconnected at the storey height by horizontal panels or prefabricated floor systems (planks). In these structural systems, all loads are transferred to the ground through the walls and the foundation structure.

The mass construction of large-panel structures is not only taking place in the European countries: during the last few years, many countries outside Europe have increased the application of large-panel systems, mainly in large series. Large panel systems with high level assemblage procedures enable efficient, fast and economic construction of residential buildings.

The design of these systems for seismic regions is based on theoretical (analytical) and experimental investigations which put special emphasis on the construction and performance of the joints between the panel elements. Prefabricated large-panel systems in seismic regions are most frequently designed to have cast-in-place monolithic joints; the resulting system is assumed to behave as a monolithic one, without taking into account the occurrence and development of cracks, i.e., the nonlinear behaviour of joints and some panels under seismic effects.

From the structural viewpoint, large panel systems can be classified into three main groups: cross wall systems, longitudinal wall systems and two-way systems.

For systems with shear bearing cross walls, the panels in the longitudinal direction are not load bearing and are usually constructed of light material. For systems having longitudinal bearing walls, the panels in the transverse direction are not load bearing and are constructed of a light material.

Two-way systems having bearing walls in both directions provide for easier and more economic foundation designs, even in cases of relatively unfavourable soil conditions. These systems are widely applied throughout Europe and are considered to be a very appropriate structural solution for construction in seismically-prone regions.

Large-panel systems have been used exclusively in the construction of a large number of similar buildings according to typical designs; this standard design approach increases the seismic hazard and risk problem. The design of buildings of this type has been carried out in full accordance with regulations which have been especially established for the construction and analysis of large-panel structures, with the regulations being used mainly as minimum requirements but not as an exclusive basis for the design of the structure.

1.3. Observed Behaviour of Large Panel Structures during Earthquakes

The experience gathered from the failure of several prefabricated buildings caused by the Agadir earthquake of 1960 provided little data concerning the behaviour of precast structures during earthquakes. However, a general conclusion was drawn that precast structures suffer heavier damage than monolithic ones.

It could be said that up to the Romania earthquake of March 4, 1977 there were almost no data about the behaviour of precast structures during strong

earthquakes. During this event, it was possible for the first time to examine the behaviour of the entire range of precast systems, especially the large panel systems which have been used for mass construction in Romania during the last twenty years. The large-panel systems constructed throughout the country, amounting to 120,000 - 150,000 apartments, provide a good possibility for analysis of the behaviour of such systems and of the influence of such parameters as earthquake intensity, frequency content, soil conditions, height of the building, types of members, connections and so forth.

The epicenter of the March 4, 1977 Romania earthquake was on the slope of the Carpathian chain, at a depth of about 100 km; it had a Richter magnitude of 7.2.

Earthquake failure and damage were experienced over an area of 80,000 km^2 which is one-third of the whole of Romania. Furthermore, some destruction was evident in Bulgaria along the Danube River, and the earthquake was also felt, with varying intensity, in Yugoslavia.

The observed behaviour of the precast structural systems was better than any expectations, in spite of the different quality of construction of different types of structures.

Following usual European practice, Romania has adopted the two-way large-panel system; usually all panel walls, both internal and in the facade, are bearing walls. Both the horizontal and vertical connections of the panels are usually wet joints having concrete placed in situ and welded anchor reinforcement; this is a characteristic of European systems.

Structural systems have mainly been designed and analyzed according to the existing seismic regulations, applying static methods for definition of the static loads; the stresses are defined for ultimate stress state.

The principal structural characteristics of the systems used in Romania are as follows:

- Two-way systems of eight storeys with nonbearing facade panels. These structures have no basement and the prefabricated system is placed on monolithic foundations. They were constructed in series in Bucharest, using monolithic horizontal and vertical joints, welded reinforcement of vertical panels and monolithic slabs above the last precast components.

- Two-way systems of ten storeys with a precast basement structure supported on monolithic foundations.

- In Ploesti which is closer to the epicentral region, construction of large-panel structures is limited to 5 storeys. They always have monolithic basements with monolithic floor slabs above. The walls are arranged in a two-way system with a section of the monolithic column enlarged in order to increase its shear strength.

In the Romanian towns all the large panel structures behaved very well and did not suffer any significant structural damage. The overall performance of members within the structural system was described as follows:

- No damage of the foundation structure has been observed.

- Horizontal panels performed as horizontal rigid diaphragms, without damage.

- In vertical panels there were no observed cracks in most cases; an exception is one building where several longitudinal internal panel walls (without openings) developed fine vertical cracks.

- Also, in some structures on the first and second floor, cracks which might have been due to shrinkage, developed in vertical joints at the contacts between the concrete placed in situ and the panels, especially in flanged joints. The width of these cracks generally was from 0.1 - 0.3 mm. The

cracks were mainly concentrated on the first floor and less on the second floor, and as a rule in the intermediate infilled panel walls.

- The horizontal joints occasionally developed cracks close to the place where vertical cracks appeared and extended 1 - 2.0 mm in the floor panel from the contact edges towards the middle of the room.

- It should be mentioned here that such cracks in vertical joints close to horizontal cracks are observed on a much smaller number of structures, regardless of the system and the location (Bucharest, Ploesti and Kraiova).

- Sometimes, very fine cracks appear in the connection with a prefabricated staircase.

The precast large-panel system performed very well during the March, 1977 earthquake, compared with other systems such as cast-in-place structures. This superior performance can be explained by the following:

- High design base shear coefficient according to the predominant natural dynamic characteristics of structures, soil conditions and the intensity of the earthquake motion and its frequency content.

- The large number and favourable distribution of the panels and the length of joints required for architectural reasons in the two-way systems.

- The whole building worked as a box system with capacity for energy dissipation in the ground at the foundation level.

- Increased damping of the whole system due to the energy dissipation in the fine cracks on the contact areas in vertical and horizontal joints in the zones of shrinkage cracks.

- The quality of concrete was much better than in the case of monolithic structures even if there were some faults in the cast-in-place joints and welding of reinforcement.

However, these conclusions should not be generalized since the real behaviour of structures during earthquakes depends in each case upon the earth quake intensity and frequency content, the soil conditions and the structural parameters.

1.4. General Principles of Configuration of Structural Elements

European design engineers consider large-panel structures to be monolithic reinforced concrete systems having bearing walls capable of sustaining vertical and horizontal loads. On the other hand, achieving good performance of the large-panel system depends upon the production technology, prefabrication and the architectural design.

The seismic stability and safety of the structure depends upon the following concepts:

- Aseismic structural elements should be provided in both orthogonal directions of the structure in order to assure sufficient stability of the system under seismic effects. The two-way system mobilizing all walls to resist seismic effects has been accepted in all European seismic regions and especially in the countries of East Europe. Introducing vertical structural panels in both directions is particularly effective in the construction of smaller flats. However, it would be desirable that in the future the concept of considering only part of the walls to behave as structural elements during an earthquake be adopted. In this way, the external facade walls as well as part of the internal walls could be made to behave as non-bearing walls. This would decrease the total length of structural joints and provide the possibility of using light materials for the non-structural elements. Such a system would be a much simpler configuration and would provide a more clearly defined response to

earthquake motion.

- Generally speaking, walls may have different cross-sections, rectangular or with flanges; even the possibility of applying strengthened flanges, the so-called "barbell" cross-section should be considered, although panels with such cross-sections have not so far been used in practice. As to the reinforcement, it may be longitudinal, transverse or it may have additional tensile "confinement" reinforcement. Such combinations improve the whole system, contributing to more favourable behaviour during an earthquake.

- It is desirable to define in advance zones of allowable nonlinear deformations, especially those due to slipping along the vertical and horizontal joints. Nonlinear deformations in structural panels should take place by yielding of reinforcement as a result of the overturning moment. In some cases, it may be necessary to consider the possibility of designing a building by casting in place certain parts in which nonlinear deformations are expected.

1.5. The RAD Large-Panel System: Characteristics of the Structure

The RAD large-panel prefabricated system consists of walls in both longitudinal and transverse directions, and a horizontal rigid floor structure, which constitute a rigid space structure with the required strength and deformability [3,4].

The construction of a large number of buildings using the same members, in seismic zones having different expected intensities, imposed the need for intense experimental and analytical studies of structural connections, members and portions of structures, as well as for full-scale testing in order to determine requirements for uniform application of the system in all the seismic

zones and for buildings of different story heights. The results of these intense studies and of the industrialized production of typical members now make the uniform application of the system possible in zones of any seismicity for construction of buildings of different heights, with unlimited possibilities for different configurations; this proves the system to be adaptable and to satisfy all the requirements of modern construction.

1.5.1. Structural System

From the structural aspect, the system consists of vertical bearing panel walls, horizontal panel floor structures and a connection system, which, linked together, constitute the load carrying structural system capable of withstanding gravity and additional loads.

Concrete is the basic material for production of the members. Its crushing strength depends on the selected structural system and the corresponding calculation, while steel reinforcement is of the usual variety.

The members produced in the factory and assembled at the building are connected to form a structurally-functional unit by in-situ casting of the horizontal and vertical reinforced concrete connections, while steel ties linked by specially elaborated connections provide full continuity of the assemblages.

The main structural members and their distribution and interconnection are shown on the characteristic plan of the building presented in Fig. 1.1. The building structure is completed by full assembly, in stages by floors, as illustrated in Fig. 1.2.

1.5.2. Vertical and Horizontal Panels

The bearing walls of the structural system consist of independent members

which are vertical reinforced concrete panels. The dimensions of the panels are determined by the designs and the technical and technological conditions in production and assembly. In practice the members which have been used are up to 6.60 m in length and 3.0 m in height, with a minimum thickness d = 16 cm. The vertical edges of the panels are indented and designed to form closed vertical connections of the system. The upper and lower horizontal edges can also be indented, if necessary; this is determined by the design and depends on the results of the structural analysis.

The panels are reinforced with welded web reinforcement (one-side or two -side) which is designed according to the geometry of the panel, its role in the structure, openings in the panels, production and technological requirements, transportation and other conditions (Fig. 1.3).

In addition to the reinforcement of the panel itself, the greater part of the section of the vertical reinforcement passes through the panel, while a smaller part of it is placed in the vertical connection between two adjacent connection walls. The continuous panel vertical reinforcement is extended and joined to the panel below by special connections.

The panels with openings (Fig. 1.4) are reinforced similarly to the panels without openings, but with additional reinforcement above and around the opening. By considering the force distributions in the walls with openings and the possibility of developing plastic hinges in the lintel parts of the panels because of strong earthquake effects, these walls can improve the ductility characteristics of the structure if they are properly designed.

The facade walls may be constructed as multi-layer panels with an archi- tectural facing and an interior reinforced concrete layer which acts as a bearing part of the panel, if they are intended for use as bearing walls. In

this case, the thickness of the interior portion should be determined by calculation; the minimum thickness is 8.0 cm.

The reinforcement of the facade bearing panels is carried out in the same way as in the remaining bearing panels. If these panels are not load carrying the reinforcement depends, exclusively, on the production needs as well as the transportation and assembling requirements.

The horizontal panels in the RAD structural system are interconnected with special connections, thus forming the floor structures. The horizontal panels form rigid horizontal diaphragms connecting all the vertical panels. The horizontal panels as well as the connections between them are constructed so that they transmit the seismic effects to vertical walls without nonlinear deformations, and do not require additional protection for transportation and assembling, but enable assembling without application of supporting scaffold and additional equipment.

The shape of these slabs can vary depending on the position of the members within the building structure. The edges of the members are designed to have profiles which enable easy assembling and casting of the connections between these panels themselves, as well as between the horizontal and vertical panels. The cross section of the ceiling is constructed so that it is possible to install necessary electrical systems in them.

The dimensions of the floor structure members are variable and their thickness depends on the span. The most frequently applied span for residential buildings is up to 6.00 m with a thickness of 16.5 cm.

1.5.3. Connections of Structural Systems

The connections between the prefabricated panels constituting the structural system are provided by in-situ cast reinforced concrete joints and

by special steel reinforcement details.

The main purpose of the connections is to make the prefabricated members act as a monolithic structural system. The typical joints are closed and self-formed, which means that they form their shape from the prefabricated members themselves, without application of additional forms. The connections are reinforced and poured with concrete at the building site, and according to their position, function and structure, they can be horizontal or vertical.

The horizontal connection between the vertical wall panels and the horizontal floor panels is shown in Fig. 1.5. The connection consists of floor structures supported by the lower wall panels and free standing vertical panels whose contact is provided by additionally cast, monolithic horizontal connections. Horizontal floor structure panels are connected through extended stirrups placed alternately in both directions, longitudinal belt course reinforcement and additional closed stirrups in the connection.

The continuity of the joint at the ends of the panels is provided by connecting the reinforcement of the upper and lower floor panels. The vertical load carrying reinforcement in the wall panels is interconnected as bolt connections, as shown in Fig. 1.6. The horizontal connection between the floor panels is shown in Fig. 1.7.

From the structural aspect, the connections should make the prefabricated floor structure panels act monolithically. The contact surfaces of the horizontal panels are indented. Reinforcement is extended from the sides of the prefabricated panels in the form of closed stirrups, so by placing longitudinal reinforcement and casting the concrete, the panels form a rigid diaphragm.

The horizontal connections are constructed to provide the elastic resistance mechanism for gravity, dead and moderate seismic loads, while in the

case of extremely high seismic effects it provides seismic isolation because of favourable nonlinear behaviour.

Connection of adjacent vertical wall panels is carried out by vertical connections. The shape of the vertical connections depends on the position of the vertical walls. There are two characteristic types of vertical connection: connection of longitudinal and transverse walls (Fig. 1.8) and connection of walls in the same direction (Fig. 1.9).

Figure 1.8 shows the connection of vertical panels in longitudinal and transverse directions along the height of the panel. It is constructed as a closed connection, so that the surfaces of the prefabricated panels close the space for the cast-in-situ concrete, thus forming a monolithic section. The connection is reinforced by horizontal stirrups extended alternately from the vertical panels along the height where the contact area of the panels is indented. The vertical reinforcement in the connection includes two bars of 12 mm diameter and is constant along the whole height of the building.

The indented contact areas as well as the extended stirrups provide the special characteristics of the connection which differs considerably from flat nonreinforced connections. These connections should provide continuity between the longitudinal and transverse panels of the structure along the height of the storey.

Concrete used in cast-in-situ connections is designed to have suitable strength and consistency for injection [5].

1.6. Experimental and Analytical Investigations

The stability of the RAD large-panel prefabricated system against normal live loads is identical with the stability of cast-in-place panel systems [4]. However, the behaviour of the large-panel prefabricated structural systems

during violent earthquakes and other severe dynamic effects differs from the behaviour of monolithic structures and depends on the design of the structural system and the system of connections.

For the determination of the seismic stability of the buildings constructed in the RAD structural system, intensive experimental and analytical studies were carried out in order to define the stability criteria. The results of the experimental studies of the system for shear cyclic loads, the pseudodynamic load tests of the three-storey models, as well as the shaking table tests on the three-storey models applying actual seismic motions, and also the analytical studies of the structural response to actual seismic loads prove that buildings constructed in the RAD large-panel prefabricated system can be made suitable for regions of severe seismic intensity.

In this study the following experimental investigations were carried out:

- representative joints of the system were subjected to cyclic loading with variable axial stresses,

- representative walls in three-storey models were subjected to pseudodynamic cyclic loading,

- representative walls in three-storey models were tested on a shaking table simulating the effects of an actual earthquake,

- small amplitude dynamic testing was carried out on full-scale structures, in which strong earthquake motion recording instruments (SMA-1) were installed.

Analytical investigations followed the long-term program of experimental testing: special attention was paid to the response of structures to actual dynamic earthquake effects including the nonlinear behaviour of the horizontal wall joints.

A prototype multi-storey building was designed and constructed and represents the prototype "test model", shown in plan view in Fig. 1.1. The experimental program covered all members and joints of this system.

The panels of all wall and connection models were constructed in the Apartment Construction Factory in Belgrade under the same conditions as the prototype structure, while assembling and filling of connections was carried out under laboratory conditions. The Dynamic Testing Laboratory of IZIIS was the site of all static and pseudostatic tests. Testing of three-storey models on a shaking table was carried out at EERC. The panels used in the connection tests were full scale while those used in the three-storey models were one-third scale.

The procedure and results of testing have been given in detail in References 1 and 2. Brief summaries of the information contained in these references are presented in Chapters 2 and 3 of this report, respectively.
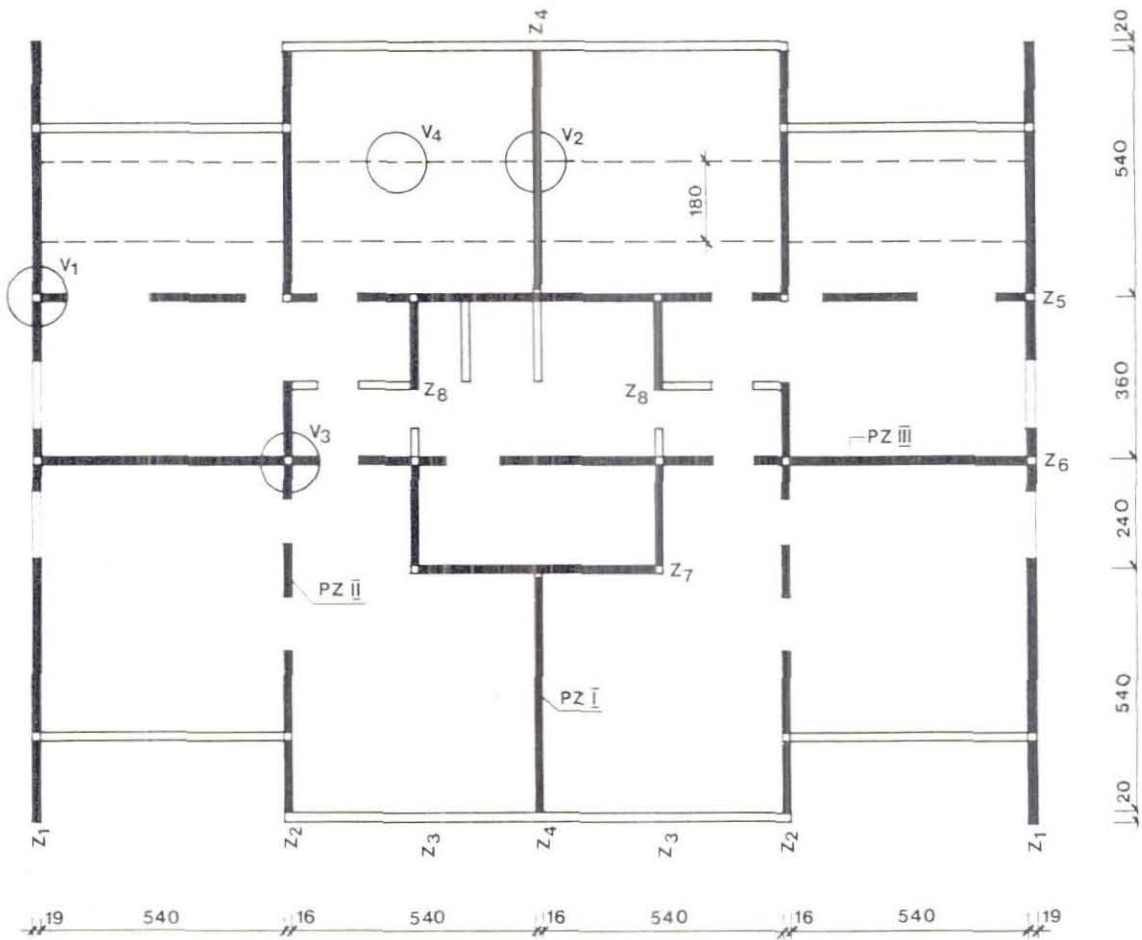
Fig. 1.1. Plan of the Building "Testing Model" with Tested Members
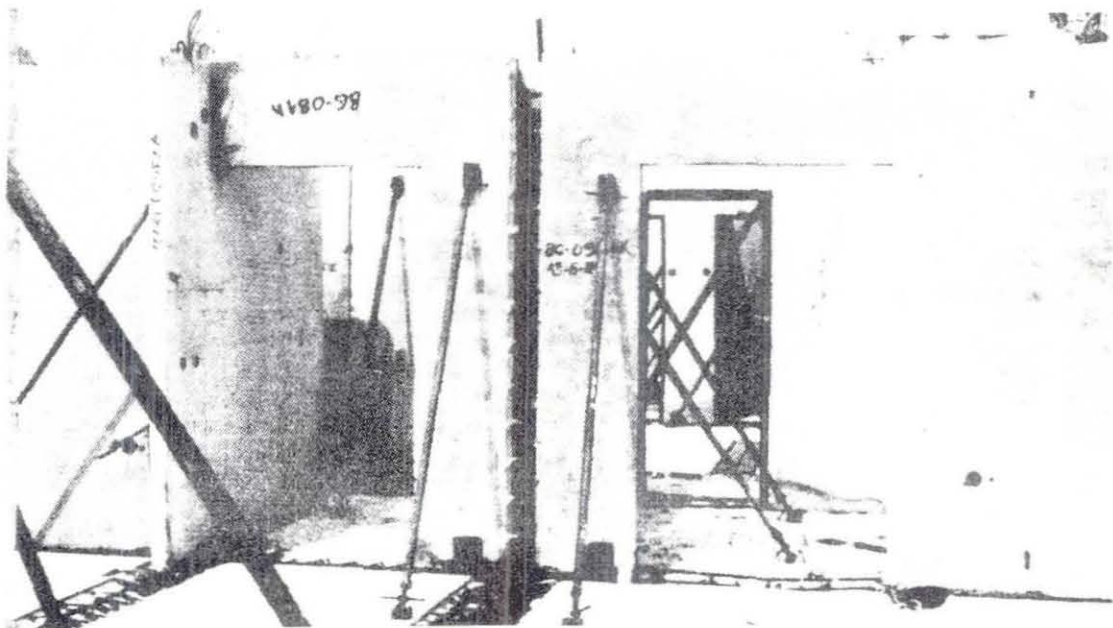
Fig. 1.2. Assembling of Structure
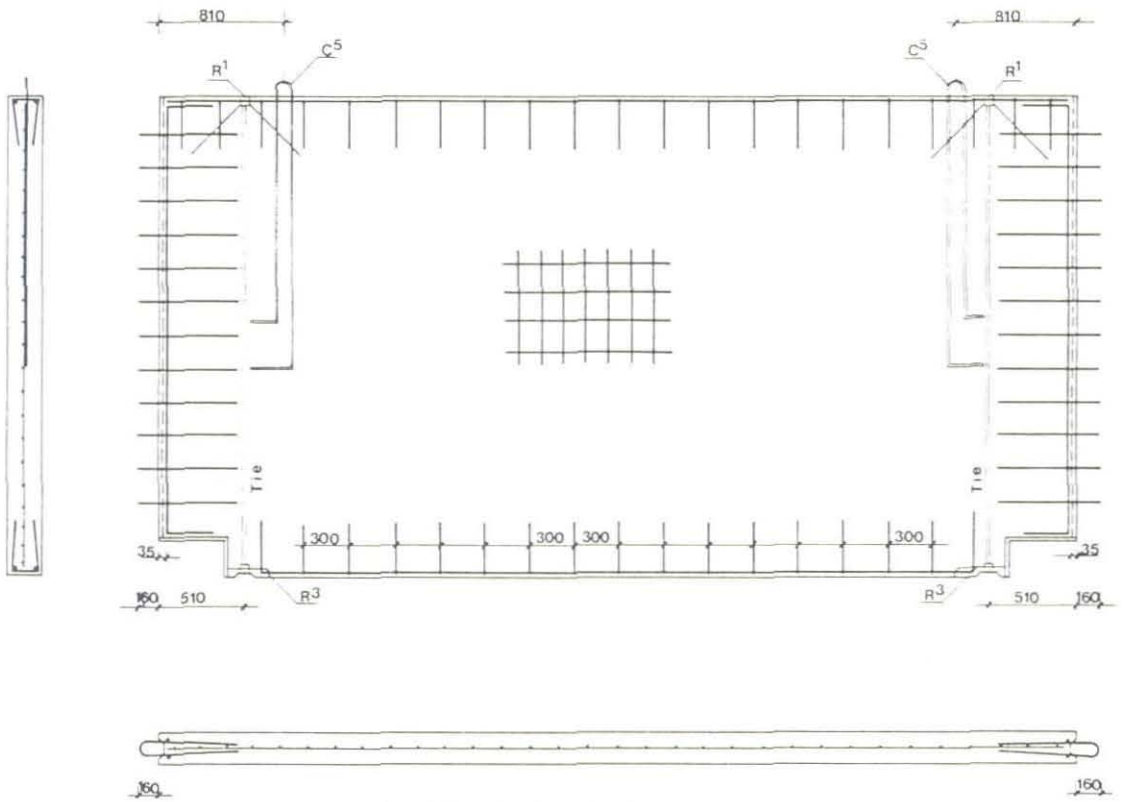
Fig. 1.3.   Detail of Bearing Vertical Panel
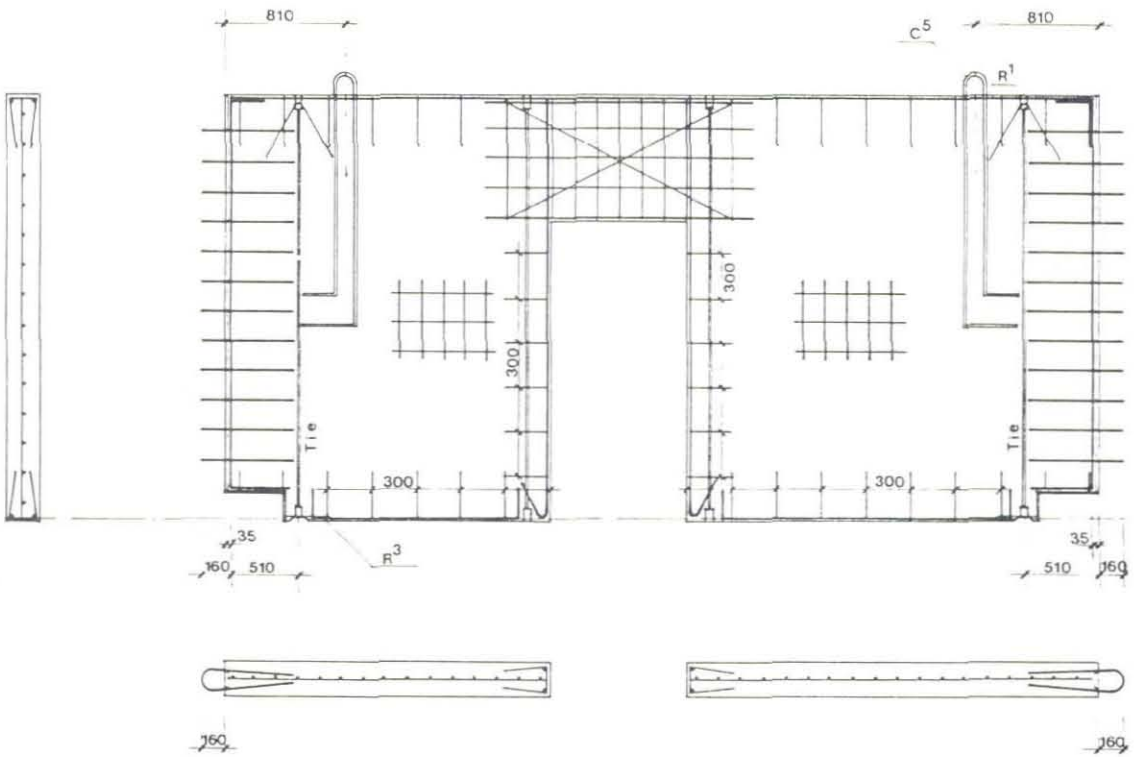
Fig. 1.4.   Detail of Bearing Vertical Panel   with Opening
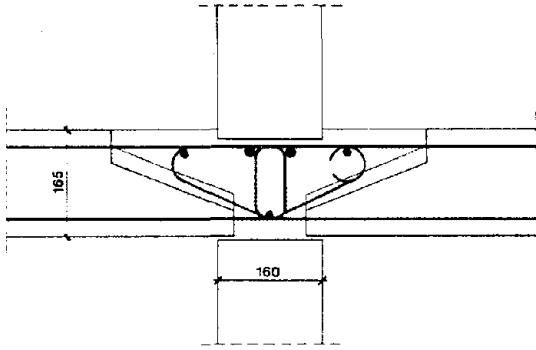
Fig. 1.5.   Horizontal Connection of Vertical Panels
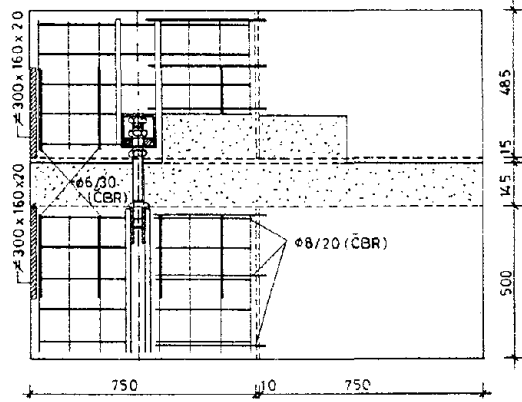
Fig. 1.6.   Bolt Connection
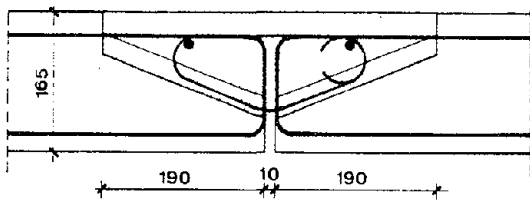
Fig. 1.7.   Horizontal Connection of Floor Structure Panels
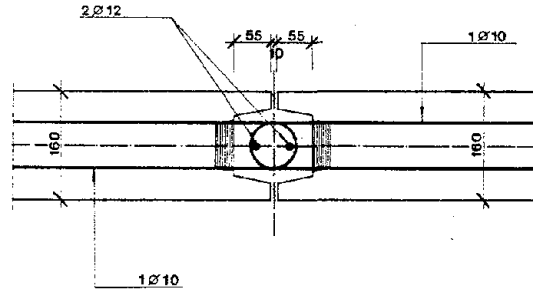
Fig. 1.9.   Vertical Connection of Bearing Walls in the Same Direction
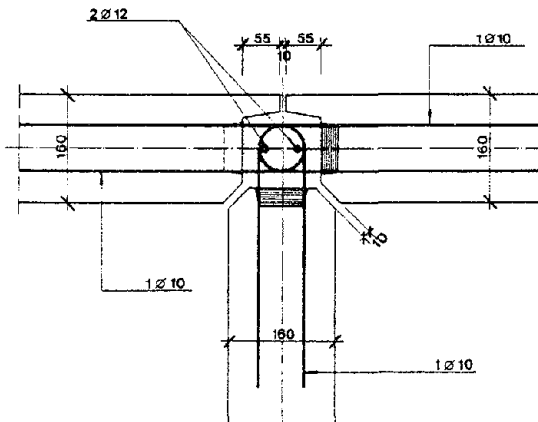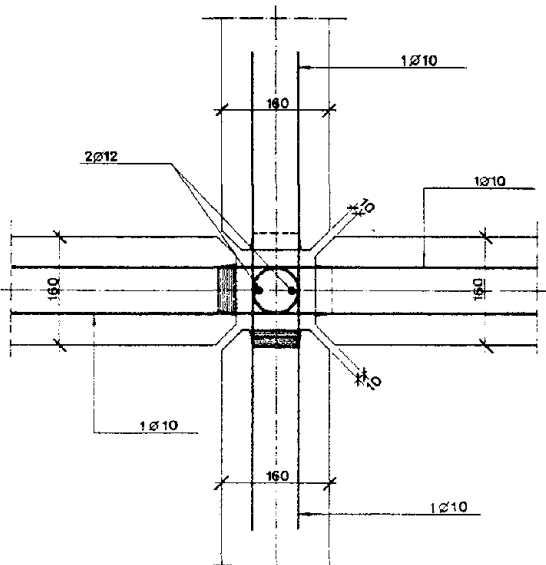
Fig. 1.8.   Vertical Connection of Vertical Bearing Panels of Longitudinal and Transverse Panels

2.   PSEUDOSTATIC EXPERIMENTAL STUDIES

2.1. Introduction

Experimental studies using pseudostatic (slow-cycling) methods were carried out on representative connections of the system for shear force-displacement relationships with variable axial stresses, and on representative bearing walls in three-storey models.

The testing of the connections in the system was intended for evaluation of shear resistance and deformability, while testing of structural parts (walls) was aimed at investigation of the simultaneous action of moments, axial and shear forces.

The design and construction of the models were based on a detailed static and dynamic analysis of the prototype "testing model building" (Fig. 1.1) including linear and nonlinear response to actual earthquake effects. For the purpose of experimental testing of structural subassemblages, three representative walls were selected: (i) rectangular panel walls, (ii) panel walls with openings and (iii) "flanged" panel walls (taking into account the influence of connected perpendicular walls). All wall models were designed in the scale of 1:3. Three identical models were constructed for each wall. The first two were used for pseudostatic testing while the third model was tested on the shaking table.

The pseudostatic experiments described in this chapter were performed in the dynamic testing laboratories of IZIIS.

2.2. Experimental Investigation of Connections

On the basis of analyses of representative structures, four joints were selected defining the structural characteristics of the system, the load carrying capacity and deformation characteristics for serviceability and

ultimate loads. Vertical joints of bearing panels, horizontal joints of vertical panels, and horizontal joints of the floor panels were tested. All joint models were constructed and tested with equipment which provides for displacement control and automated data acquisition.

For each of these four types of connections, two full-scale models and one one-third scale model were considered. A brief summary of the test results is presented below.

2.2.1. Horizontal Connection

Horizontal wall joints provide connections between vertical wall panels and floor panel slabs. The bottom edge of the contact area with the connection is plane and has no cantilevered stirrups, so that the contact between the panel and the joint is provided by cast-in-place concrete, as shown in Fig. 1.5.

The experimental tests of horizontal wall connections under cyclic shear force loads were carried out on different models having different intensities of axial stress.

The horizontal wall connection results for the full-scale model loaded by a gravity load q = 0.85MPa are shown in Fig. 2.1.

First the model was loaded by a force simulating the gravity load of q = 0.85MPa which remained constant throughout the testing. Then, the model was loaded by a cyclic horizontal shear force of 160kN which was calculated to induce the occurrence of the first crack. The displacement Δ caused by this loading was enlarged to 2Δ, 3Δ, ... $n\Delta$ until a relative displacement of 8.5 mm was achieved at which there was no further decrease in the shear resistance of the joint. Three cycles were performed at each displacement amplitude. The force-displacement results obtained for one of the models of this type are

shown in Fig. 2.1. Similar results were obtained with the one-third scale model.

On the basis of the results of the experimental studies the following conclusions may be drawn: (i) the behaviour of the models under cyclic loading at the same displacement amplitude shows considerable decrease of the resistance to moment loading; (ii) maximum shear resistance is achieved in the range of relatively small displacements (from 1.4 to 2.8 mm) and is followed by cracking between the monolithic and the prefabricated concrete giving rise to a range in which shear resistance is constant and proportional to axial forces representing the dry friction mechanism, not only from the aspect of bearing capacity but also from the viewpoint of deformability, as can be seen from the hysteresis loop presented in Fig. 2.1.

2.2.2. Vertical Connection

Vertical joints connect longitudinal and transverse wall panels. The panels at the contact surface with the connection are indented and have stirrups connected by longitudinal bars.

Figure 2.2. shows the hysteresis relationship from experimental testing of vertical connections in vertical panels due to shear forces, for full-scale models; and Fig. 2.3 shows the hysteretic behaviour of the same connection for the one-third scale model.

The main characteristic of the behaviour of vertical joints is the high shear capacity in the first stage up to the initial occurrence of large inelastic deformations, which is very close to the shear capacity of cast-in-place reinforced concrete elements and connections. In the next cycle of loading there is an abrupt decrease of stiffness and strength which is in inverse proportion to the size of the inelastic deformations. Examining any

cycle of loading in Fig. 2.2, it is quite obvious that the narrow hysteresis loop is due to the low shear resistance of concrete as a material and the fact that there is no normal force in the connection. The indented contact area between the loaded panel and the connection contributes to the development of high shear resistance in the range of small deformations. The increase of deformations results in breaking of the indentation teeth, then the remaining capacity of the concrete is quite small because there is no axial force to induce friction. From a comparison of Figs. 2.2 and 2.3 it can be concluded that there is a good agreement between the full-scale and one-third scale models with differences in shear stresses of less than 20 - 25%.

2.3. Experimental Studies of Three-Story Models of Panel Walls

The main objective of the research was to determine the hysteretic behaviour of panel walls as a basis for studying the stiffness, strength, ductility capacity, modes of failure, energy dissipation and contribution of different mechanisms to the overall deformation.

2.3.1. Program, Test Models, Equipment and Test Procedure

The experimental study of the behaviour of structural walls included three representative arrangements of wall panels: rectangular panel wall, panel wall with opening and flanged panel wall.

A model of a panel wall with rectangular cross-section (PZ-I) is presented in Fig. 2.7 with details of joints and reinforcement. Presented in Fig. 2.15 is a model of a panel wall with opening (PZ-II) and details of its joints and reinforcement. Figure 2.20 shows a model of a flanged panel wall (PZ-III), i.e., connected perpendicular walls. All models were designed and produced in the scale of 1:3.

The panel elements were manufactured in a factory and transported to the laboratory at IZIIS where they were assembled using joints of monolith concrete.

As has already been stated, identical elements of panel walls were shipped to the laboratory of EERC where the models were assembled and prepared for testing on the shaking table.

This chapter presents the results of the pseudostatic testing of the panel walls.

The testing of the models was performed using pseudostatic test equipment including three hydraulic actuators having a total capacity of 200 tons. All the elements were supported in a horizontal position, with the equipment arranged as shown in Figs. 2.4 - 2.6. Actuators 2 and 3 simulated axial loads, while actuator 1 simulated the horizontal shear force. The instrumentation of the models was installed according to the schematic presentation in Fig. 2.5, using external and internal instrumentation for collection of such data as displacement, deformation, dilatation, strains, etc. The measuring equipment, the data acquisition system and the loading control system were operated by means of a processing PDP 11/45 computer. According to the program, the loading procedure included application of forces for simulation of axial load (actuators 2 and 3) which remained constant throughout the application of the horizontal shear force (actuator 1) simulating cyclic load.

2.4. Experimental Results

The results are presented for the first (denoted el.1) of the two identical models for each of the three wall models; PZ-I, PZ-II and PZ-III, which were designed, constructed and tested for correlation with the models tested on the shaking table. Because the technical possibilities associated with testing on a seismic shaking table are limited (limited weight) the

models presented in this report were designed to simulate the upper storeys of the building prototype. Because of the large amount of data, the results are presented mainly in the form of diagrams, but numerical values also are indicated for the main parameters. The hysteresis diagrams presented in this chapter are plotted as functions of the horizontal shear force.

2.4.1. Test Results for the Rectangular Wall - Specimen PZ-1

The specimen PZ-1 (Fig. 2.7) was subjected to the loading program presented in Fig. 2.8, and the measured hysteresis relationship (force-displacement) is presented in Fig. 2.8b. At first, the element was loaded by axial forces $N_1 = N_2 = 41.5 kN$, i.e., a total axial force of $\Sigma N = 83 kN$ corresponding to nominal axial stress of $\sigma_0 = 0.80 MPa$. The horizontal force applied at the top of the element varied according to the loading program (Fig. 2.8a) resulting in total cyclic behaviour for different levels of forces and strains.

During the first loading phase up to the level of the occurrence of the first visible cracks ($P_{CR} = 54.3 kN$) the behaviour was linear (loading points LP.29-69). In the next phase the element was loaded up to the yielding point (LP.62) resulting in yielding force Py=84.8kN and corresponding yield displacement $\Delta y = 4.55 mm$; LP.71 was selected as the yield point for loading in the opposite direction (see the hysteresis relationship shown in Fig. 2.8b). This state can be regarded as initial yielding at which the displacement ductility is $\mu_y = \frac{\Delta y}{\Delta i} = 1$, and resulted in the occurrence of the first visible shear cracks at the ends of the panel walls propagating continuously through the cast-in-place and the prefabricated concrete (Fig. 2.9). The element subsequently was subjected to cyclic loading with displacement amplitudes which correspond approximately to the displacement of $2\Delta y$, $3\Delta y$, ... $n\Delta y$ — up to failure. The characteristic part was LP.149-157 - a state corresponding to

displacement ductility of $\mu = \dfrac{16.50}{4.55} = 3.63$ when damages to the panel occurred (Fig. 2.10); this was in the form of shear cracks and a characteristic crack along the joint line propagating continuously during the loading process, while the cracks in the upper part of the panel were blocked. This failure mechanism was of the "gap opening" type which became predominant especially in the range of large deformations. During the next loading cycle (LP.211-231) a maximum yield strength of Pu=95.8kN and yield displacement $\Delta u = 24mm$ were obtained corresponding to displacement ductility of $\mu = \dfrac{24}{4.55} = 5.30$ which can be estimated as the ultimate value since at that moment, on the left side of the panel, the ties in the prefabricated part of the panel were separated, while concrete failure due to compression took place on the other side (Fig. 2.11). This state was followed by an abrupt strength deterioration (on the left side of the diagram in Fig. 2.8) as well as decrease in rigidity with considerable increase of damage to the model. The analysis of the results and of the form of damage to the model point to the fact that the predominant effect is "gap opening", i.e., moment deformations which are clearly seen in Fig. 2.12, showing the relationship between strength variation and gap at the end of the panel wall. The influence of the shear slippage effects was negligible as is shown in the relationship presented in Fig. 2.13.

On the basis of the damage to the wall which included cracks in the precast panels, dominant opening of the horizontal connection of the lower level panel, yielding of the vertical reinforcement in the vertical joints and tensile reinforcement in panels with rupture in the case of larger top displacement, crushing of concrete and buckling in bars (Fig. 2.14), it can be concluded that the major failure mechanism occurred as gap opening in the horizontal joints with limited shear sliding and limited shear failure in the precast panels.

On the basis of the experimental results showing the load carrying and deformability capacity as well as the failure mechanism and hysteretic behaviour, it can be concluded that the precast wall panels are ductile elements of the structural system, and are capable of withstanding a considerable amount of nonlinear deformation (effective displacement ductility of $\mu > 5$) with energy absorption as shown by the dense hysteresis loop.

2.4.2. Test Results for Wall with Openings - Specimen PZ-II

The model PZ-II is a wall with openings; its characteristics are shown in Fig. 2.15. The loading scheme shows that the element was loaded by axial forces $\Sigma N = 83kN$, while the cyclic loads were applied with three successive cycles at the same displacement amplitude.

The force-displacement relationship for the entire loading sequence is shown in Fig. 2.16, while the displacements of the first and the second storey are given in Figs. 2.18 and 2.17, respectively. The maximum horizontal force is about $P_{max} = 100kN$, the maximum displacement initiating failure is about $\Delta_{fail} = 40mm$; however, the loading point 204 with $\Delta_{ult} = 30mm$ should be considered as an ultimate state, since a sudden force drop occurred then. Hence the displacement ductility is evaluated as

$$\mu_{displ} = \frac{\Delta_{ult}}{\Delta y} = \frac{30}{6.50} = 4.60 .$$

In the displacement to the initial yield point, cracks appeared in the parts of the wall under tension and diagonal cracks appeared in the beams as well as considerable cracks in the contact zone between the precast and the monolith concrete, all on the first floor. The increased displacements widened the cracks and resulted in appearance of cracks on the second floor (LP.111); however, localization of the damage to the contact zone also was noted. The failure mechanism developed successively from the crushing of concrete in the

compressive zones in which widened cracks already existed, so that almost complete failure took place in the cast-in-place concrete at the edges of the panels. The real failure took place in the final stage as failure of the panels due to compression (Fig. 2.19).

From the experimental results and the observed behaviour of models of walls with openings under cyclic loading, the following conclusions can be made:

- The failure mechanism, i.e., the stress and strain distribution, in walls with openings is different from that in the panel wall of the rectangular section without openings.

- The connecting beam above the openings in these walls is of special importance, first of all for the force distribution and moment reduction in the lower stories, as well as for increasing the energy absorption capacity through the beam failure, shown first by initial cracks and then by formation of plastic hinges.

- The expected plastic hinge development in the beams did not occur because of the constraint provided by the loading beam at the wall top; thus it will be necessary to perform a new test of walls with openings to avoid this effect.

2.4.3. Test Results for Flanged Wall - Specimen PZ-III

The structure of the flanged panel wall model PZ-III displaying a middle longitudinal wall from the building prototype is presented in Fig. 2.20. The main objective for testing the flanged panel wall is to study the participation of perpendicular walls in the total bearing capacity of the walls.

The model PZ-III was loaded by an axial force of $\Sigma N = 153kN$, and by the cyclic shear force P(N) according to the loading program. The measured hysteresis relationship is presented in Fig. 2.21 which shows all the

characteristic phases: occurrence of the first cracks (Pcr), serviceability load level (Psv), design earthquake level (Pde), initial yielding (Pᵧ), ultimate stress (Pu) and state of failure (Δcl). Under cyclic loading of about 15 mm top displacement, failure of the compressed flange occurred (which may be characterized as local failure of a flange) followed by abrupt force deterioration (LP.156) and a considerable increase of slippage. Although failure occurred quite early, a displacement ductility higher than 4 was achieved.

As to the behaviour of the flanged walls, it may be concluded that efficient shear resistance is contributed by the perpendicular walls, not only in the elastic but also in the post-elastic range.

2.5. Summary of the Pseudostatic Test Observations

On the basis of the experimental test results and observed behaviour of the models it can be concluded that testing of all the models was successful and the results obtained provide a good basis for correlation of the static results with dynamic tests, for establishment of analytical models and for developing recommendations for design and construction.

It can be concluded that the system connections are efficient and that the structural parts behave as ductile structures in the nonlinear range. The cast-in-place part of the vertical panel joints and the continuity of vertical reinforcement between the panels aid in prevention of panel sliding or brittle failure due to shears along the contact zones. The end result was an increase of energy absorption capacity during earthquakes, which is a significant prerequisite for creation of a universal system to be applied under all seismic conditions.

It should be mentioned that the design modifications incorporated in the vertical panels ensured that the precast panels themselves contributed to the inelastic work of the system, as is evident from the experimental results. This justifies the method of construction and reinforcement of the panel walls which was intended to provide for their optimum performance in the nonlinear range.

The very large contribution of the flanges to model PZ-III behaviour demonstrates the importance of three-dimensional study of panel structures, which will have to be done in a future investigation.
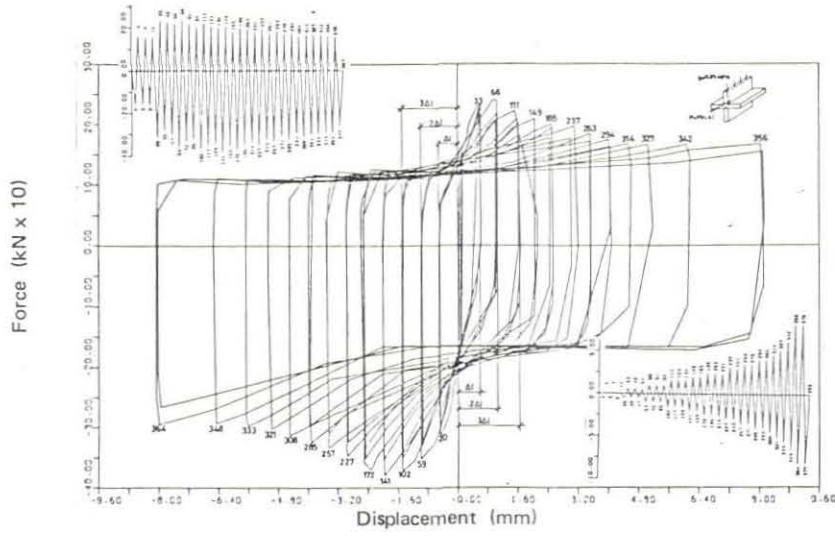
Fig. 2.1.   Hysteresis Relationship of Horizontal Joints in Vertical Panels
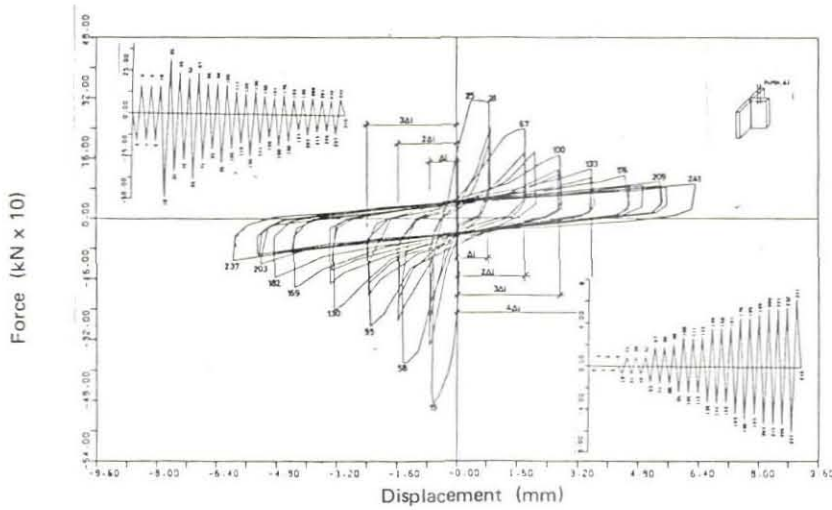
Fig. 2.2.   Hysteresis Relationship of Vertical Joints in
Vertical Panels (Model in Scale of 1 : 1)
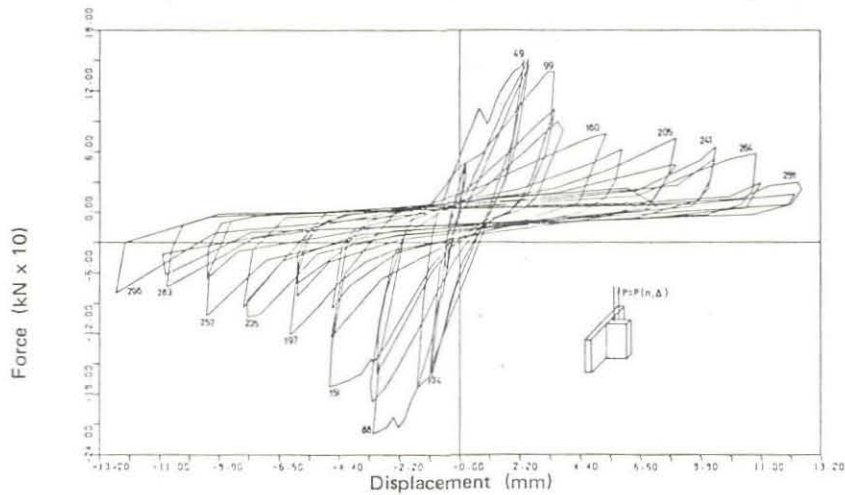
Fig. 2.3.   Hysteresis Relationship of Vertical Joints in Vertical
Panels for the Model in Scale of 1 : 3
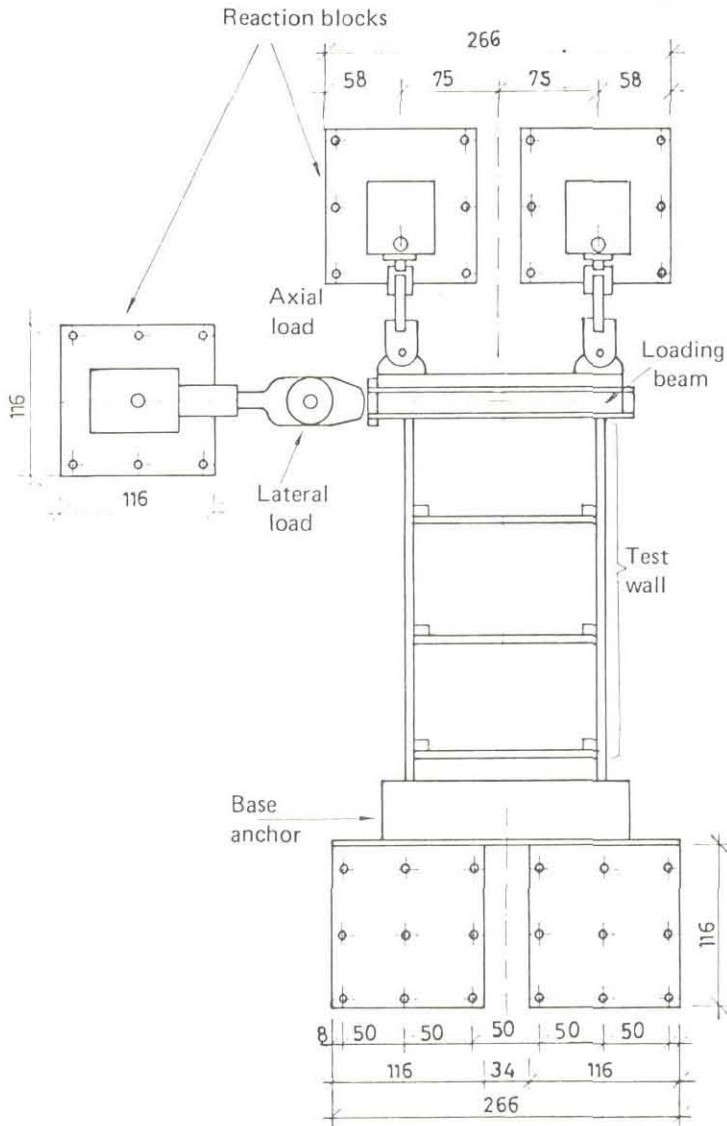
Fig. 2.4. Configuration of Test Systems for Experimental Investigation of Panel Walls
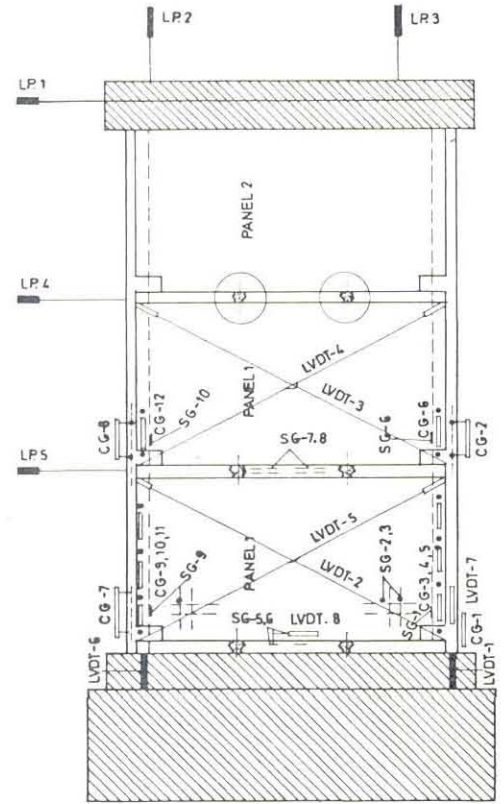
Fig. 2.5. Instrumentation of Models for Pseudostatic Tests
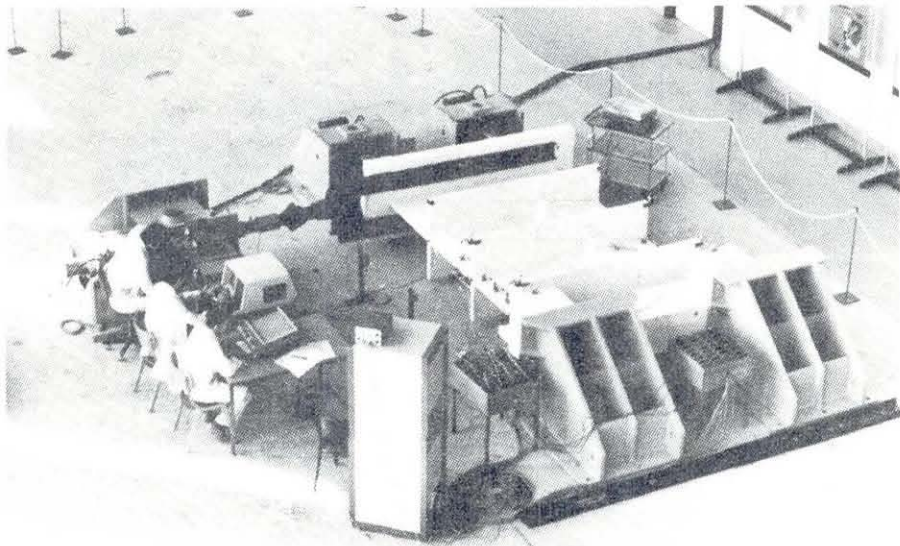
Fig. 2.6. Photograph of the Test Model

Fig. 2.7.   Details of the Panel Wall Model PZ–I
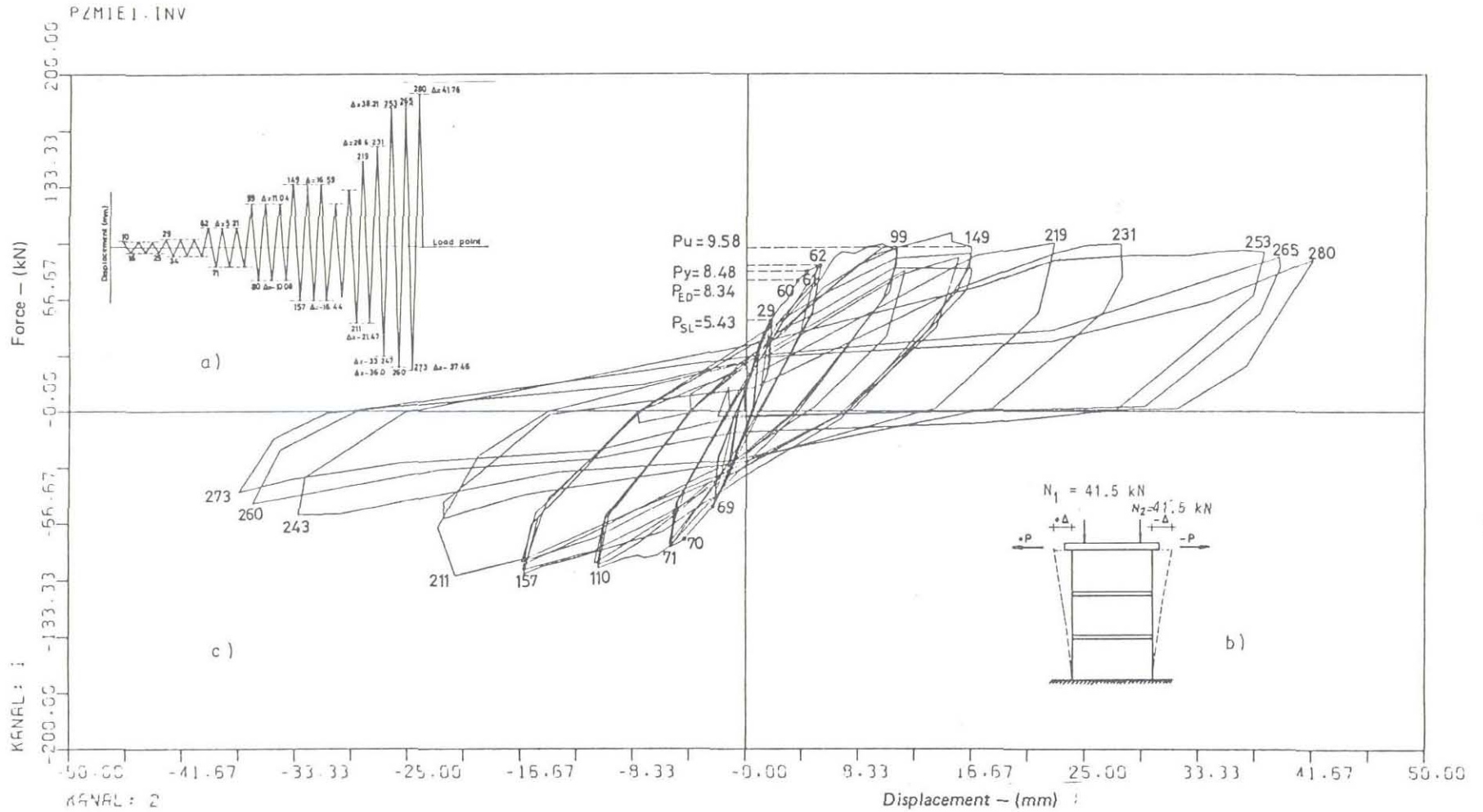
Fig. 2.8. Hysteresis Loop of the Model PZ–I, el. 1
a) Loading Program, b) Force Application Scheme,
c) Hysteresis P–Δ Relationship at the Top of the Model
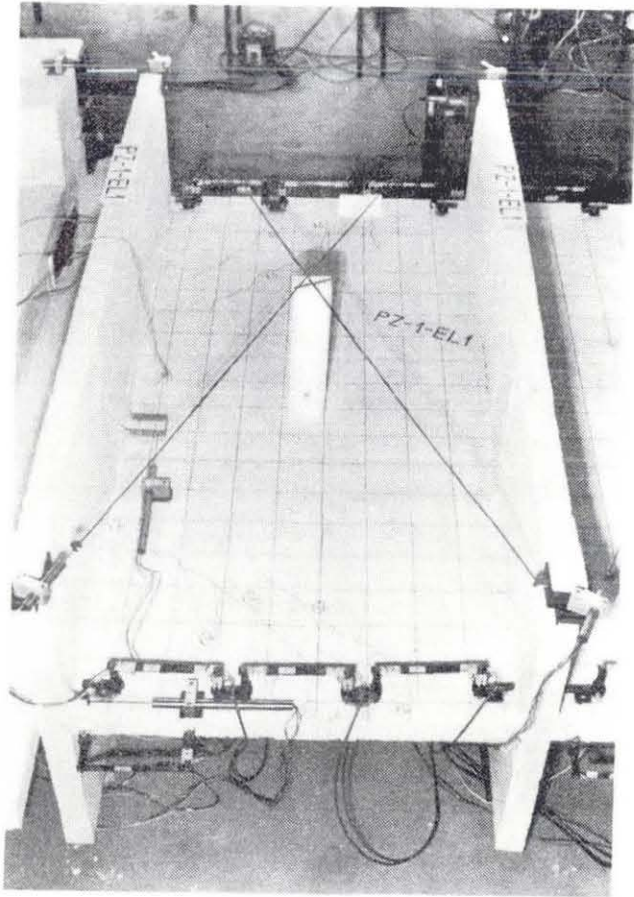
Fig. 2.9.   Cracks in the Wall Occurring in the First
            Yielding State
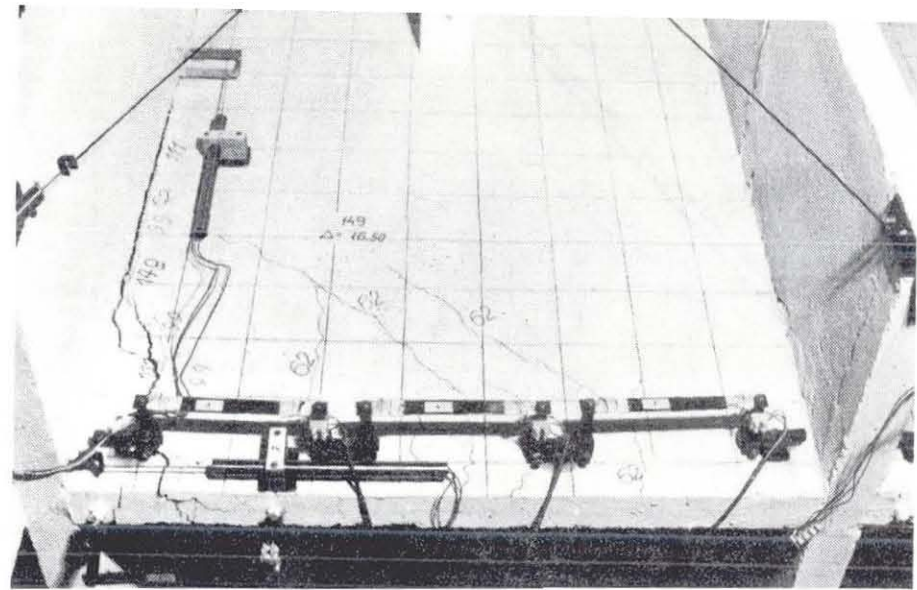
Fig. 2.10.   Cracks in the Panel Wall Occurring at Top
             Displacement of $\triangle$ = 16.4 mm
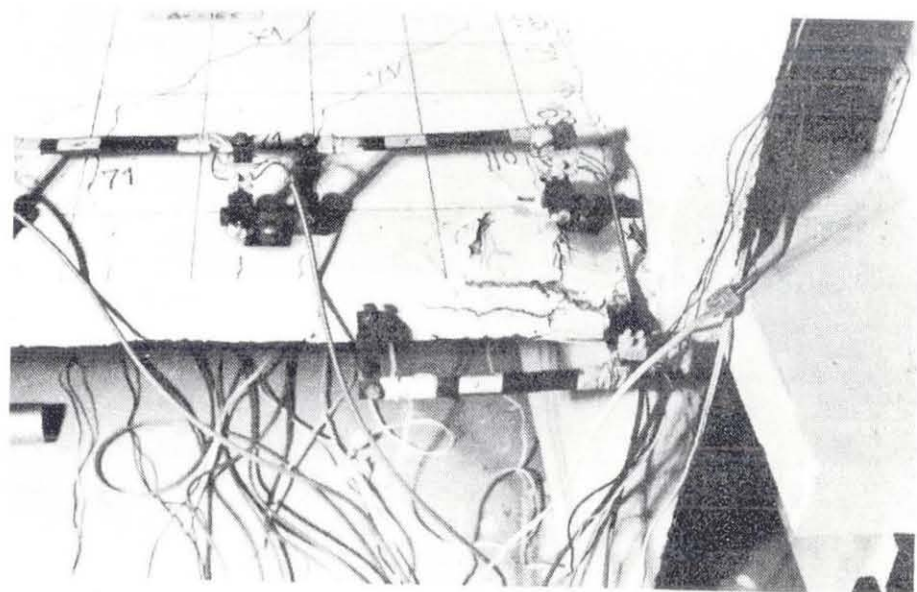
Fig. 2.11.   Crushing in the Compression Zone of the Panel Wall
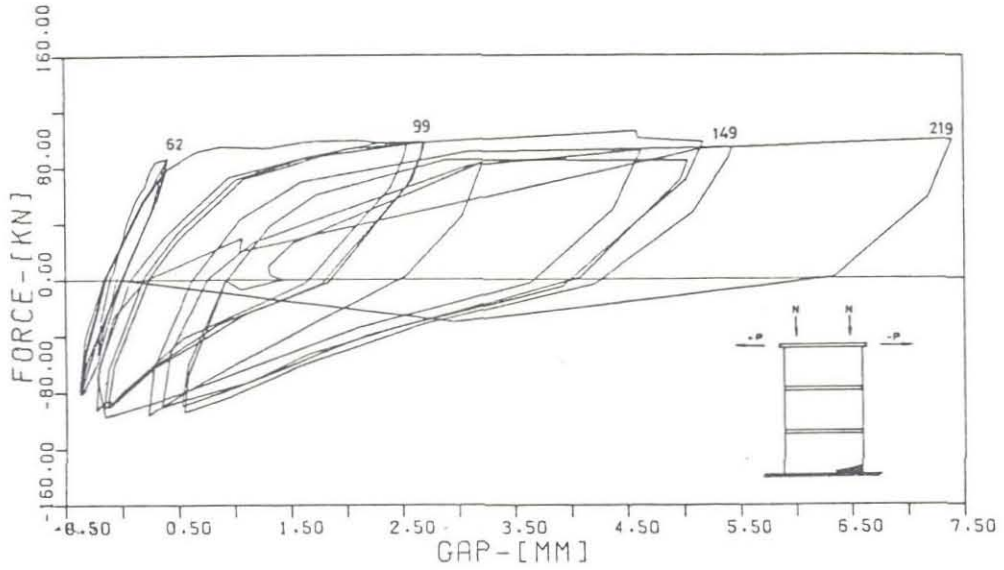
Fig. 2.12.   Gap - Opening - Force Relationship (PZ–I)
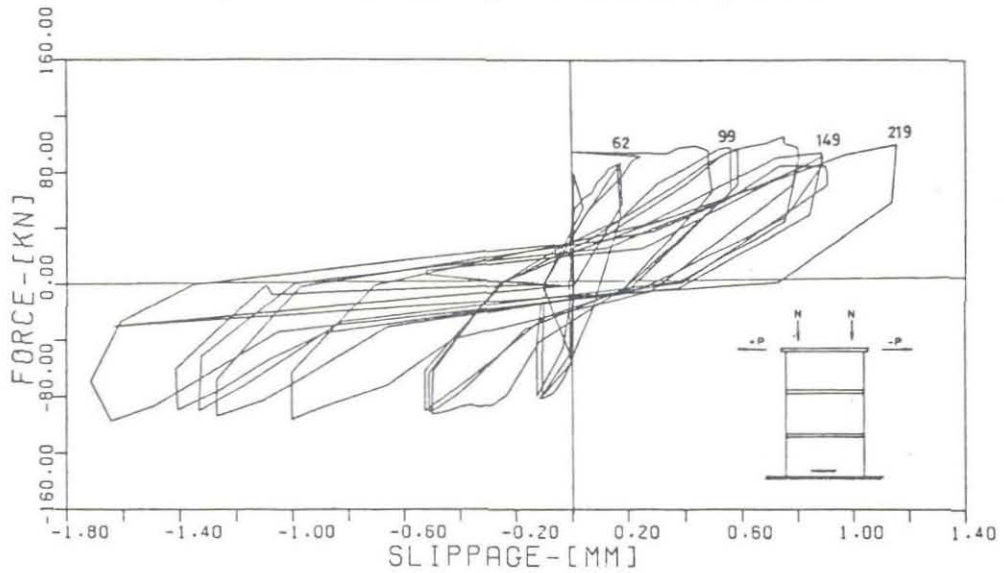
Fig. 2.13.   Shear Slippage - Force Relationship
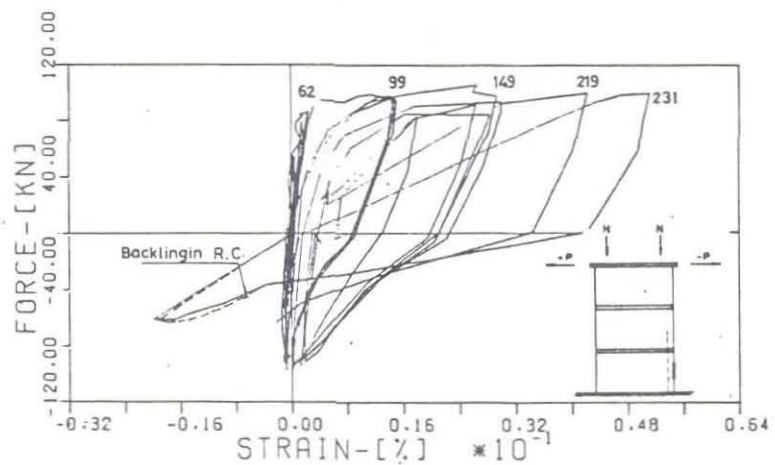
Fig. 2.14.   Strain in Tensile Reinforcement - Force Relationship
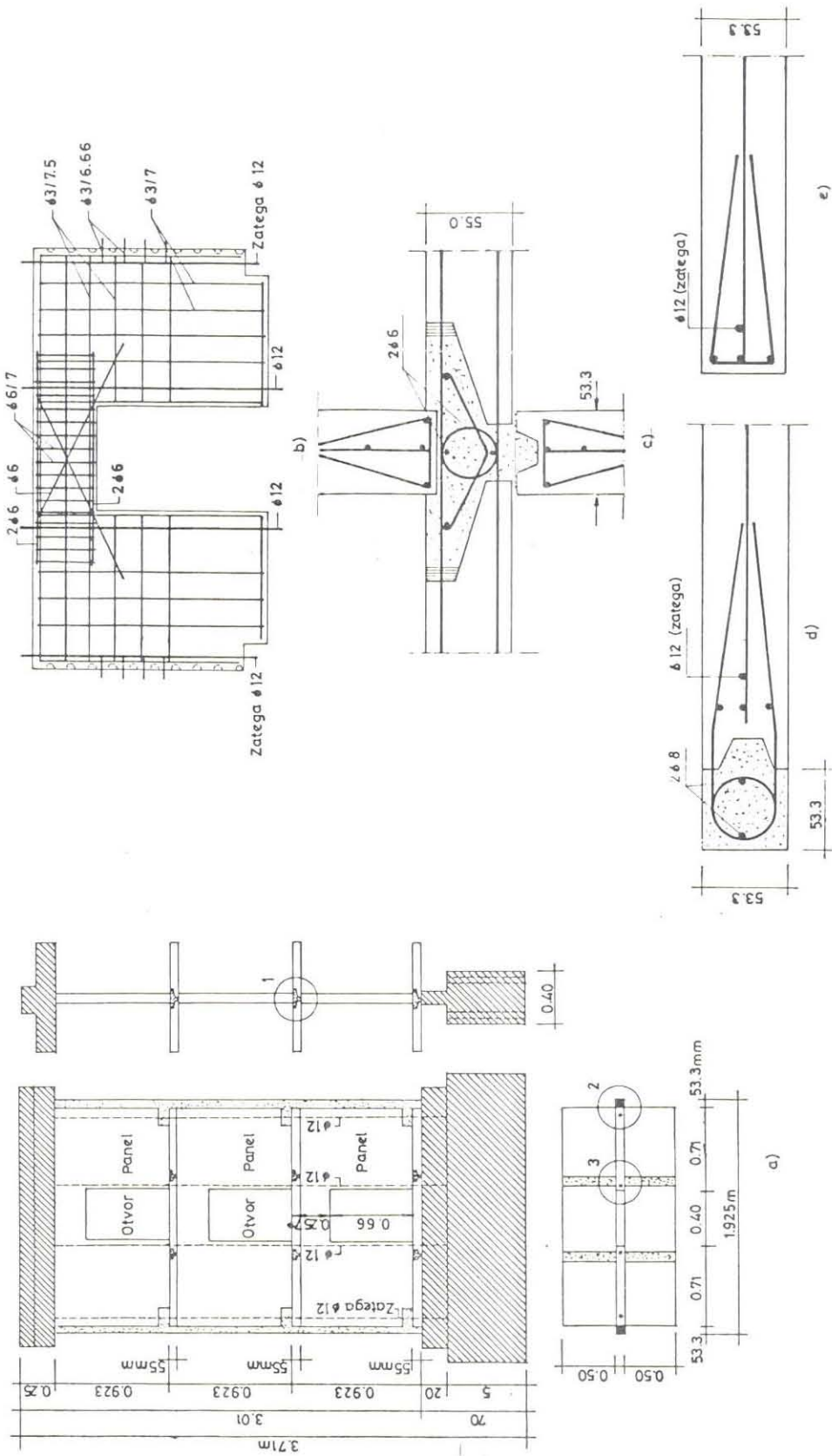
Fig. 2.15. Details of the Model of a Panel Wall With Openings (PZ—II)
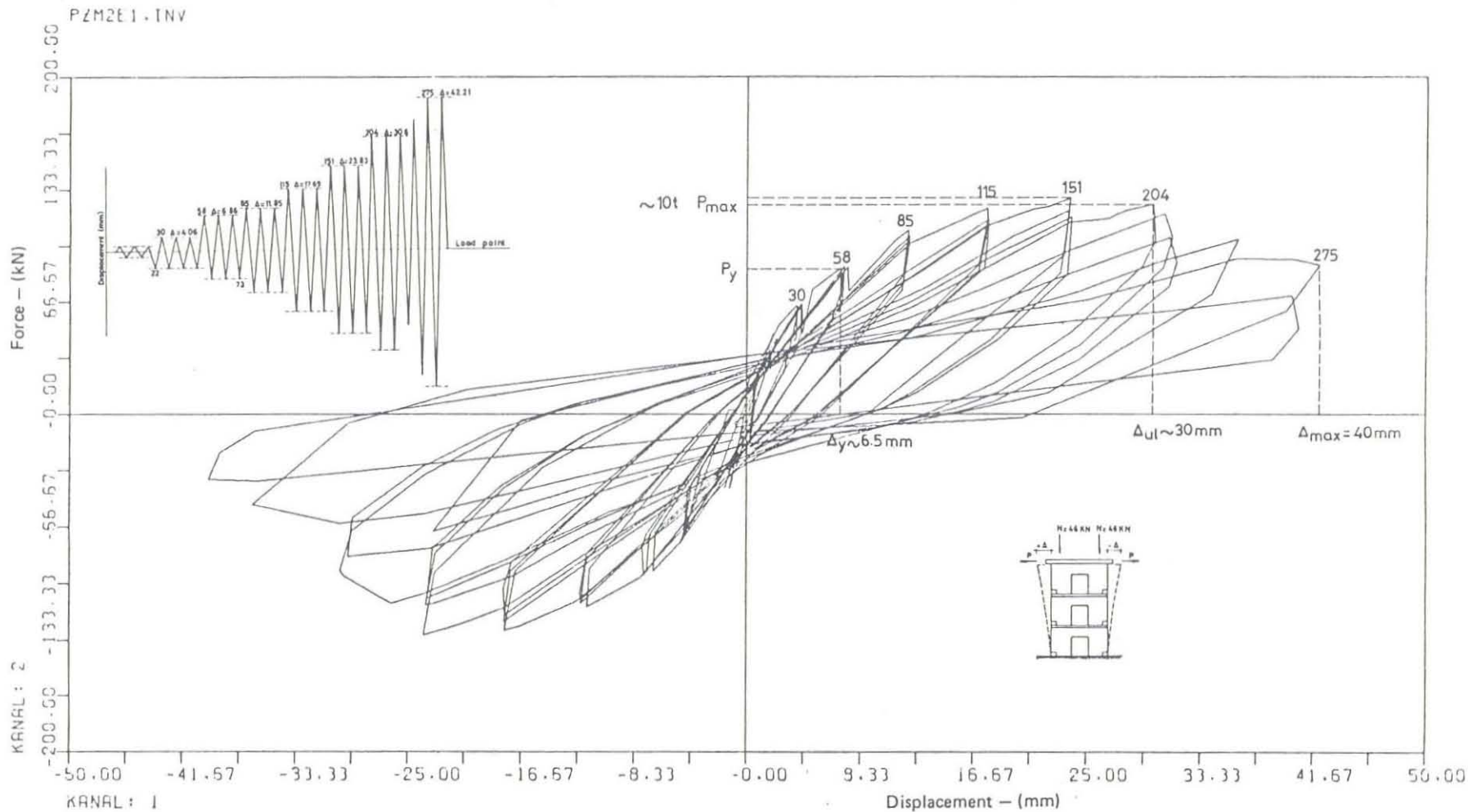
Fig. 2.16. Hysteresis Loop of the Model of a Panel Wall with Openings (PZ–II, el. 1)
a) Loading Program, b) Force Application Scheme, c) Hysteresis P–Δ
Relationship at the Top of the Model
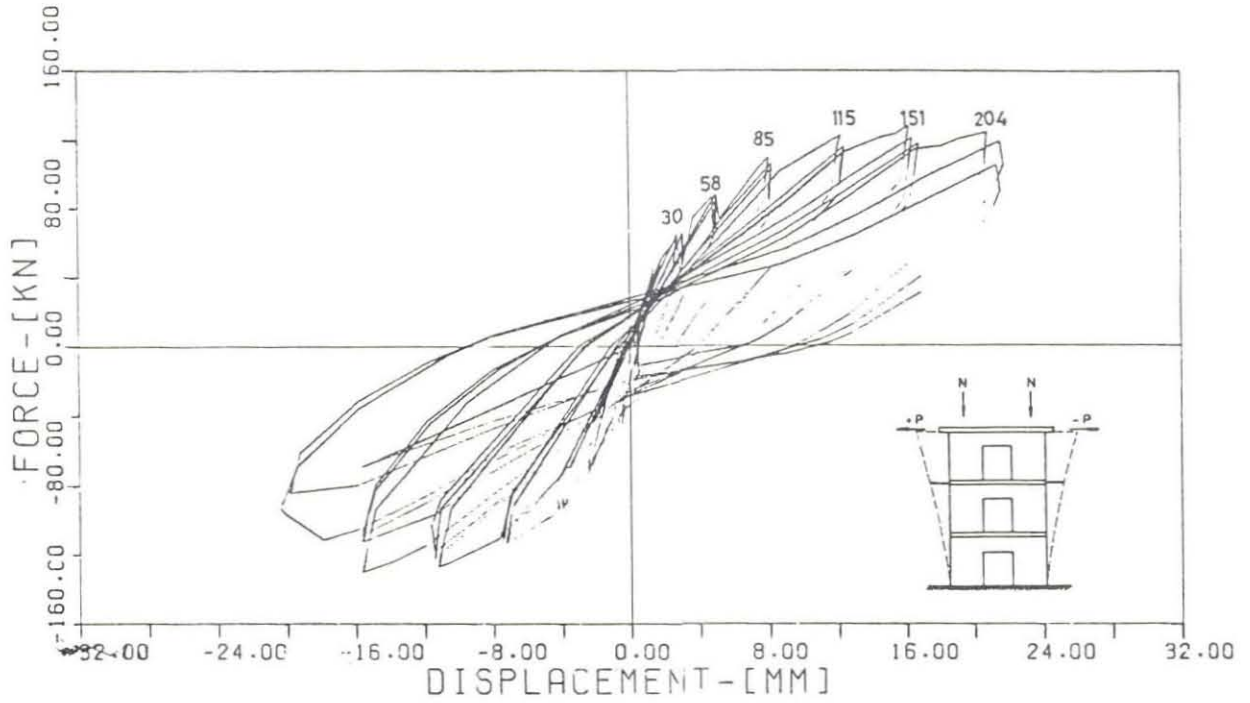
Fig. 2.17. P—Δ Relationship for the Second Storey Level
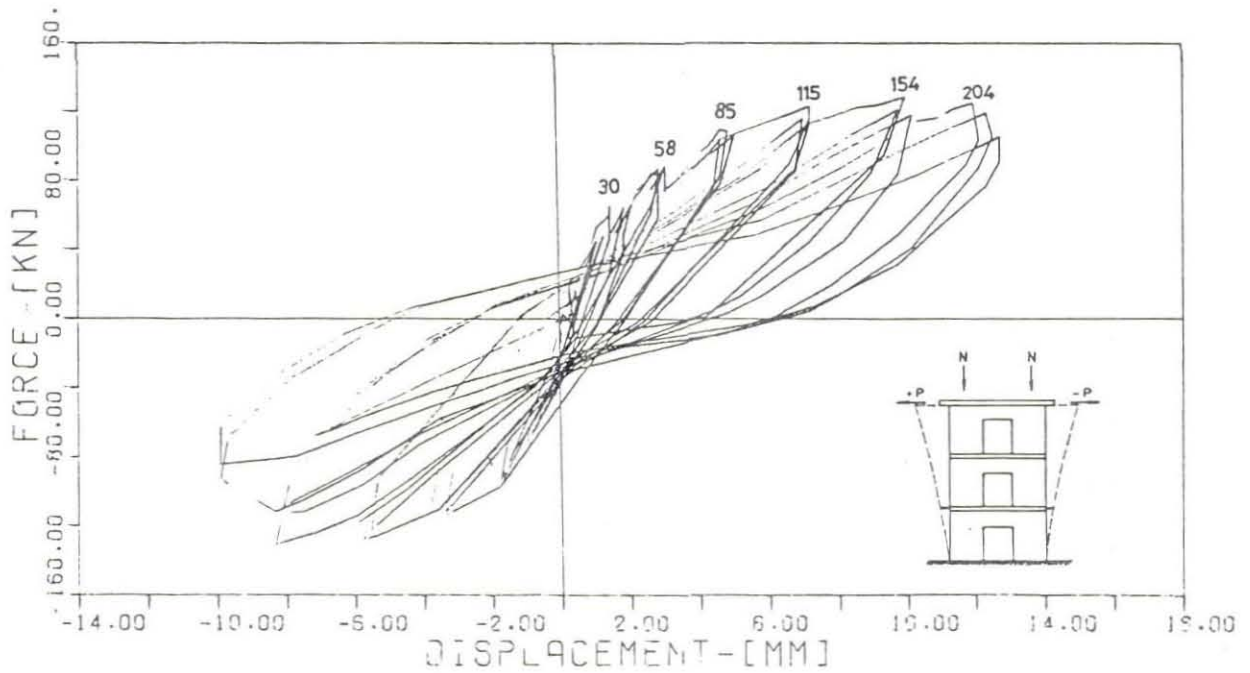
Fig. 2.18. P—Δ Relationship for the First Storey Level
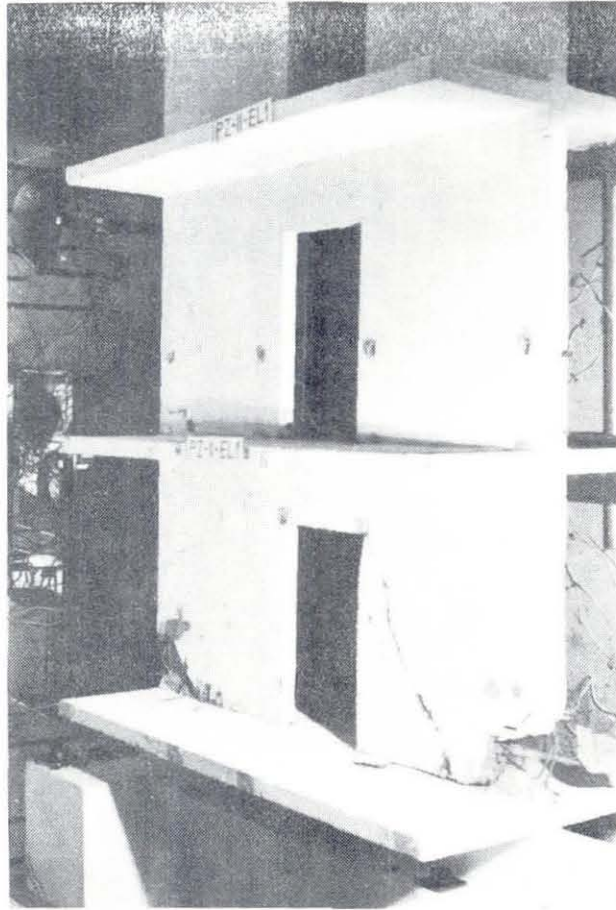
Fig. 2.19. Photograph of Damage to the Model
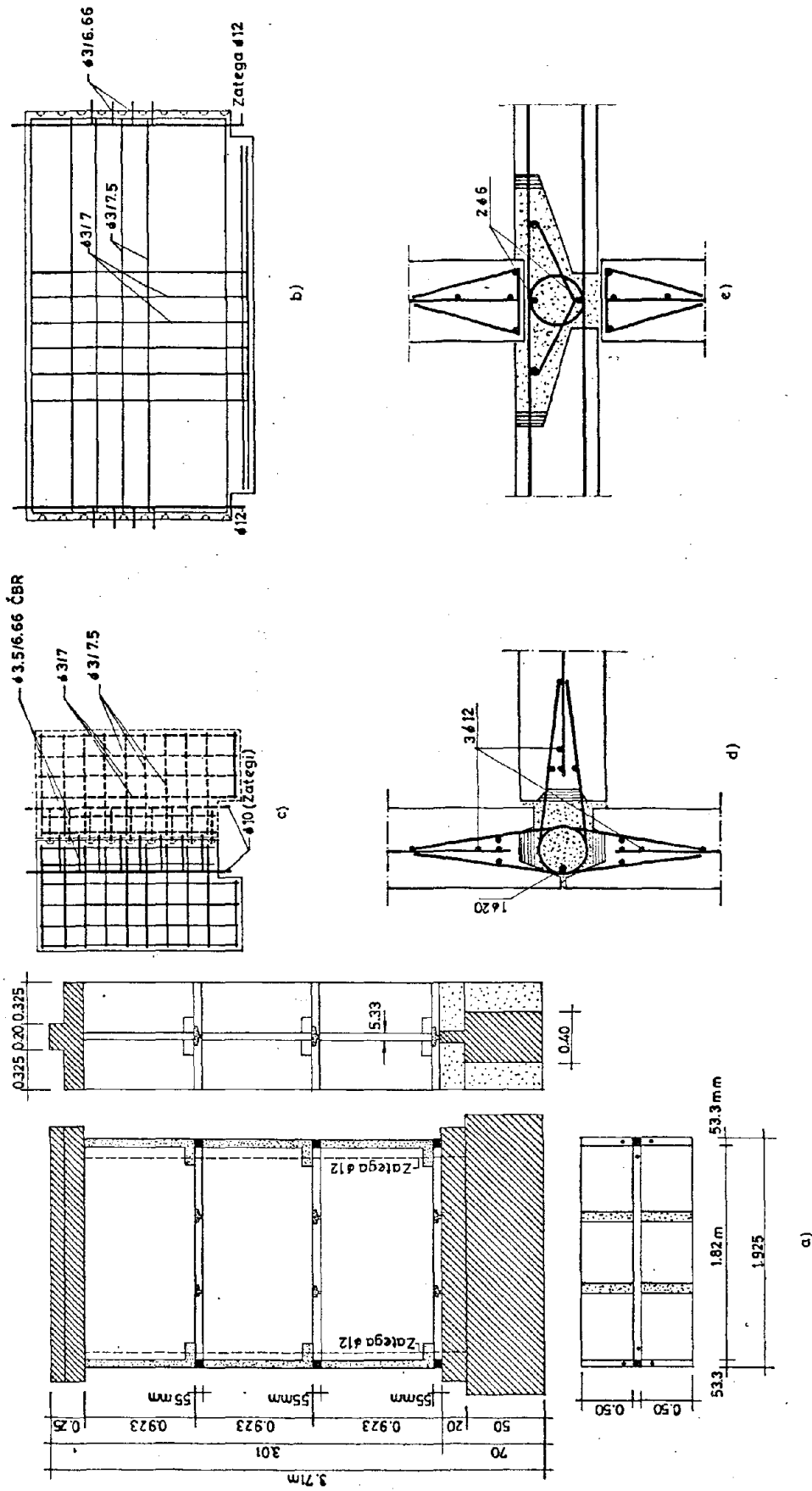
Fig. 2.20. Details of the Panel Wall Model PZ–III

PZM3E1.INV
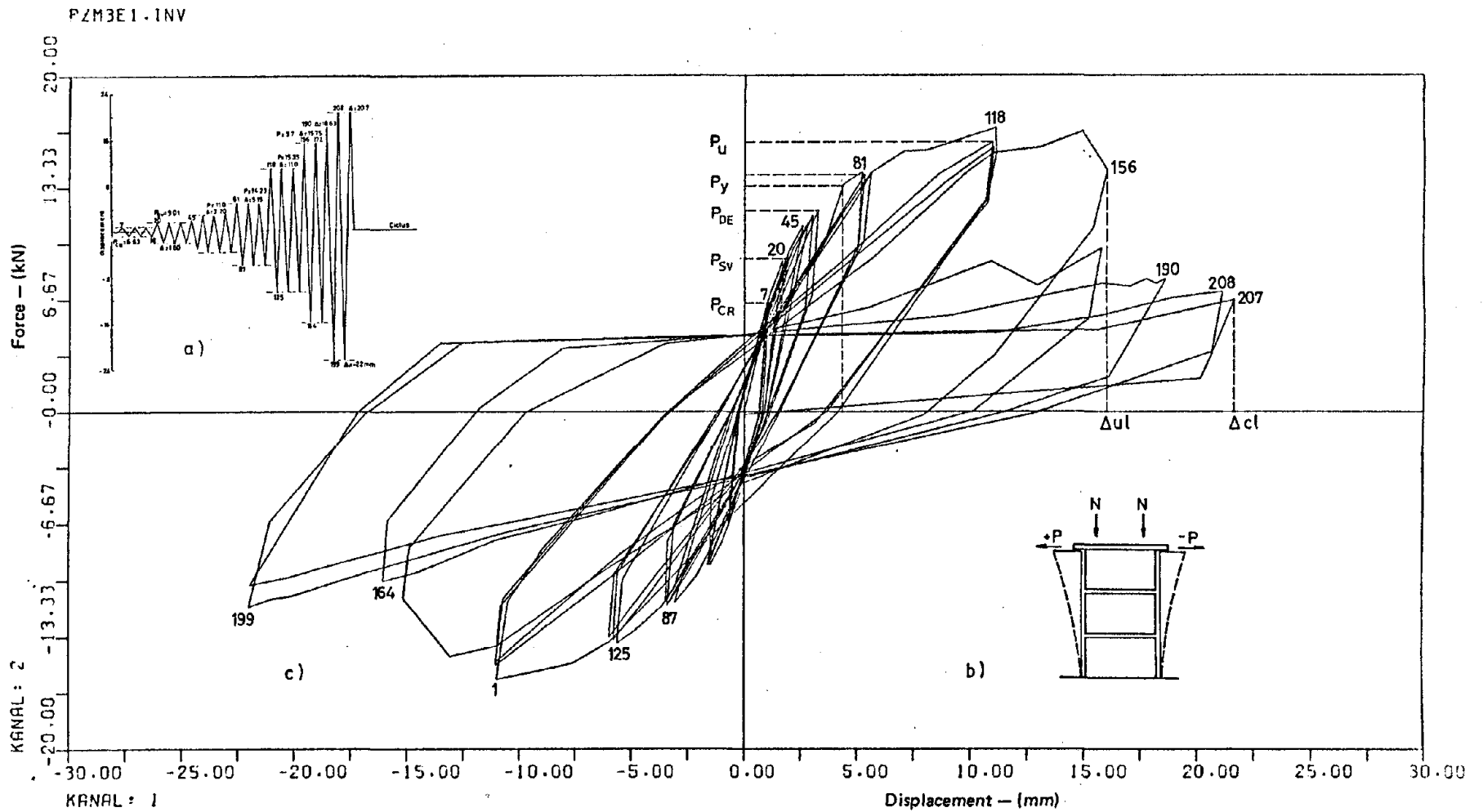
Fig. 2.21. Hysteresis Loop of the Model PZ–III

a) Loading Program, b) Force Application Scheme,
c) Hysteresis P–Δ Relationship at the Top of the Model

3. SHAKING TABLE EXPERIMENTAL STUDIES

3.1. Introduction

From the earliest phase of planning this research program on the seismic resistance of large-panel precast concrete apartment buildings, it was recognized that shaking table experiments would be an important part of the study. The pseudostatic test program described in the preceding chapter was intended to demonstrate the capacity of the RAD structural system to resist earthquake type loads, and to accommodate deformations that might be imposed during an earthquake. The strength and deformability of the typical joint systems used in assembling the precast panels were investigated, and then the earthquake capacity of three different three-storey assemblages of the panels was calculated. Such testing provides an ideal approach to planning design improvements, because the relative capacity of different design proposals can be determined quickly and at small cost.

However, the pseudostatic testing method has one major deficiency - it does not provide any information on the strength and deformation demand to be made on the structure by a specific design earthquake. Strength and deformability are essential characteristics of any earthquake-resistant structure, and as mentioned above these properties are easily measured for any structural component or assemblage by a cyclic testing method. But a prescribed earthquake motion does not require the structure to have any specific strength, deformation limit or energy absorption capacity. Satisfactory performance may be obtained with structures having widely differing values of these properties and a true dynamic response experiment is the best way to establish whether a specific design will perform satisfactorily in resisting a prescribed design earthquake; the response mechanism involves the combined action of strength,

deformability and energy absorption.

An important concept in planning the shaking table experiments was that they should be performed on test specimens as nearly identical to the pseudostatic specimens as possible in order to relate the demand imposed by the earthquake motions to the capacity indicated by the static tests. Thus the shaking table test assemblages designated PZ-I, PZ-II and PZ-III were fabricated from one-third scale panels manufactured by RAD in the same way as the corresponding pseudostatic models. Also the properties of the concrete and steel used in the two sets of models were essentially the same. The only significant discrepancy was in the compressive strength of the concrete used in IZIIS specimen PZ-II, which was only about half as strong as that used in the other panels; however the shaking table arrangement used for testing this model proved to be unsatisfactory (as was mentioned above for the pseudostatic test) so it was not included in the comparison of the two types of test results.

In the following sections of this chapter, brief descriptions will be presented of the shaking table test system, of the instrumentation used to record the performance of the models, of the tests performed and resulting damage, and finally of the dynamic response behaviour of specimens PZ-I and PZ-III. The specimens themselves are equivalent to those described in the preceding chapter so their descriptions are not repeated here. Complete details of the entire shaking table test programs are published in Reference 1.

3.2. Shaking Table Test System

The dynamic tests of the three-storey test specimens were performed on the Earthquake Simulator at EERC. This 20 ft. square shaking table can be controlled to produce any specified earthquake motion in one horizontal component together with an equally arbitrary vertical motion. The maximum

weight of the structures that may be tested is 100,000 lb, and with this full capacity load the table can produce accelerations of up to 2/3 g horizontally and 1/3 g vertically.

The data acquisition system to record data from the dynamic tests can take signals from as many as 128 transducers and can record these in digital form at the rate of up to 155 readings per second from each instrument. Information recorded in typical tests of structural systems included dynamic displacements and accelerations as well as strains measured at selected points on the structure. All test data are stored on magnetic disks from which it can be recovered as desired for use in preparing plots of the response quantities.

To perform a test of any of the precast panel assemblages, the model was supported on a steel foundation system which in turn was bolted to the shaking table. A steel platform also was attached to the top of the model and concrete blocks were supported on the platform to provide the desired added load of 19,100 pounds. The purpose of this load was to induce dynamic stresses and displacements of the model equivalent to those expected near mid-height of a 10 to 20 storey building during the design earthquake.

Because each test structure represented only a single wall section of the prototype building, it was necessary to use a test fixture to provide stability in the lateral direction (i.e., perpendicular to the earthquake excitation axis). This fixture is a rigid steel frame which surrounded the test specimen on the shaking table. A linkage system between the fixture and the specimen provided lateral support but offered no resistance to displacements in the vertical plane of the dynamic response. Figure 3.1 is an elevation view of a typical test specimen on the shaking table, also showing the top steel platform and concrete mass blocks. Figure 3.2. is an equivalent view of specimen PZ-II seen through the side of the structural steel lateral support fixture.

3.3. Instrumentation

Instrumentation used in these experiments was designed to monitor three kinds of dynamic response : (1) shaking table motion, (2) accelerations and total displacements of the model measured from a stationary reference frame, and (3) local deformations (i.e., relative displacements) and strains within the model. Details concerning some of the more important measurements are presented in the following paragraphs; Reference 1 contains complete information on the instrumentation system. In general, an average of 85 channels of test data were recorded for each test specimen studied during this test program, readings of each channel being taken at the rate of 100 samples per second.

The most important data recorded from the shaking table were its horizontal acceleration and displacement. No vertical earthquake component was applied in these tests because such motions have been observed to produce negligible effects on the performance of test buildings.

Displacements and accelerations in the horizontal direction were measured at the base, at each floor level, and at the top of the test structures. Additional gages were installed to measure rotational displacements and accelerations at the top of the assemblage. Local deformations measured within the test specimens included the shear slip at vertical and horizontal joints, uplift at the bottom floor joint, and panel shear distortions. In addition, resistance wire strain gages were welded to reinforcing bars at critical locations, notably on the vertical bars cast-in-place at the sides of the panels and on the horizontal bars in the horizontal panel joints.

One further type of response information was provided by a set of force transducers connecting the base of the test system to the top of the shaking table. These four gages were calibrated to indicate the shear forces developed

at the four corners of the support frame, and thus provided a check on the inertial forces derived from the horizontal acceleration measurements.

3.3. Test Program

During the test program, each specimen was subjected to a sequence of simulated earthquake motions. In each case, the test signal was first applied at low intensity in order to check the functioning of the instrumentation without causing damage to the structure. Then the specimen was subjected to base motions of sufficient intensity to cause appreciable damage. In all tests, the applied motion was proportional to the N-S component of the earthquake recorded at El Centro, California in May 1940, the intensity being set as desired by appropriate adjustment of the control system. In general the earthquake intended to cause the initial major damage of the specimen was set to have a peak acceleration value of about 2/3 g. After the main test, each specimen was subjected to an "aftershock earthquake"; for specimen PZ-I this was less intense than the main shock, but for specimen PZ-III it was made significantly greater than the main shock. The test sequence for these two specimens is summarized in Table 3.1.

Table 3.1.   Shaking Table Sequence

Specimen	Test No.	Input Signal	Maximum input acceleration (g)
PZ-I	1	El Centro (150)	0.179
	2	El Centro (700)	0.666
	3	El Centro (500)	0.495
PZ-III	1	El Centro (200)	0.223
	2	El Centro (750)	0.689
	3	El Centro (1000)	1.081

In order to assess the degree of damage induced during each test, the free vibration frequency of the test structure was measured before testing and after each simulated earthquake. The frequencies were determined by applying a low-intensity "white-noise" table motion and analyzing the response signal of an accelerometer mounted at the top of the specimen; thus the frequency indicated is that of the test structure on the operating shaking table. The measured frequency results are listed in Table 3.2. The reduction of frequency shows that the stiffness was reduced by about 50% as a result of the damage incurred during the main shock; however the structure still supported the applied load even after being subjected to an additional severe earthquake.

Table 3.2.   Free Vibration Frequencies in Shaking Table

Specimen	Test Program Phase	Frequency (Hz)
PZ-I	Prior to test	5.20
	Post EC -150	5.10
	Post EC - 700	3.90
PZ-III	Prior to test	6.30
	Post EC - 750	4.32

Damage Observations

Observations of the performance of the specimens during the tests and examination of the damage after the tests provided valuable information supplementary to the instrumental data. In all cases there was no visible deformation during the preliminary low intensity test. A summary of the damage resulting from the severe shaking tests of specimens PZ-I and PZ-III follows.

PZ-I: The obvious visible response mechanism during intense excitation was rocking motion associated with uplift separation at the first floor horizontal joint; no shear slip could be noted. Uplift occurred over at least half of the north end of the joint length and was accompanied by compression damage to the north end column and shear key.

Subsequent cycles of rocking caused the two reinforcing bars of the

south end cast-in-place column to buckle and ruptured the adjacent panel bar. Figure 3.3 is a photograph of this damage area; only minor cracks were noted at the corresponding north end column.

PZ-III   This specimen was similar to PZ-I except that it had flange walls at each end oriented perpendicular to the main wall; its visible motion also was dominated by rocking associated with alternating uplift of the ends of the wall and flanges. The principal damage consisted of crushing of the shear key at the south end and spalling of the adjacent flange panels; lesser but similar damage occurred at the north end. Careful study of the south end damage regions revealed that the outer column bar had ruptured a short distance above the floor and the inside bar buckled; also the flange and wall panel bars had ruptured. The lesser damage at the north end included buckling of the two column bars and rupture of one of the flange panel bars. Photographs of these damage areas are presented in Figs. 3.4 and 3.5.

3.5. Experimental Results
3.5.1. Test Results - Specimen PZ-I

The instrumentation records confirmed the type of response behaviour described above. For both specimens the preliminary test was intended to induce deformations within the linear elastic range and the shaking table motions applied to specimen PZ-I, shown in Fig. 3.6, indicate a peak acceleration of only 0.18 g. As shown in Fig. 3.7, the acceleration of the concrete blocks at the top of the test system was considerably greater, about 0.4 g, but this increase is mostly associated with a rocking motion of the shaking table and does not indicate significant deformation of the wall assembly. The essentially

linear response behaviour is demonstrated in Fig. 3.8 in which the shear force exerted by the shaking table at the base of the test structure is plotted as the abscissa while the horizontal response of the wall relative to the table is indicated by the ordinate. The nearly constant slope of this force-displacement relation during the entire 20 seconds history of the table motion shows that the test structure did not lose any of its original stiffness property.

The much more severe table motion applied in the second test of this specimen is evident in the peak acceleration of 0.67 g indicated in Fig. 3.9, but comparison of the displacement trace of this figure with that of Fig. 3.6 shows that the two tests were equivalent except for intensity. The significant amplification of motion with height is shown by the acceleration traces from the different floor levels in Fig. 3.10. In this test the amplification results mainly from rotation of the model relative to the table, a phenomenon that was indicated by the uplift gages at the base of the model. The nature of this uplift mechanism may be deduced by study of Fig. 3.11, which shows the history of vertical displacement relative to the table measured at three points at the base of the wall. Gauge U6 is located in the shear key at the left (north) end of the wall; it clearly shows that the wall uplifts and returns to the table top, alternately, as the top of the wall displaces right and left. Also it is clear that the uplift never completely returns to zero; apparently the yielded (elongated) vertical reinforcing bars and loose concrete particles support the wall in a slightly elevated position. The displacements at gages U7 and U8 show lesser amounts of uplift indicating that the wall is pivoting about the right (south) end during top displacement toward the right; however smaller uplifts also may be seen between the main rocking cycles, demonstrating that similar pivoting is taking place about the left end of the wall.

The second type of relative motion measured at the base of the wall was shear slip, that is, horizontal sliding of the wall along the crack resulting from the uplift mechanism. This sliding history is shown in Fig. 3.12; careful study shows that sliding towards the south is in phase with uplift at the north end of the wall, and that the peak slip displacements are essentially proportional to the amount of uplift but only about one-tenth as great. The sliding towards the north as the wall rocks in the opposite direction has noticeably smaller peak motions, but it is interesting that the average sliding motion (especially during the latter part of the earthquake) tends to be more north than south.

The shear force exerted by the table on the base of the wall was measured by the force transducers supporting the test specimen, as mentioned earlier; however the horizontal force also could be calculated as the product of the mass of the test structure at various levels and the corresponding measured accelerations. The values of total base shear force obtained by each approach are compared in Fig. 3.13, the solid line showing the sum of the shear indicated by the base transducers and the dashed line indicating the sum of the horizontal forces calculated from the accelerometer values. The close agreement between the two types of data is apparent in the lower sketch, which presents the first 4 seconds of the test using an expanded time scale. The relation between the base shear force and the motions of the wall is shown clearly in Fig. 3.14, which indicates the first four seconds of the test. As expected, the displacement of the wall towards the south coincides with the shear force towards the south and with the uplift at the north end.

The final indication of the performance of this wall to be considered here is the top displacement vs. base shear force history shown in Fig. 3.15. This plot is equivalent to the low intensity test result of Fig. 3.8, but the nonlinear nature of the response behaviour is quite obvious in Fig. 3.15. It is

apparent in the lower plot (which shows the first two seconds of response) that the behaviour was essentially linear during the beginning of the test, but then when the shear force exceeded about 13 kips (negative) the displacement increased suddenly - indicating yield or fracture. On the return (positive direction) motion the stiffness was noticeably less than in the first phase response; also positive direction damage is observed when the shear force exceeds 15 kips. The sudden drop of shear force at B, between points A and C of the trace, coincide with rupture of some of the north side reinforcement, but it is interesting that most of the shear force was recovered after the rupture on this cycle of deformation. However, it is apparent that this same maximum force was not attained in subsequent cycles, demonstrating the degree of damage associated with the rupture of the reinforcement.

3.5.2. Test Results - Specimen PZ-III

In the preliminary low intensity test of specimen PZ-III, the table motions were essentially equivalent to those applied to specimen PZ-I, as shown in Fig. 3.6, except that the shaking intensity was set a little higher (peak table acceleration of 0.22 g rather than 0.18 g) in recognition of the greater strength of the wall with flange panels. The plot of base shear versus top displacement shown in Fig. 3.16. shows that the average lateral elastic stiffness of the flanged specimen was about 106 k/in, well above the value of 54 k/in shown in Fig. 8 for PZ-I.

The first high intensity earthquake motion applied to PZ-III is shown in Fig. 3.17. from which it may be seen that the peak table acceleration was 0.69 g. The acceleration response of this flanged model is shown in Fig. 3.18; the increased acceleration at the successively higher floor levels is due mainly to base rotation associated with uplift of the lower wall panel from the foundation walls, as was true for specimen PZ-I. The uplift displacements

measured at three locations across the base width are shown in Fig. 3.19. These plots show that the cyclic motions are supplemented by two major permanent offsets occurring at about 3 and 16 seconds from the start. It is probable that both yield elongation of the reinforcing bars and the presence of crushed concrete in the uplift crack prevented the return of the wall to its original level after these displacements. The reinforcing bar strains shown in Fig. 3.20 are consistent with the uplift history described above. All three main bars exhibit major yielding at 3 and 16 seconds; on the other hand an adjacent vertical panel bar shows only elastic strains.

3.6. Summary of Shaking Table Test Observations

(a) These tests demonstrated that seismic inputs with accelerations as large as 0.22 g or 0.18 g could be resisted without any apparent damage to the three-storey test specimens with and without flange walls, respectively, at the ends of the main shear wall. In these tests there was no visible evidence of either of the most likely types of displacement at the horizontal joints of the shear wall - uplifting associated with overturning moments or sliding associated with horizontal shear forces.

(b) When the shaking table motions were increased by factors between three and four, significant damage to the base joints of the models was observed. Yielding of the vertical reinforcing bars at the two sides of the model's base joints allowed rocking motions to develop. The uplift associated with this rocking and pivoting about the opposite end of the base joint was the dominant deformation mechanism; very little horizontal shear displacement was found at the base of either model.

(c) Even though some of the vertical reinforcing bars ruptured and there was some crushing damage to the concrete at the two ends of the base joints, both models were able to support the large static vertical loads after the table motion stopped; in fact, each model survived a severe "aftershock" test without any danger of collapse.
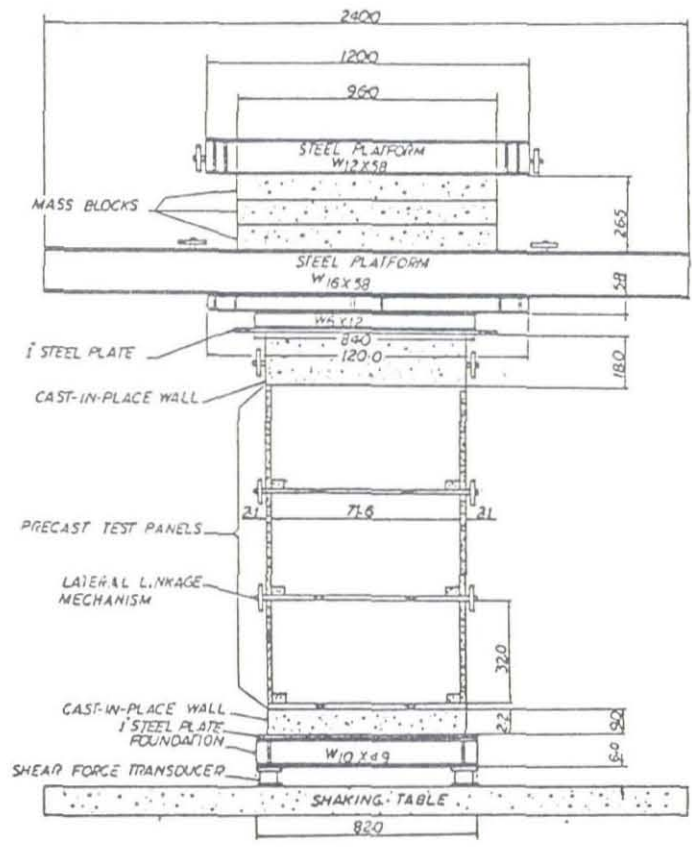
Fig. 3.1.   Front Elevation of the Test
Specimen Layout
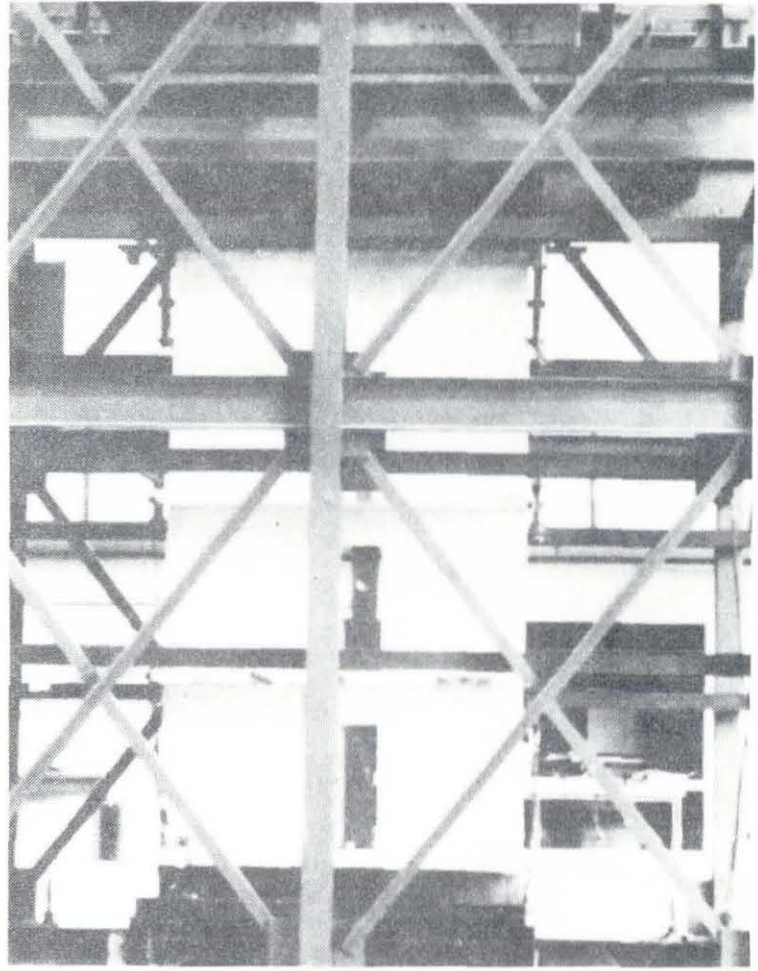
Fig. 3.2.   Front Elevation of Specimen PZ–II
Seen Through Test Fixture
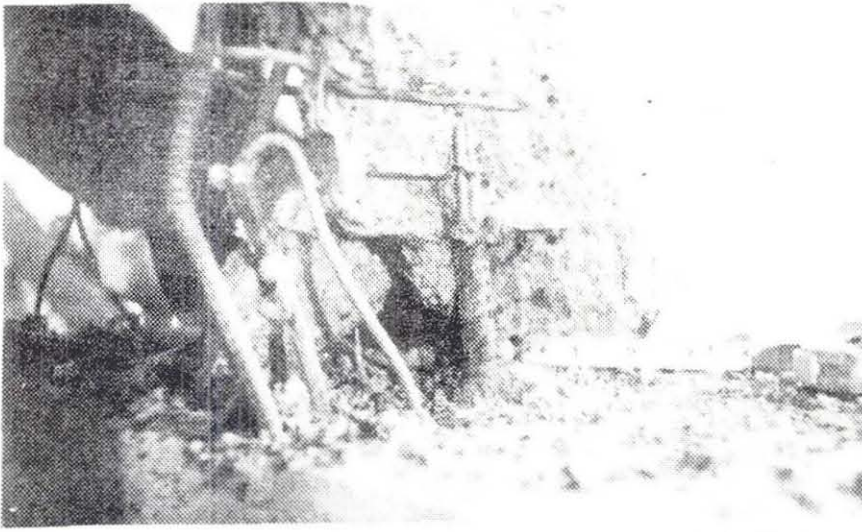
Fig. 3.3. Specimen PZ–I
Damage at SE Corner
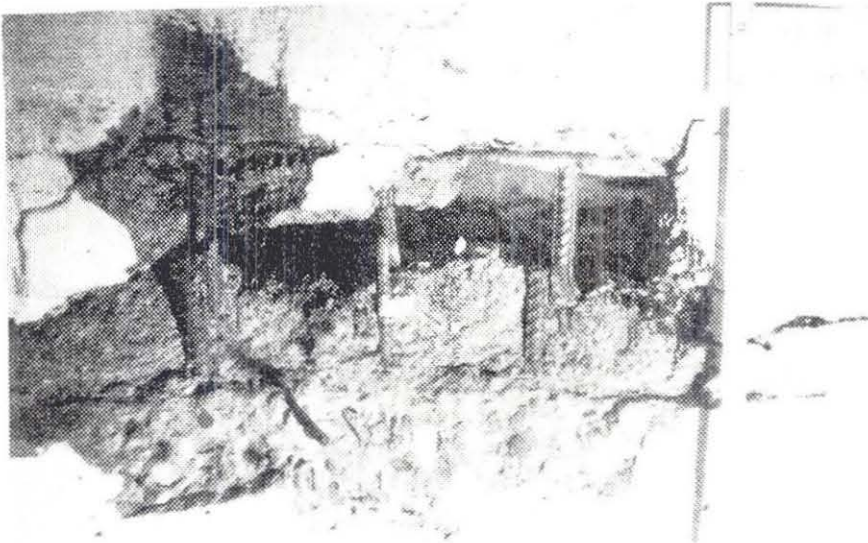
Fig. 3.4. Specimen PZ–III
Rebar Failure at South Flange
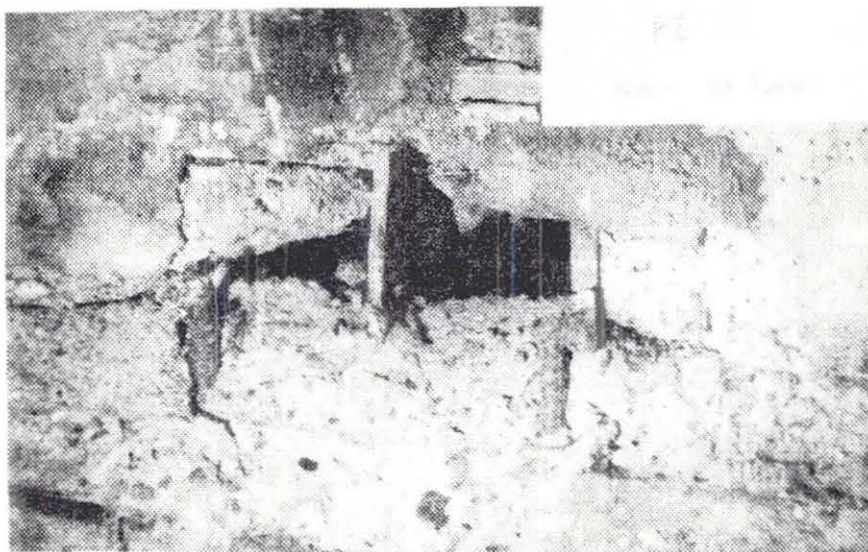
Fig. 3.5. Rebar Failure at North Flange
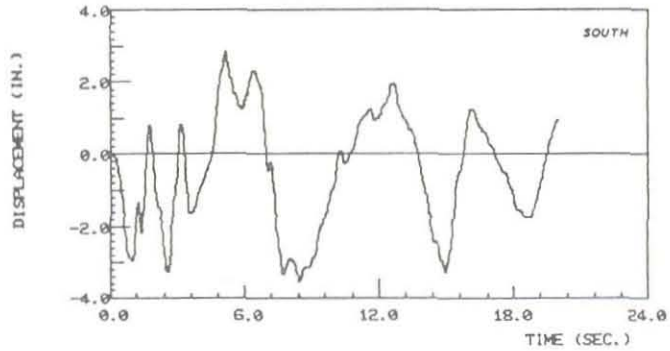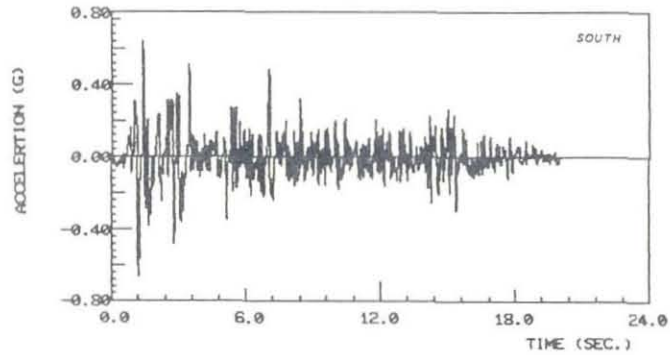
Fig. 3.6. Horizontal Displacement and Acceleration of the Shaking Table (EC–150, 0.18 g)
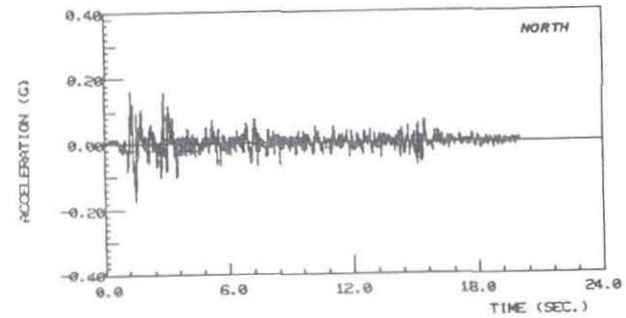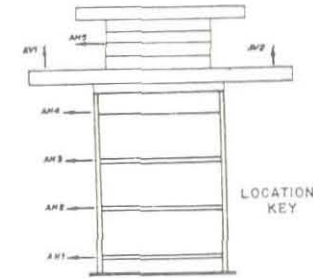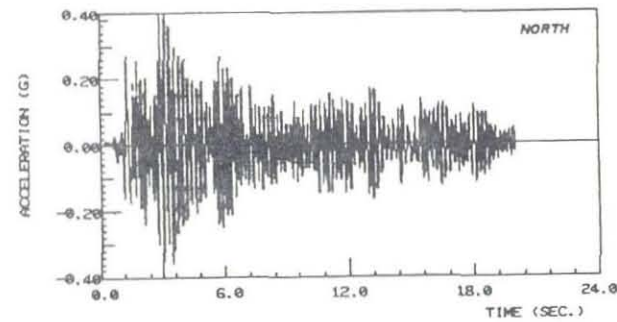
Fig. 3.7. Accelerations at Different Locations, Simple Wall, EC–150, 0.18 g

BASE SHEAR — TOP DEFLECTION

PZ-I (EC-150)
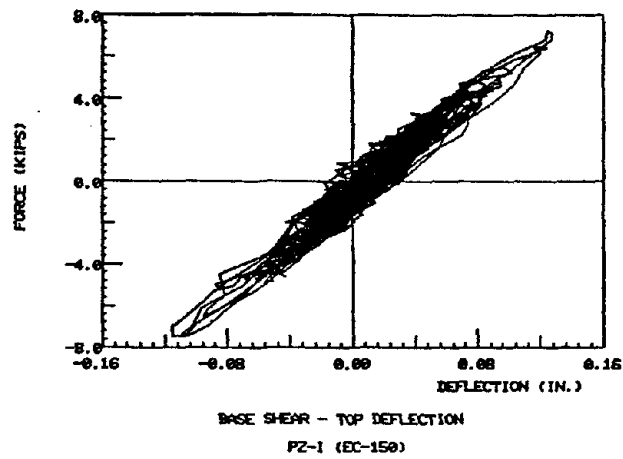
Fig. 3.8. Overall Behaviour of the System, Simple Wall, EC—150, 0.18 g, Top Deflection and Simulations Base Shear

TABLE DISPLACEMENT

PZ-I (EC-700)

TABLE ACCELERATION

PZ-I (EC-700)
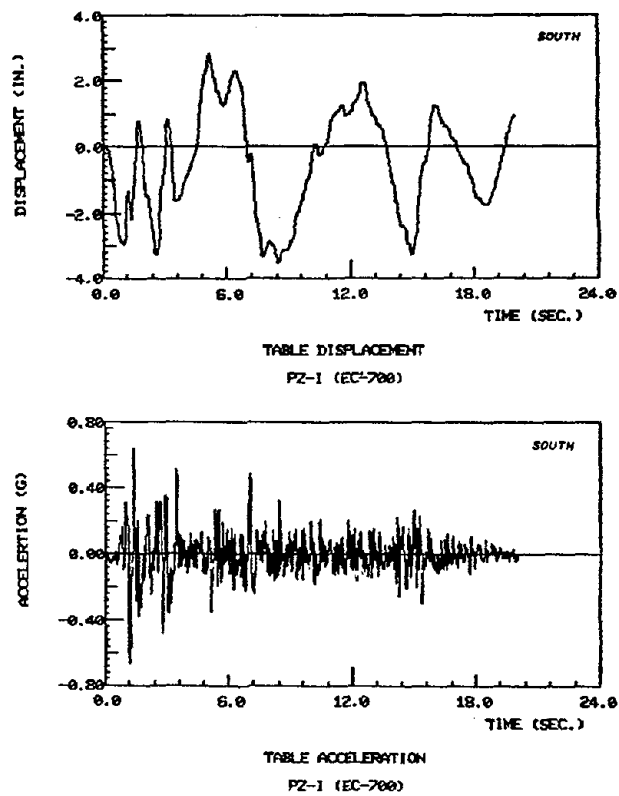
Fig. 3.9. Horizontal Displacement and Acceleration of the Shaking Table, Simple Wall, EC—700, 0.67 g.
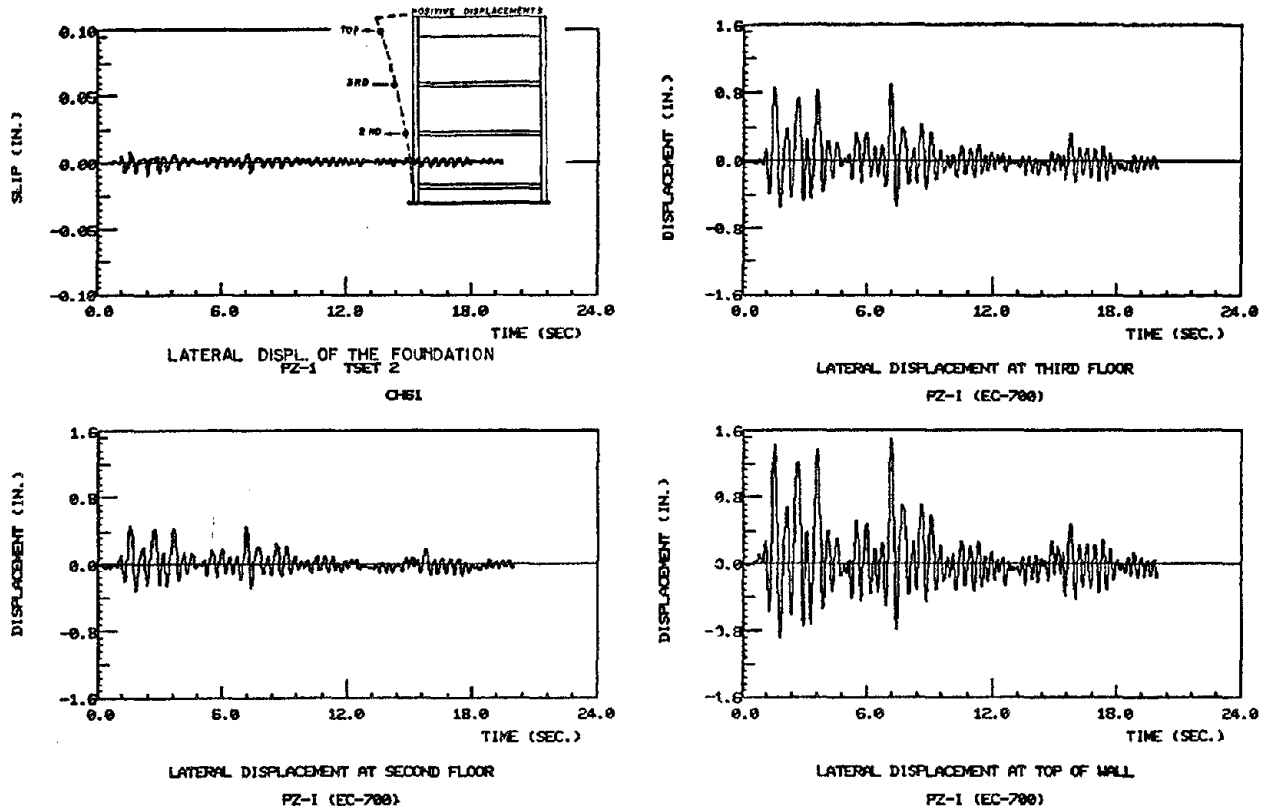
Fig. 3.10.   Relative Lateral Displacements, Simple Wall, EC—700, 0.67 g.
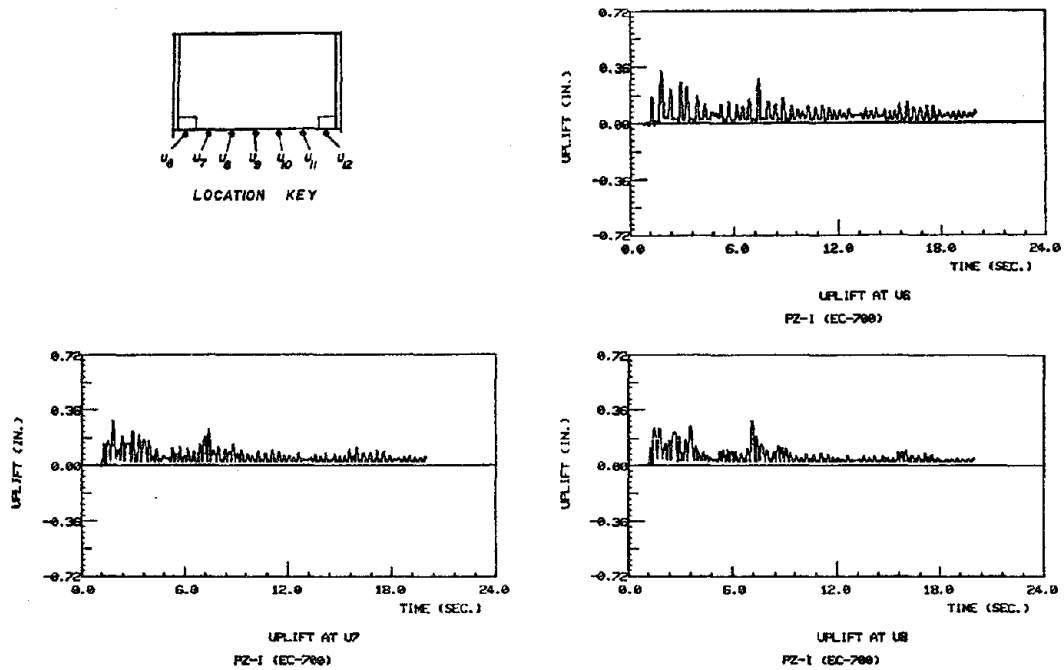
Fig. 3.11.   Lower Panel Uplift, Simple Wall, EC—700, 0.67 g.
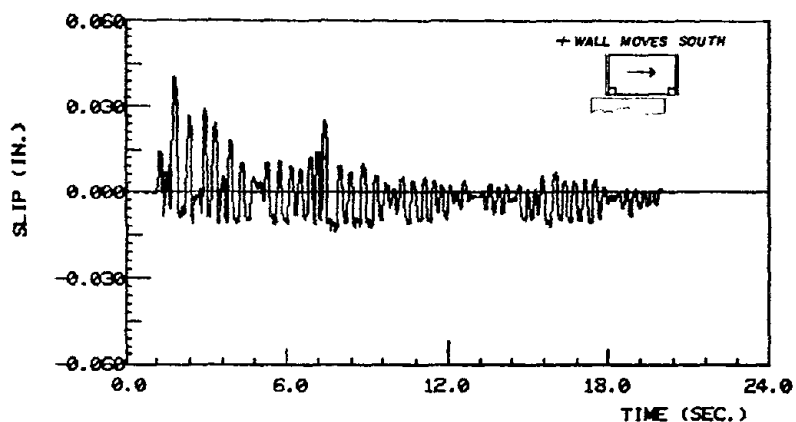
SHEAR SLIP AT BASE OF WALL
PZ-I (EC-700)

Fig. 3.12.   Shear-Slip at Base of the Precast Wall,
Simple Wall, EC—700, 0.67 g.
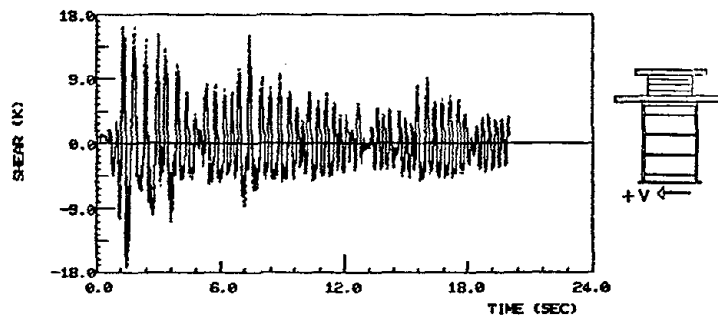
PZ-1 TEST 2
SOLID= TRANSDUCER SHEARS, DASH= INERTIAL SHEARS

PZ-1   TEST 2
SOLID= TRANDUCER SHEARS, DASH= INERTIAL SHEARS

———————— = experimental results
- - - - = computed, from Eq. 2 of Figure 7.6

Fig. 3.13.   Comparison Between Computed Inertial and Experimentally
Measured Base Shear, Simple Wall, EC—700, 0.67 g.

BASE SHEAR
PZ1 TEST2

DISPLACEMENT- TOP OF WALL
PZ1 TEST2

UPLIFT AT SOUTH END
P1 TEST2
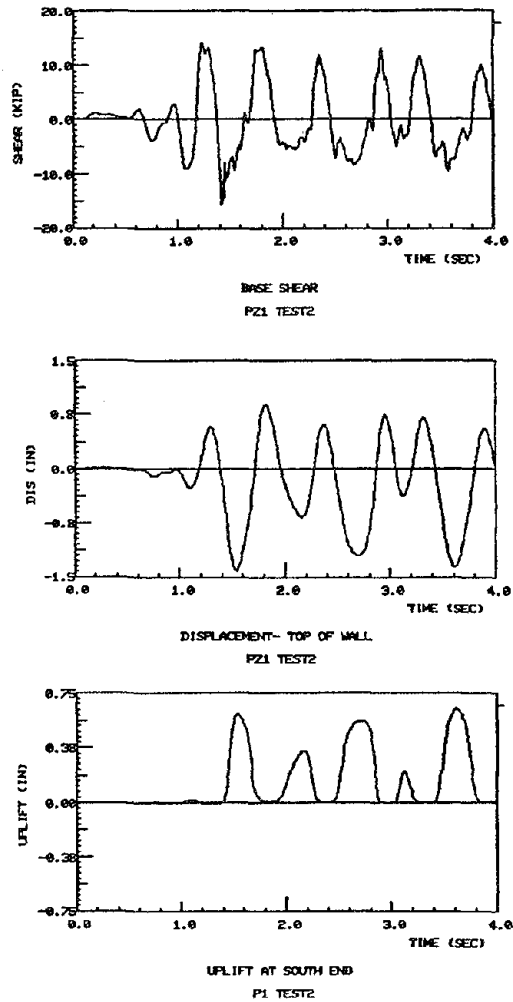
Fig. 3.14. Response During Initial Four Seconds

BASE SHEAR - TOP DEFLECTION
PZ-I (EC-700)

BASE SHEAR - TOP DEFLECTION (1ST 2 SECONDS)
PZ-I (EC-700)
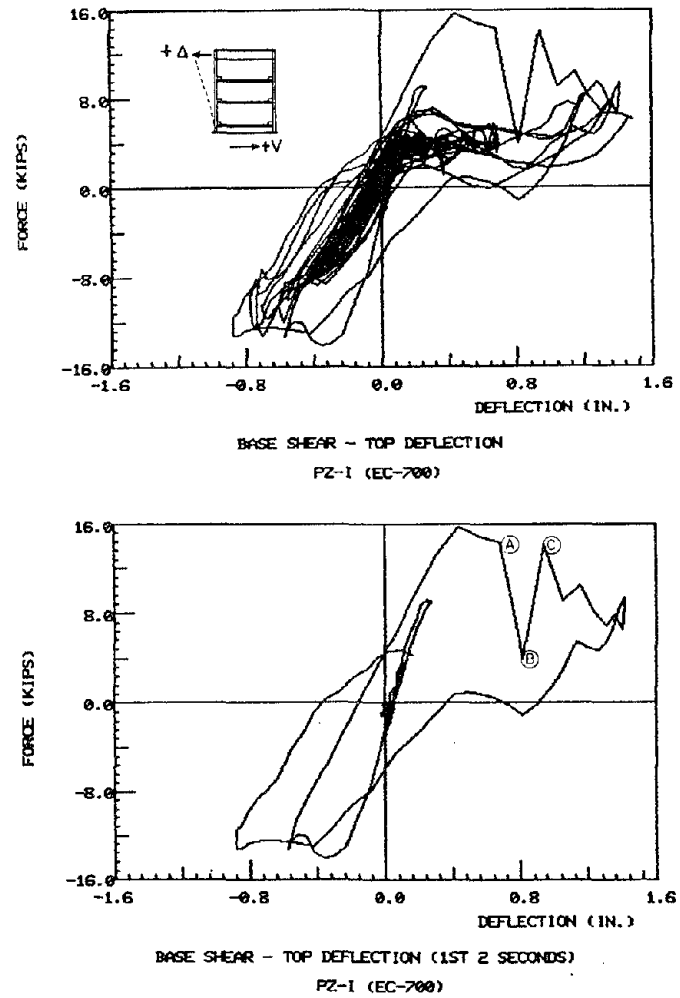
Fig. 3.15. Overall Behaviour of the Wall,
Simple Wall, EC—700, 0.67 g.
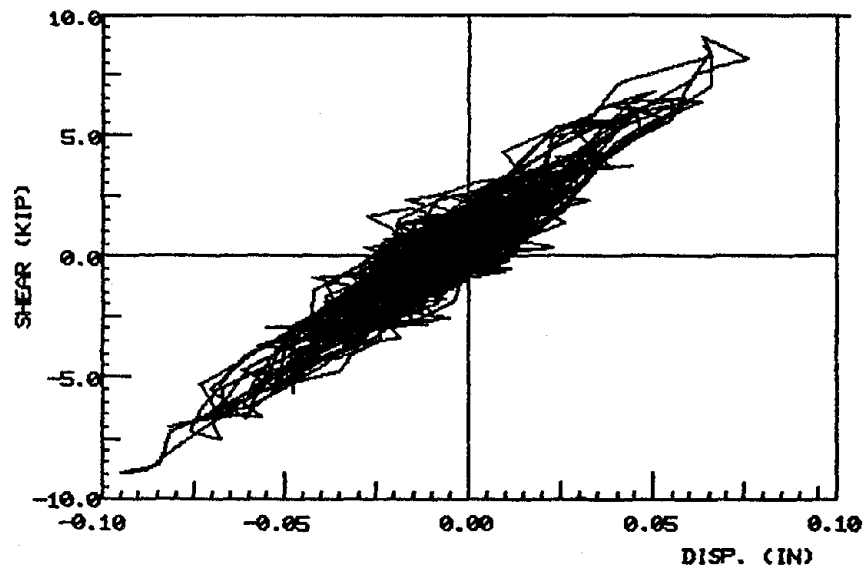
Fig. 3.16.   Base Shear and Top Displacement,
Flanged Wall EC—200, 0.22 g.
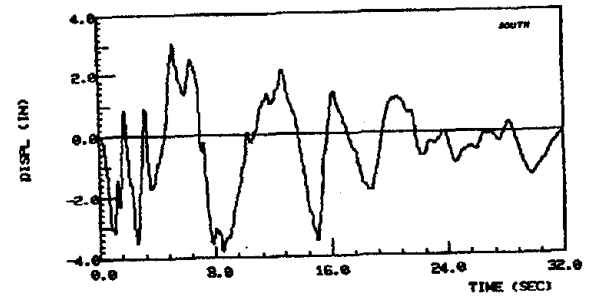
HORZ TABLE DISPLACEMENT
PZ3 T2 250383.03 CH0
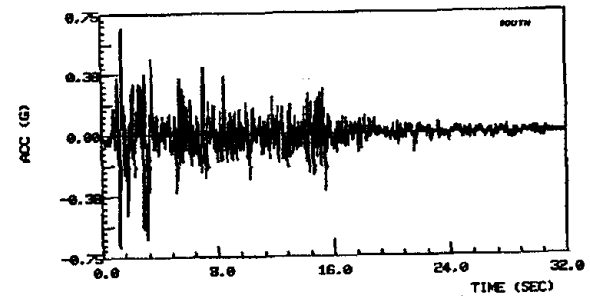
HORZ TABLE ACCELERATION
PZ3 T2 250383.03 CH2
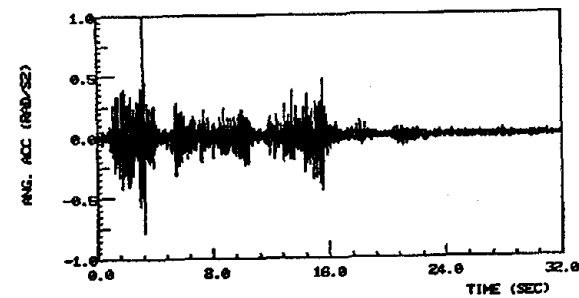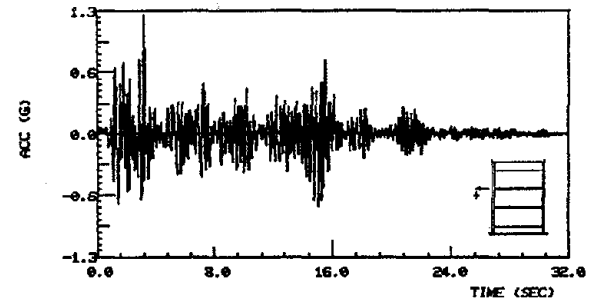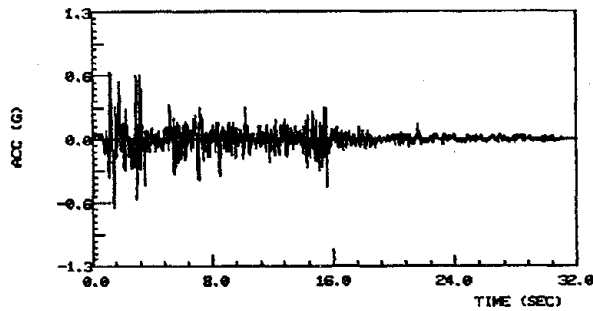
TABLE PITCH ACCELERATION
PZ3 T2 250383.03 CH4
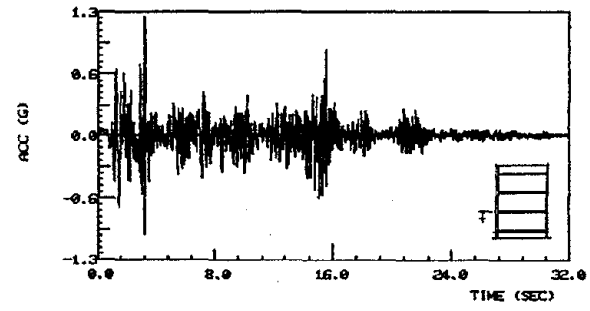
Fig. 3.17.   Table Motion, Flanged Wall, EC—750, 0.69 g.

Fig. 3.18. Story Accelerations, Time Histories, Flanged
Wall, EC–750, 0.69 g.
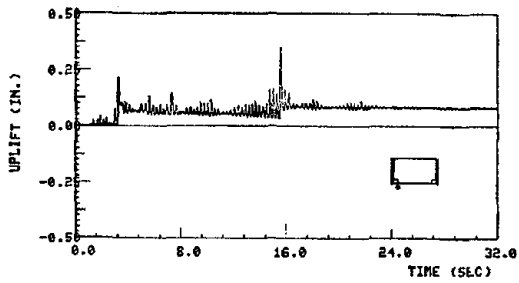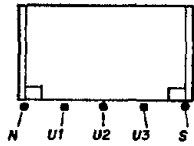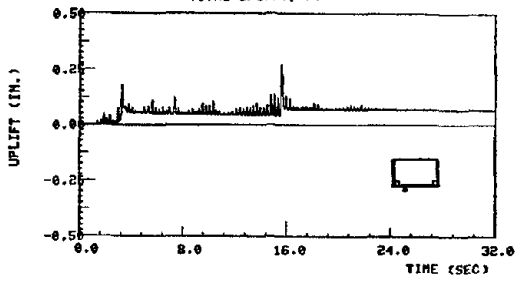
Fif. 3.19.   Uplift of the Lower Web Wall,
Flanged Wall, EC—750, 0.69 g
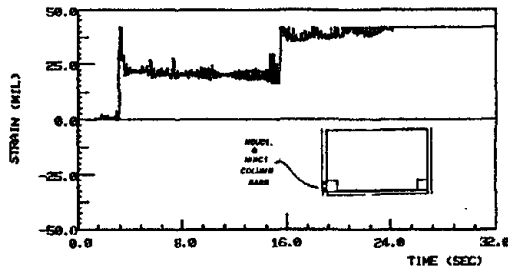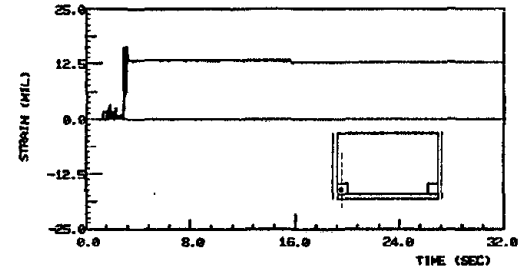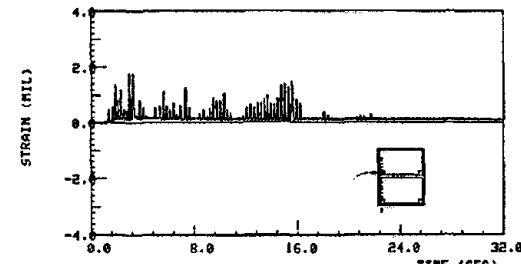
Fig. 3.20.   Reinforcing Bar Strains at North End of the Wall,
Flanged Wall, EC—750, 0.69 g. .

4. CORRELATION OF SHAKING TABLE AND PSEUDOSTATIC TEST RESULTS

4.1. Similarity of Test Models

The test specimens used in the static and shaking table tests were nearly identical. All of the precast elements were fabricated by the RAD Construction Company in Belgrade and shipped to the two laboratories where their assemblage and testing were completed. Minor differences existed in the strengths of materials in the specimens, in the means of applying load at the top of the specimens, and in the orientation of the walls during testing.

The cast-in-place concrete used to join the precast panels was designed to similar specifications and used similarly graded aggregate. The compressive strengths of the joint material in the static and shaking table tests differed slightly because of differences in the materials used and age at testing. The areas and strengths of reinforcing bars used in the cast-in-place joints also differed because of basic differences in the properties of the steel bars obtained in the two testing locations. The overall effects of these variations appear to be minor. Properties of the materials used in the static and dynamic tests are compared in Table 4.1.

A second difference in the static and shaking table specimens resulted from the boundary condition which was provided at the top of the three-storey model. A cast-in-place top beam was used in the static test and a cast-in-place wall element was used in the dynamic test with additional steel members above as portrayed in Fig. 4.1.

The remaining difference was in the orientation of the walls during testing. The static walls were tested in a horizontal position to allow convenient anchorage of the foundation and the actuator reaction blocks to the laboratory test floor. The shaking table specimens were tested in their natural

vertical position. The orientation of the specimens may have had an effect on their behaviour as noted below in the comparison of their stiffness variation.

4.2. Similarity of Test Loading

The static walls were loaded by applying a controlled series of cyclic displacements to the top of the wall. The displacements included complete reversals and were intended to simulate the range of displacements which might occur during an earthquake. The shaking table tests used ground motion records which were derived from historical earthquake accelerograms. The actual loads and displacements developed during the shaking table tests were dependent on the ground motion, the instantaneous stiffness and damping of the structural system, and the preceding response history.

The location of the resultant lateral load or lateral inertial force differed slightly in the static and dynamic tests. The lateral load was applied through an actuator in the static tests at a constant distance above the specimen base. Data indicated that the resultant inertial load in the shaking tests, due to the distributed mass, remained at a fairly constant distance above the specimen base but differed from the location in the static tests by a factor of 1.8.

Axial load was applied to the static test specimens through two hydraulic actuators operated under force control at the top of the specimen. The actuators maintained a constant axial load independent of the lateral motion. Axial load was provided in the shaking table tests by the added mass system at the top of the structure. The axial load applied in the static tests was calculated for the wall specimens based on their cross section areas to provide a constant axial stress of 0.80MPa (114 psi). The total axial load acting on the two shaking table specimens was equal, resulting in an axial stress of 0.96

MPa (146 psi) in the simple wall and 0.66 MPa (96 psi) in the flanged wall. The differing axial loads in the static and shaking tests has a slight influence on the yield force levels and on the gravity restoring moment as described in a following section.

4.3. Comparison of General Response

The static and shaking table specimens all exhibited similar visually detectable damage. Damage included opening of the lower level horizontal joint, yielding and subsequent buckling of vertical reinforcing through the joint, spalling of concrete adjacent to the buckled bars, rupture of some vertical reinforcing bars through joints, crushing of concrete and limited formation of combined flexural-shear cracks in the precast panels. These types of damage may be noted and compared in Fig. 4.2 for specimens tested under both types of loading.

The horizontal joint between the panels, having less vertical reinforcing than the panels themselves and a precracked plane as well, was the location of concentrated inelastic deformations and damage in both test series. The damage in the gradually deformed static specimens started with cracking of the horizontal joint followed by limited cracking of the panel in a manner which would result from combined flexural tension and shear stress at the tension ends of the panel. The horizontal joint opened and a gap formed at the tension ends as the lateral top deformations increased. Gap opening was accompanied by yielding of the tension steel across the joint and subsequent buckling when the top displacements were reversed. Combined steel buckling and compression forces in the concrete caused the concrete in the vicinity of the buckled bars to spall or crumble away. Further loading caused rupture of some of the vertical joint reinforcing. The exact sequence of damage formation could not be followed

during the shaking table tests on account of their short duration, but the observed damage was consistent with a process similar to that recorded in the static tests.

Damage in the dynamic tests was generally not symmetrical since the top displacements did not have equal complete reversals as they did in the static tests. Once damage develops at a particular location during dynamic tests, further motion tends to compound the inelasticity within that region since the motion which occurs subsequently depends on the remaining force capacity of the damaged region and the instantaneous structural characteristics of the system. Though similar damage occurred in both test series the shaking table tests resulted in unsymmetrical damage because of unsymmetry of the earthquake motions.

The overall behaviour of both systems was characterized by a rocking of the three precast panels at the lower horizontal joint. Shear slip was effectively limited during most of the tests by cast-in-place keys at the ends of each joint and panel. Specific values of various force and displacement quantities are compared in Table 4.2 for the two test series.

4.4. Specific Behaviour Characteristics

The two basic mechanisms of deformation in precast panel walls are often characterized as moment rocking and shear-slip. The features of each of these two types of mechanisms are compared here for the static and shaking table tests. The rocking mechanism was predominant in both series of tests with shear-slip having minor effects for the simple walls. Shear-slip became important with large top displacements in the static flanged wall test.

4.4.1. Moment and Rocking

The location of the resultant lateral forces differed in the static and shaking tests but rocking motion is primarily a result of the moment at the base of the structure. The comparison of rocking behaviour in the two test series will not be affected by the differing moment arms to the lateral forces since moments are used as the basis of comparison. The primary characteristics of structural response to earthquake motion - strength, stiffness, deformability, and energy dissipation noted in the test series are discussed.

The overall load resisting quality of the systems and strength capacity are shown in the envelope of the moment vs. top displacement response plotted in Figs. 4.3 and 4.4. The overall agreement between the envelope obtained from the static tests and shaking table tests is very good indicating that both tests provide similar information regarding the overall strength, strength deterioration and stiffness of the wall systems. The primary difference in the envelopes is a result of the unsymmetric deformation which develops in the dynamic tests. The capacity deterioration seen in the envelopes is a result of rupture of continuous vertical steel through the lower horizontal joint and to a lesser extent due to deterioration of the concrete at the ends of the lower horizontal joint. The displacement at which the rupture occurred was controlled by the method of connecting the vertical panel reinforcing which was made continuous through the joints. The rupture displacement level was reduced in these tests as compared with typical field construction performance because the bars used in the tests were connected by welding which resulted in embrittlement that would not develop with the connections normally used. Both types of tests showed very similar rupture levels or welded bar capacity. The level at which strength deterioration occurs will differ for other connecting methods.

Rupture of some of the vertical through joint reinforcing led to the development of major rocking in both test series. Rupture of the continuous panel bar occurred with large displacements and gap openings. The remaining bars had yielded and considerably elongated. On subsequent cycles they provided no restraint against rocking until displacements reached levels near to their previous maximums. Until these bars became active again the only restoring force in the rocking mechanism was provided by the axial gravity load which remained constant as displacement increased. The amplitude of the rocking was effectively limited by the cyclic reversing nature of the earthquake ground motion in the shaking table specimens and the applied displacement in the static tests. Both test series exhibited nearly unrestrained deformation with rocking after bar rupture occurred. The effect of the varying moment-rocking stiffness and of the constant restoring force was to act as a load limiting mechanism ending the spread of inelastic deformation upward in the wall system.

The varying stiffnesses of the moment-rocking mechanism of the simple wall are shown in Fig. 4.3 for both test series, with the near perfectly plastic condition created by rocking apparent. An excellent agreement in behaviour and stiffness is exhibited by the hysteresis loop envelope of the static test and the first major response cycles of the shaking table tests. Rupture of the continuous panel bar occurred in the static tests during the 17th cycle of loading when top displacement reached 21.5 mm (0.85 in.). A similar rupture occurred during shaking table tests at 1.42 seconds during the second cycle of major yielding with a displacement of 15 mm (0.59 in.). Both tests show a significant loss of strength and stiffness after the rupture. The post-rupture hysteresis plots from the shaking table test clearly show the rocking phenomena and load limiting behaviour with increasing negative displacement. The moment level at which nearly zero stiffness elastic deformation starts is consistent

with rocking of the wall and an axial load restoring force. Upon reversed deformation the shaking table test elastically follows the zero stiffness loading path until the section closes and rocking ceases. The stiffness variation apparent in the static test result is significantly different after the tension bar ruptures and rocking occurs. The low stiffness under increasing deformation is apparent as in the shaking tests. However, when the deformation is reversed, the wall does not unload elastically as in the dynamic test. The moment becomes negative before displacements return to the level at which the low stiffness rocking started. It is believed that the rapid drop in moment at displacement reversal may be a result of loose concrete material becoming lodged within the gap which had slowly been opened during loading, providing an immediate low compression capacity and reversed moment when the gap begins to close. This difference from the dynamic tests behaviour may have occurred because the static specimens were tested in a slow manner and in a horizontal position.

The moment rocking mechanism's stiffness in the flanged wall tests also was studied, and the static and dynamic test results showed very similar characteristics in the initial load cycles before rupture. Both of the walls appeared to sustain rupture of some of the tension bars in a nearly identical fashion when the top displacements exceeded 15.00 mm (0.60 in.). However, the response after rupture was completely different in the two test series. The shaking table test had an apparent rupture (detected by strain gauges) of the north web panel bar at 16 seconds into the earthquake record. The displacements at the early peaks were not sufficient to cause rupture like that seen in the simple wall (0.7 in. vs 1.3 in.). Only a single large displacement occurred following the rupture, thus the load limiting and rocking noted in the simple wall test did not have an opportunity to develop in the flanged wall. The

static tests showed the low stiffness load limiting behaviour during displacement cycles beyond the rupture level. More bars ruptured in the positive displacement direction than in the negative producing unsymmetrical hysteretic behaviour. In this static case the low stiffness was not a result of rocking but of shear-slip and is discussed in the following section.

The deformability produced in each of the test series was nearly identical. The maximum displacement as a percentage of the yield displacement, for each wall is listed in Table 4.1. Structural ductility is normally determined by comparing the displacement at maximum load capacity to that at yield. The ductility determined in such a manner would have little meaning for these tests since the load capacity was limited by the capacity of welded reinforcing bars in the panel to panel connection. In actual construction practice other means of connection are used to avoid the brittle fracture of welded bars. The large deformability and load limiting behaviour of the horizontal joint prevented serious inelastic damage from spreading upward into the remainder of the structure. The large deformability with rocking allowed the walls to withstand a strong seismic load but is dependent on maintaining stability out of the plane of the walls. That stability was provided in the tests by the configuration of the loading fixtures.

The wall's energy dissipation capacity always appeared larger in the static tests than in the shaking table tests. Two explanations may be made for this deviation in behaviour. The deformations applied in the static tests were achieved in a very slow manner. The structural system appeared to take advantage of the slow test rate and redistributed the forces and deformations slightly so that less concentration of deformation at a specific point may have occurred. Second, the hysteresis loops of Fig. 4.4 after rupture appeared larger for the static tests than for the dynamic because debris may have

accumulated in the open horizontal joint of the static test. This material initially tended to resist gap closing until it crushed and energy was dissipated. The shaking table test showed little energy dissipation during the elastic bi-linear deformation with negative moment and rocking. Energy dissipation in this type of jointed structure is naturally lower than in well-reinforced monolithic structures since deformations are concentrated in a small volume of material within the joints. It is important to note, however, that the energy dissipation may not be essential since acceptable deformability was available during all the tests.

4.4.2 Shear-slip Mechanism

The shear-slip mechanism had very little effect on the system behaviour in all of the tests on the simple walls. Slip accounted for less that 7% of the total maximum top displacement in those tests. The shear-slip mechanisms in the flanged walls differed significantly between the static and shaking table tests. Slip contributed 6.3% of the top of wall displacement in the shaking table test with moment-bending being the dominant behaviour. Slip made up nearly 75% of the total maximum top motion during static tests on the flanged wall. The statically tested flange wall developed significant plastic displacement, rupturing, and buckling of the through joint reinforcement at each end of the web and flanges due to the large applied displacements and full reversals. The buckled steel caused spalling of concrete in the flanges near the horizontal joint and substantially reduced the shear capacity of the system. The steel deformation which developed in the shaking table tests occurred primarily at one end of the wall allowing the full joint and key mechanism at the other end to remain effectively intact. As a result this intact joint maintained the restraint against slip.

4.5. Summary of the Correlation between Shaking Table
and Pseudostatic Test Results

The tests of each type of wall exhibited similar damage in the systems regardless of whether the loading was statically applied with controlled displacements or was a result of shaking table motions. Damage invariably consisted of initial cracking at the lower horizontal joint between cast-in-place concrete and the vertical panel above. Continued increase in the top displacement of the walls caused yielding of vertical steel across the joint, steel buckling and steel rupture with spalling of concrete in the region near the vertical bars.

The response behaviour measured in the two test series also agreed very well. The overall force capacity vs. displacement envelopes, including the bar rupture level and loss of capacity and stiffness, were nearly identical for shaking table and static tests. Bar rupture led to development of rocking motion of the precast wall system about the lower horizontal joint in all cases. The hysteresis records of base moment plotted against top displacement, before bar rupture, were quite similar. Both types of tests on the wall systems produced nearly identical deformability. Shear-slip behaviour, which was effectively limited by cast-in-place keys, was not an important mechanism in either of the tests on the simple rectangular wall and did not exceed 10% of the wall top displacement.

Three substantial differences were apparent in results from the test series under static load and dynamic load. The energy dissipation exhibited in plots of base moment vs. top displacement was consistently higher in the static tests than in cycles of response of similar amplitude from the shaking table tests. It is believed that this is partially an effect caused by the horizontal orientation of the static specimens, allowing material to become lodged within

open joints in comparison with the vertical orientation of the shaking table specimen where loose spalled materials tended to fall away from the joint. The response of the flange walls was substantially different in the static and dynamic tests. Shear-slip accounted for 75% of the top of wall displacement at the maximum deformation cycles during the static test whereas shear-slip was limited to less than 7% of top displacement in the shaking table test. The large slip in the static test occurred because several cycles of large applied top displacement created significant deterioration of the joints at the flanges and in the keys. The shaking table specimen only experienced one cycle of deformation at the maximum level of the static test and did not develop similar deterioration. A final minor difference always apparent in a comparison of the shaking table results and static test results was in the unsymmetric character of damage from one end of the wall to the other in shaking table tests. The controlled displacements of the static test invariably led to nearly symmetric damage at both ends of the wall. During shaking table tests once damage occurs at one location in a structural system the force which can be transferred through the damaged area is usually limited and the dynamic character of the system changes because of lowered stiffness. These two effects tend to cause further damage near the already damaged region with lack of symmetry developing in overall damage.

Very satisfactory agreement in results from the static and shaking table tests occurred even though minor differences existed between the boundary conditions of the walls in the two tests, in the ratios between shear, moment and axial forces existing simultaneously, in the orientation of the specimens during testing; slight differences also existed in the material strengths and in the means of applying the loads.

Table 4.1. Properties of the Materials Used in the Pseudo-Static and Dynamic Test Models

Model	Type of test	fc' — Concrete		Tensile Steel in Panels		Tensile Steel in Joints	
		Panels	Joints	Ast	Gy	Ast	Gy
PZ – I (Simple Wall)	PS – static	45.3 MPa 6.58 KSI	30.1 MPa 4.37 KSI	1.13 cm^2 0.175 in^2	385.6 MPa 56.0 KSI	1.01 cm^2 0.156 in^2	445 MPa 64.5 KSI
	Dynamic	44.7 MPa 6.49 KSI	40.0 MPa 5.81 KSI	1.13 cm^2 0.175 in^2	385.6 MPa 56.0 KSI	1.03 cm^2 0.159 in^2	443 MPa 64 KSI
PZ – III (Flanged Wall)	PS–Static	44.8 MPa 6.49 KSI	27.94 MPa 4.06 KSI	3.39 cm^2 0.525 in^2	385.6 MPa 56.0 KSI	0.50 cm^2 0.077 in^2	445 MPa 64.5 KSI
	Dynamic	45.3 MPa 6.58 KSI	40.0 MPa 5.81 KSI	3.39 cm^2 0.525 in^2	385.6 MPa 50.0 KSI	0.62 cm^2 0.096 in^2	456 MPa 66 KSI

Table 4.2. Comparison of General Response

1. Simple Test model PZ—I

Quality	Pseudo - Static Test	Dynamic Test
1. Max. Base Bending Moment	282.43 KN-m (2499 IN-K)	397.3 KN-m (3516 IN-K)
2. Max. Shear Force	99.30 KN (21.89 KIPS)	70.7 KN (15.6 KIPS)
3. Applied Axial Stress	0.806 MPa 116 PSI	0.96 MPa 146 PSI
4. Max. Top Displacement	36 mm (1.41 IN)	37.6 mm (1.48 IN)
5. Top Displacement at the Time When Tensile Bars Ruptured	21.5 mm (0.85 IN)	23.03 mm (0.59 IN)
6. Bar Opening as a % of Top Displacement at Time of Rupture	34.4% at $\Delta T = 21.5$ mm ($\Delta T = 0.85$ IN)	3.47% at $\Delta T = 37.6$ mm ($\Delta T = 1.48$ IN)
7. Average Shear Stress at Time of Max. Shear Force	0.96 MPa (146 PSI)	0.68 MPa (104.0 PSI)
8. Shear Slip in % of Top Displacement at Specific Point	5.58% at $\Delta T = 21.5$ mm ($\Delta T = 0.85$ IN)	0.27% at $\Delta T = 37.6$ mm ($\Delta T = 1.46$ IN)

Table 4.2. Comparison of General Response
(Continuation)

2. Flanged Test model PZ – III

Quality	Pseudo - Static Test	Dynamic Test
1. Max. Base Bending Moment	485.63 KN-m (4300 IN-K)	458 KN-m (4056 IN-K)
2. Max. Shear Force	163.5 KN-m (36.04 KIPS)	97.4 KN-m (21.5 KIPS)
3. Applied Axial Stress	0.80 MPa 116 PSI	0.66 MPa 96 PSI
4. Max. Top Displacement	22 mm (0.86 IN)	40.6 mm (1.60 IN)
5. Top Displacement at the Time When Tensile Bars Ruptured	16.6 mm (0.65 IN)	15 mm (0.59 IN)
6. Bar Opening as a % of Top Displacement at Time of Rupture	40% at ΔT = 8 mm (ΔT = 0.32 IN)	45% at ΔT = 20.3 mm (ΔT = 0.8 IN)
7. Average Shear Stress at Time of Max. Shear Force	1.08 MPa (156 PSI)	0.64 MPa (93 PSI)
8. Shear Slip in % of Top Displacement at Specific Point	17.2% at ΔT = 11.6 mm (ΔT = 0.47 IN)	0.04% at ΔT = 40.6 mm (ΔT = 1.6 IN)
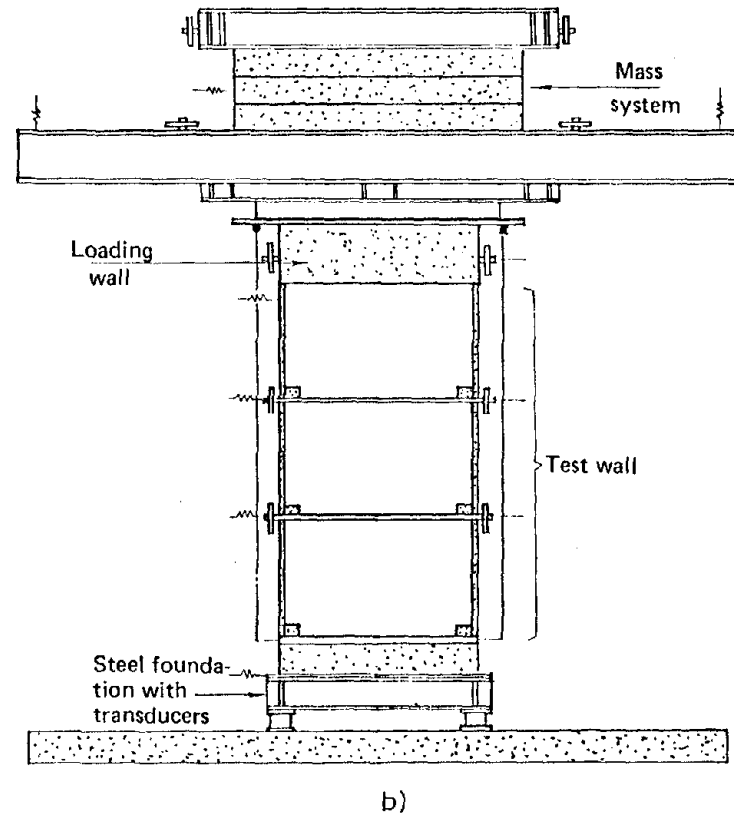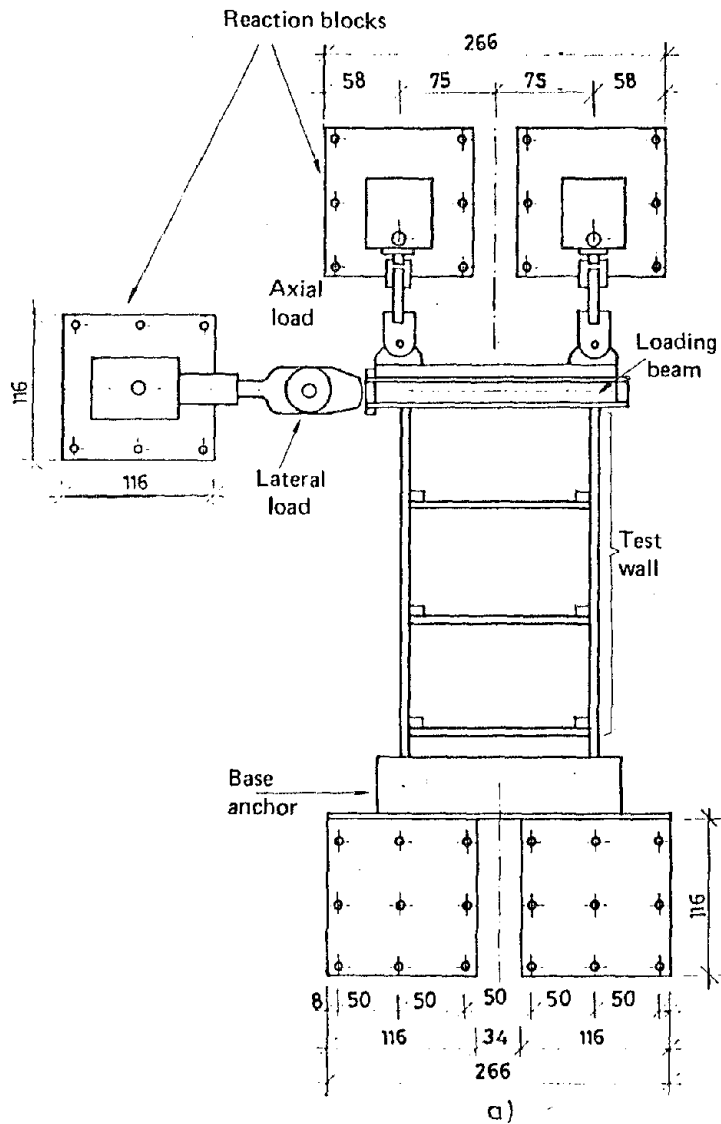
Fig. 4.I. Configuration of Test Systems
a) Pseudostatic IZIIS Test
b) Shaking Table EERC Test
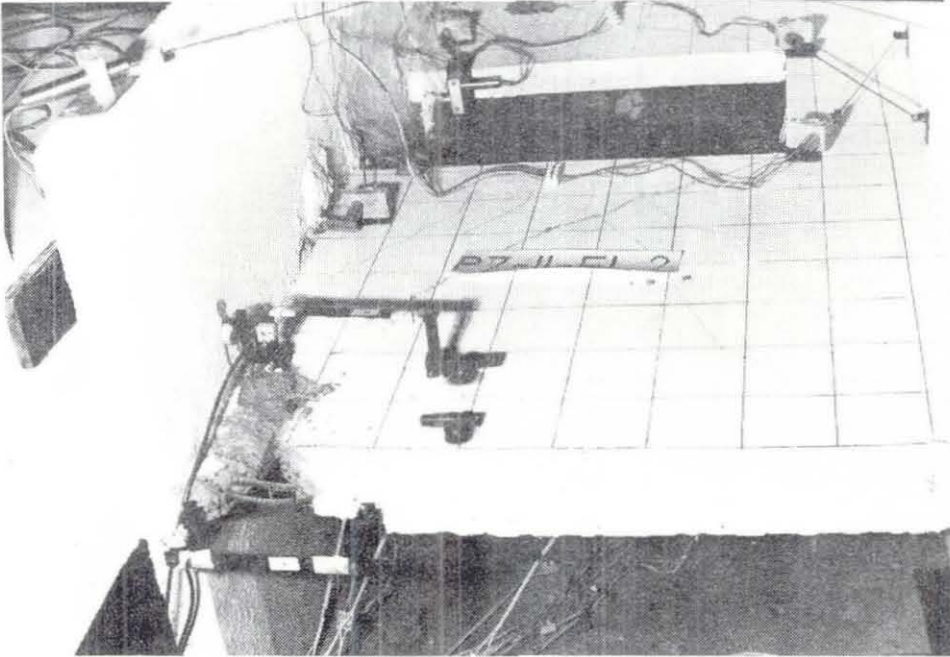
a)
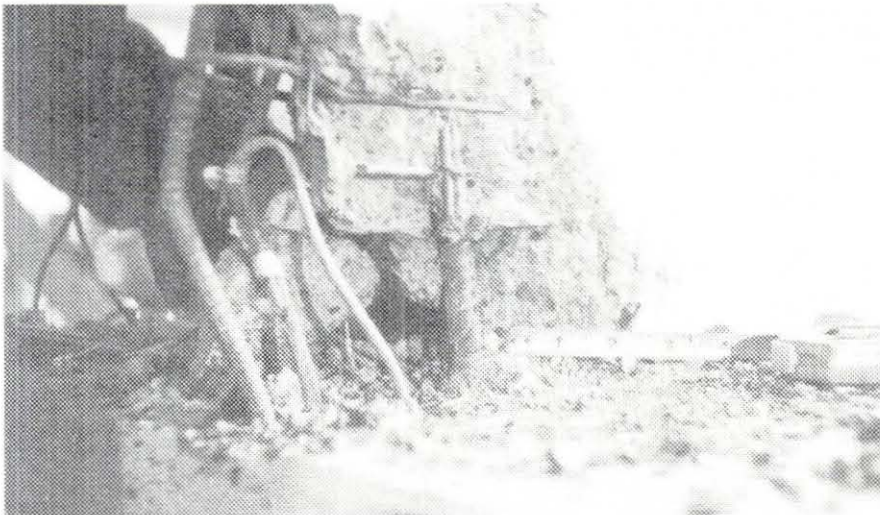
b)

Fig. 4.2. Wall Damage at End of Wall
a) IZIIS –Test, b) EERC – Test
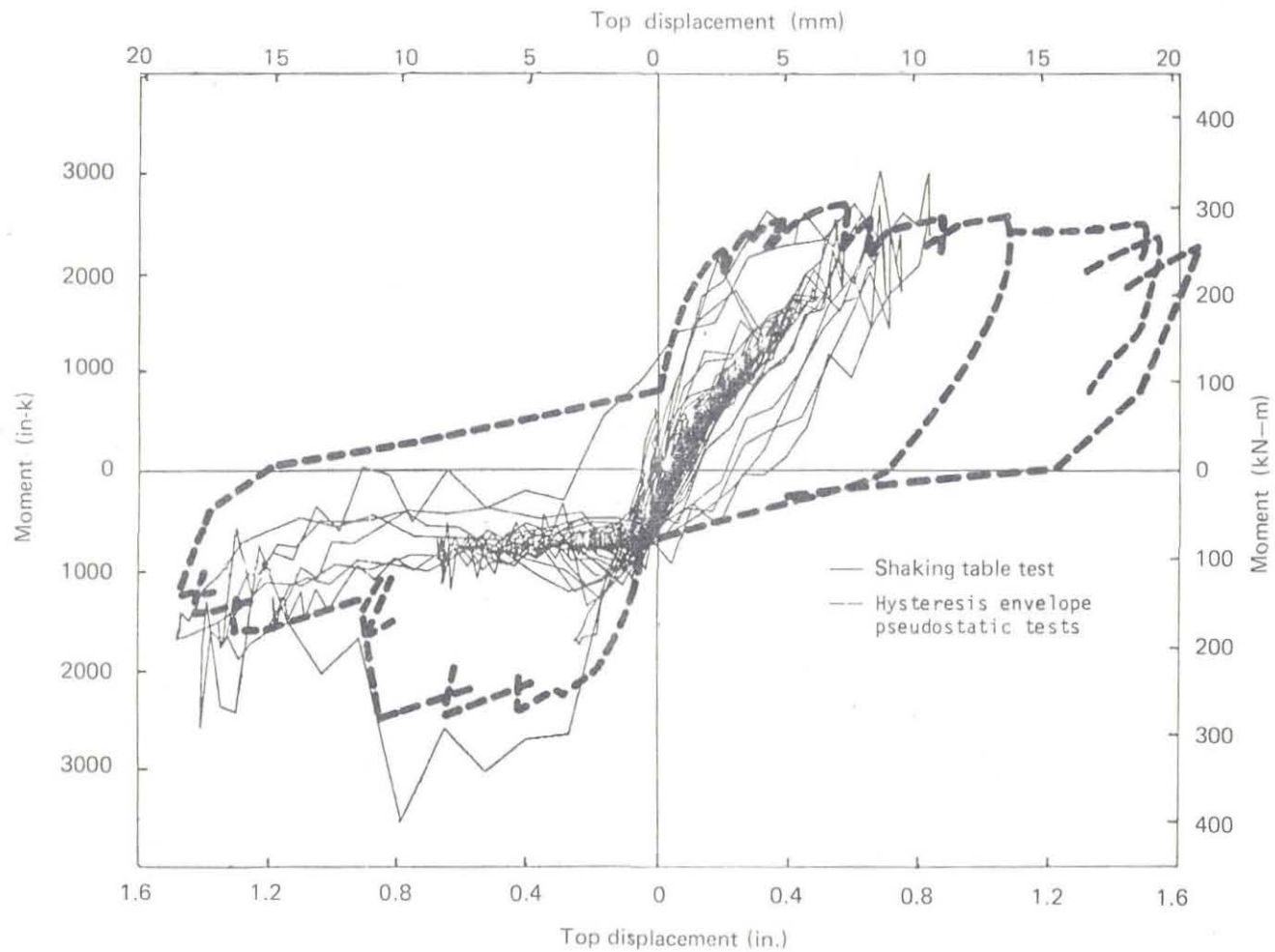
Fig. 4.3. Top Displacement - Base Moment
PZ−I, Test 2.

Top displacement (mm)

Moment (in-k) / Moment (kN-m)

— Shaking table test
—— Hysteresis envelope
pseudostatic tests

Top displacement (in)
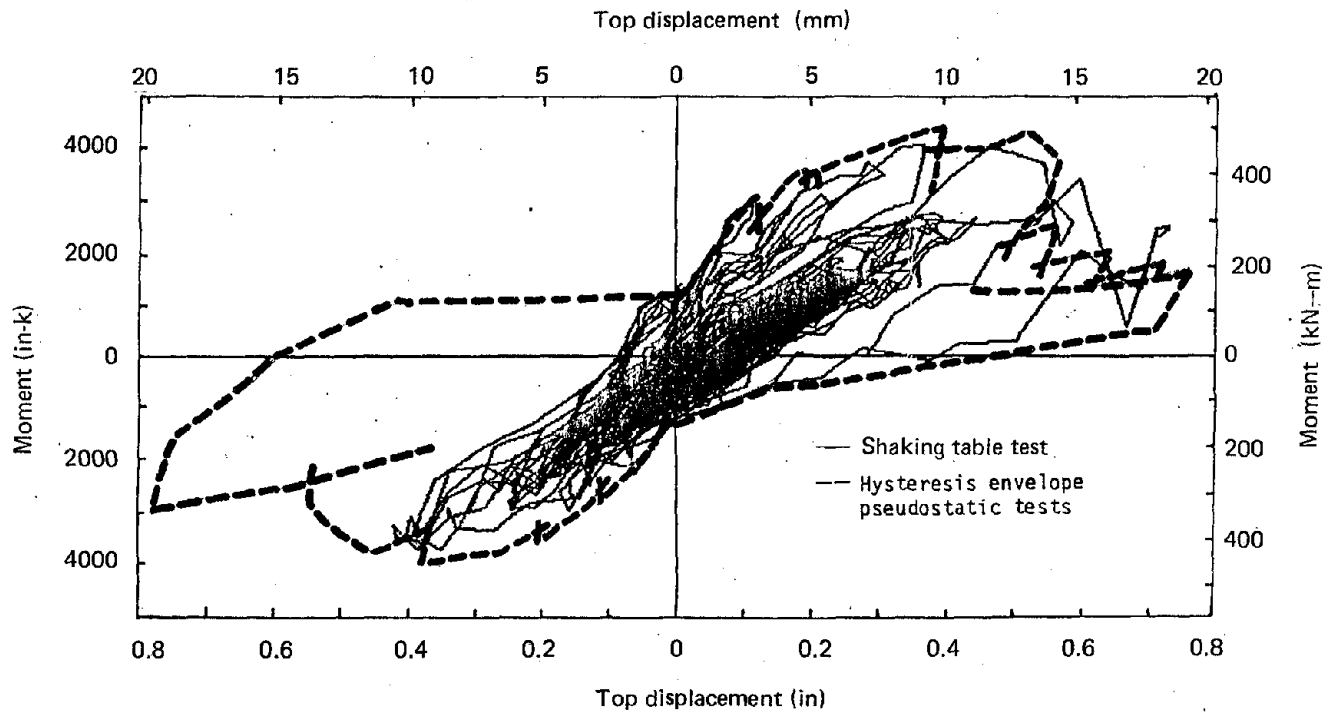
Fig. 4.4.   Top Displacement - Base Moment
PZ–III, Test 2

5. ANALYTICAL CORRELATION STUDY

5.1. Introduction

Extensive computer aided analytical studies have been completed at the University of Wisconsin using the data from the shaking table tests to verify analytical methods [7,8,9]. The analytical vs. experimental correlation studies determined the essential response mechanisms which have to be duplicated for a successful prediction of seismic response of precast panel walls at various levels of excitation. The results also verified the ability of current modelling and analytical techniques to simulate true structural behaviour correctly.

An assortment of existing computer programs was used and modified as appropriate during the correlation studies. The programs included RCCOLA [10] for predicting section inelastic flexural behaviour characteristics, ANSYS [11] for verifying specific finite element modelling techniques, DRAIN2D [12] for modelling the wall systems as vertical inelastic cantilever beams, and DRAIN2D-MarkII [13] a modified version of the preceding program for simulation of precast panel wall systems with inelastic response mechanisms in the joints.

The following sections describe the general methods involved in the correlation studies for the simple wall test specimen. A theoretical model is described which simulates the geometry of the simple rectangular wall in the test program. The physical properties of the wall will be related to the characteristics simulated in the analytical model. Results of various computed simulations of the wall response to the experimentally applied ground motions are presented and the effects of modelling assorted joint inelastic deformation mechanisms are discussed.

5.2. Physical Geometry of Analytical Model

The obvious primary portion of the analytical model consisted of the three storeys of precast panel walls and the cast-in-situ joints. Since out-of-plane motion was restrained in the actual wall tests the analytical approach used two dimensional simulation of the structure. Floor elements, which were included in the experimental specimens to form the horizontal joints correctly, were ignored in the analytical model. The dimensions used in the analytical model of the walls duplicated the dimension of the test specimens. The masses of the panels and joints were lumped at the joint locations to simplify the dynamic analysis.

An elaborate arrangement of steel platforms and concrete blocks was used in the shaking table tests to simulate the axial load expected in a wall system and to provide a means of preventing complete collapse of the structure onto the shaking table if instability developed. The analytical model included a lumped translational and rotational mass above the wall panel elements to simulate the added mass system. This mass was attached to the top of the wall element with rigid links.

The experimental wall panels were placed upon a relatively rigid steel member which was linked to the shaking table by load cells used to measure base shear. This system of steel member and load cells was referred to as the "foundation". The flexibility of this foundation was considered as being sufficiently large to affect the dynamic character of the complete system and was included in the analytical model. Deformations in the foundation were measured during the tests and used to calculate actual stiffness values for the foundation to be used in the analysis.

The shaking table itself has a detectable amount of pitching or rotation which develops because of structural interaction even though the command table

movement prescribes only lateral motion. This pitching becomes particularly evident when relatively rigid structures with high base moment are tested and has the effect of reducing the natural frequency of the full shaking table - structure system. The analytical model included a rigid table with rotational mass supported on rotational springs which simulated the actual pitching motion. The measured table lateral accelerations were used as the earthquake base motions in the analyses.

5.3. Behaviour Characteristics to be Modelled

Structural behaviour is commonly separated into elastic and inelastic response. The two base motions used during the shaking table tests were intended to produce elastic response in the first phase and severe inelastic motion in the second phase. The approaches for modelling the two types of response analytically may be considerably different. Elastic response is normally relatively simple to simulate but inelastic behaviour is considerably more complex. Two separate analytical methods were used to predict the two levels of response in this study.

5.3.1. Elastic Behaviour

The section properties of the panel elements had to be correctly selected to achieve accurate representation of the system's structural response under low level base motion. Because of the inhomogeneity of reinforced concrete structures, selection of a section stiffness could be based on either a transformed section, a gross concrete section, or a cracked section. Selection of the appropriate section depends on the internal forces and likelihood of cracking. Several techniques were used, based on results of other research studies, to estimate the base moment level at which cracking might initiate and

to compare it with internal wall moments predicted from an analysis using gross section properties, as a means of selecting the correct section properties. The joints were assumed to be precracked so that cracked section stiffnesses were appropriate.

5.3.2. Inelastic Behaviour

The internal moments and shears in the wall system become very high during the strong shaking test. Since the horizontal joints between the vertical panels contain substantially less vertical reinforcing than the panels, and generally are already cracked because of shrinkage at the panel-joint interface, any inelastic behaviour due to large shear forces or moments would be expected to occur within the joints. Thus the panels could be assumed to remain elastic with a cracked section stiffness.

Other research studies have determined that the inelasticity within the horizontal joints is likely to occur in two forms: horizontal slip of panel relative to joint due to high shear and precracked joint interface, or rocking of the panel relative to the joint due to high overturning moments and little vertical steel reinforcing. Analytical modelling of the shear-slip mechanism requires an estimate of the friction coefficient, the dowel action, the clamping effect of vertical reinforcing, the correct compressive force and behaviour of any keying mechanism. The cast-in-place keys in the wall specimens were substantial enough to assume that slip would not be an important mechanism in the response analysis. Accurate modelling of the rocking behaviour due to high overturning moments could include simulation of the yielding of vertical steel through the joints, softening of the steel due to Bauschinger cyclic effects, buckling of reinforcing under compression, rupture of tension reinforcing, opening and closing of joint cracks, and loss of concrete compressive material due to spalling and crushing.

5.4. Correlation: Elastic Model during the 0.17 g Test

The initial simulation of the simple rectangular wall's response to the earthquake ground motion with an acceleration amplitude of 0.17 g used gross panel section properties in the wall elements and cracked joint properties. The results from that analysis were used to estimate what portion of the precast wall panels would be cracked and should have cracked section stiffness. An analytical model was then prepared which would have gross section properties initially but would change to a cracked section over a limited height after the estimated cracking moment was attained. The displacement results of that simulation are plotted with the experimentally measured response in Fig. 5.1. The analysis correctly modelled the response through the major initial displacement cycles where the lower element panel cracked but did not match the low amplitude response after cracking. After cracking the system regains its initial gross section stiffness, due to the axial gravity load, when the flexural cracks close. Special spring and gap elements were used in the final analytical model to allow cracking of the panel element with an elastic behaviour and a gradual return to uncracked section stiffness when cracks close. The behaviour of this modified model is shown in Fig. 5.2. Parameter studies on the finite element modelling of the wall panels made possible the selection of the correct size mesh needed to simulate the panel elasticity and allowed the panel elements to be connected to joint elements without producing unnatural panel deformations due to concentrated joint forces. The successful correlation between predicted response from this model and the experimental results is shown in Fig. 5.2.

5.5. Correlation: Inelastic Response

Simulation of the rectangular wall's inelastic response during strong ground motion required an exceptionally complex modelling approach. The

system's response involved yielding of steel reinforcing, Bauschinger softening, buckling, rupture, opening of joints, and loss of compression concrete. The effect of these various mechanisms on modifying the predicted response of the wall system will be discussed in the following. The behaviour of the precast wall panels were modelled as being elastic with cracked section stiffnesses. All of the inelasticity was modelled as occurring within the horizontal joints between vertical wall panels.

A simple model for simulating moderate inelastic response would include the yielding of vertical steel crossing the horizontal joint and opening of the joint along an assumed precracked plane between the joint material and the lower vertical precast wall panel. It is essential that the natural elastic conditions within the panel itself be maintained while modelling the inelastic joint. The DRAIN2D-MkII program used to analyze the wall system contains a variety of specific discrete "spring type" elements which may be used in many combinations to produce the desired behaviour. The precast panels are modelled with finite elements which remain elastic. These panel elements must be subdivided into a fine mesh to provide sufficient nodes along the base of the panel for connecting with the inelastic joint springs without creating unnaturally large concentrated joint forces and local panel deformation. In Fig. 5.3, results for the first two seconds of response of the test wall are compared with response predicted using an analytical model which had distributed elastic concrete compression springs within the joint and bilinear yielding tension elements to simulate the vertical joint reinforcing. This simple model accurately simulates the true response until bar rupture occurs in the test specimen at 1.42 seconds. Figure 5.4. shows the hysteresis base moment vs. top displacement relation for the analytical model.

The inclusion of steel rupture is essential for accurate modelling of the true behaviour since the predominant rocking displacement mechanism became

active after rupture. Figure 5.5 indicates how the correlation between analytical and test results could be extended when the reinforcing in the joint was modelled with a bilinear stiffness in tension and a limiting tension rupture level. The analytical model had rupturing of the tension steel at only one end of the wall similar to the unsymmetric rupture which occurred in the test specimen. The analytical moment vs. top displacement behaviour after rupture, which is plotted in Fig. 5.6, produces the same elastic rocking response when the wall deforms in the direction where tension reinforcing had ruptured, as was indicated in the experimental data shown previously in Fig. 4.4. The maximum level of moment existing within the wall during rocking is limited to the amount which can be provided by the axial gravity load restoring force.

The wall panels do not bend in a manner that is consistent with the common theory of "plane sections remain plane" after reinforcing bar rupture occurs and rocking motion develops. The effect of the wall panels rocking with respect to the horizontal joint is to create significant uplift and gap opening at the tension end of the wall and a small region of high compression forces in the concrete at the opposite end. In this condition the true wall exhibits non-planar deformation at the joints. The error which would exist in the analytical approach if normal beam flexural theory of plane sections is assumed, is shown in Fig. 5.7; the previous analytical model was constrained to deform in a linear manner at the panel base.

The process of exact modelling of the inelastic response must include other deformation and strength degradation mechanisms such as Bauschinger softening in the remaining reinforcing and loss of concrete cross section due to spalling and crushing (Figs. 5.8 and 5.9).
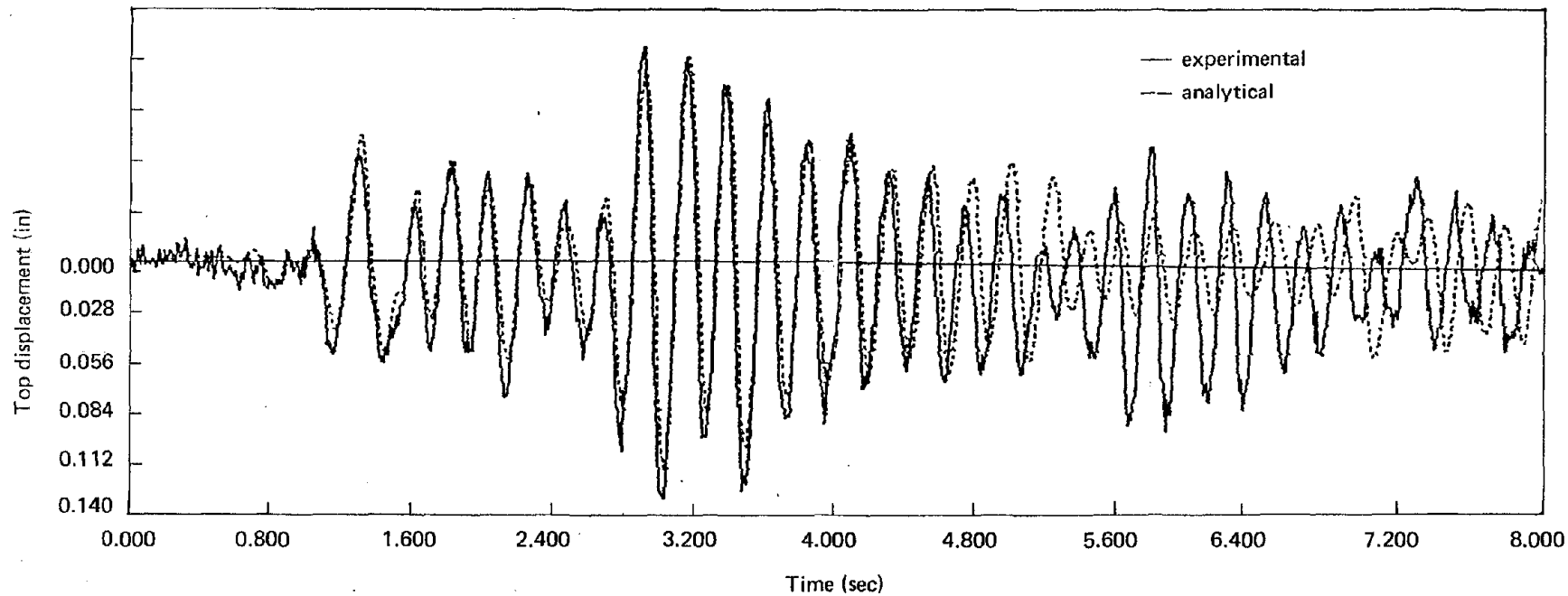
Fig. 5.1. Elastic Response of Analytical Model Which
Develops a Permanent Cracked Section
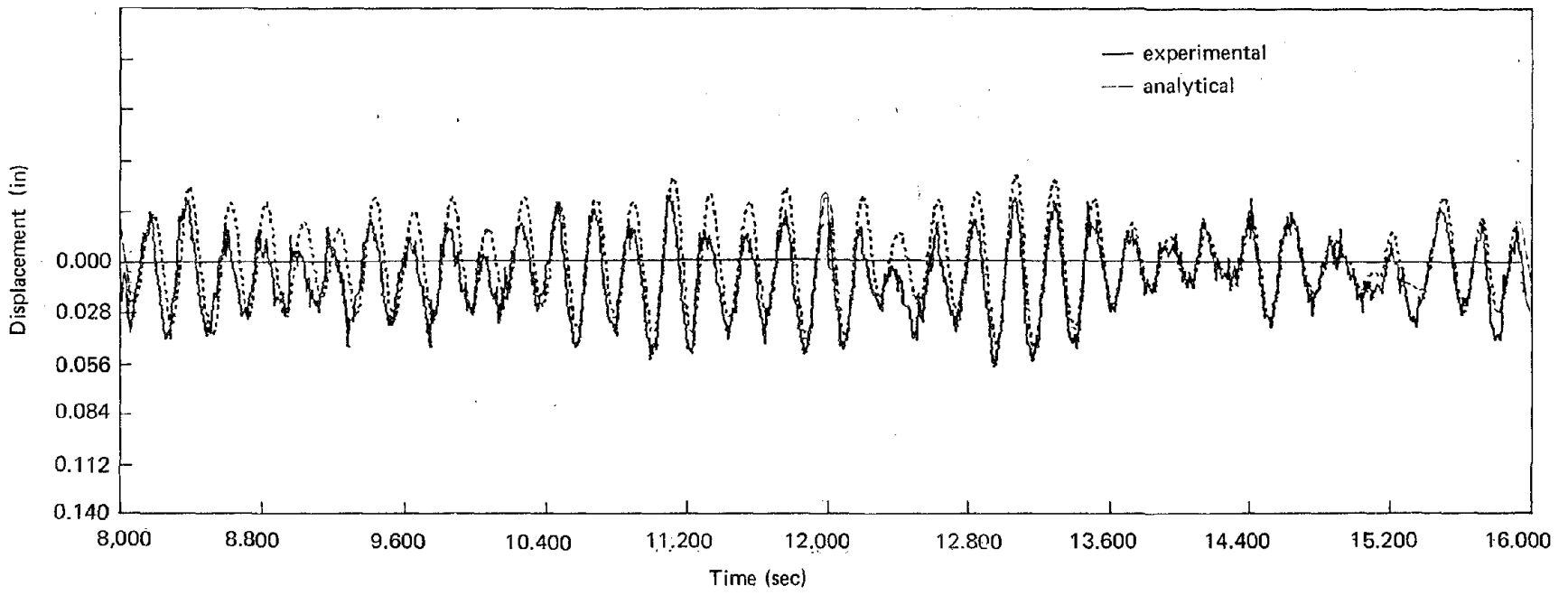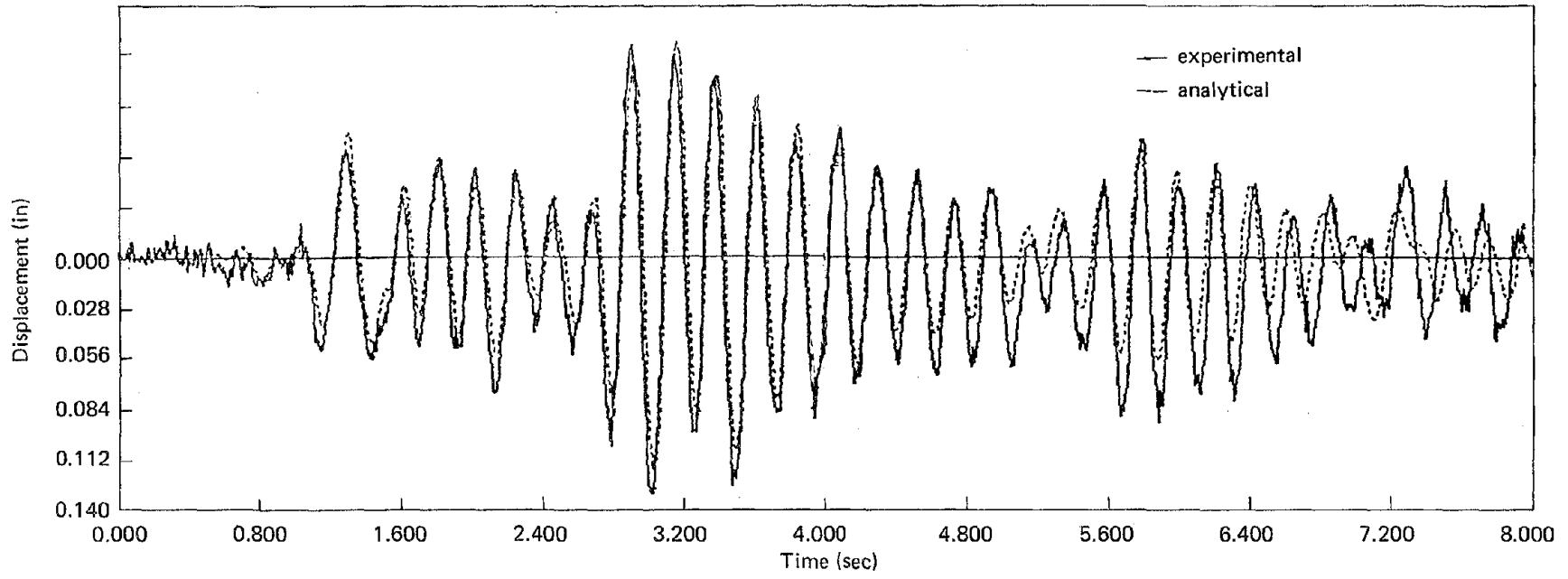
Fig. 5.2. Elastic Response of Analytical Model which Cracks
but Regains Gross Section Stiffness of Low Deformation
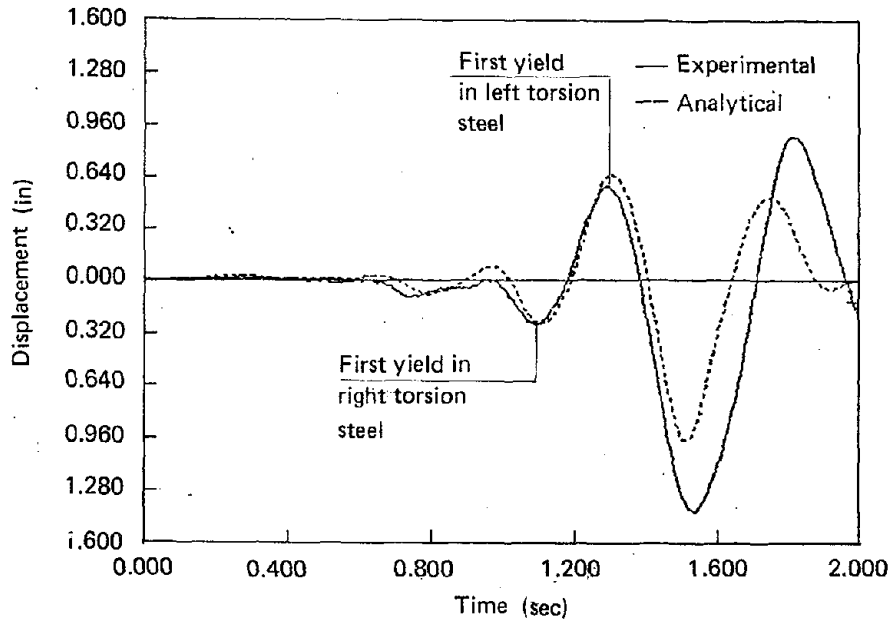
Fig. 5.3. Inelastic Response of Analytical Model with Bilinear
Reinforcing Stiffness and Gap Opening
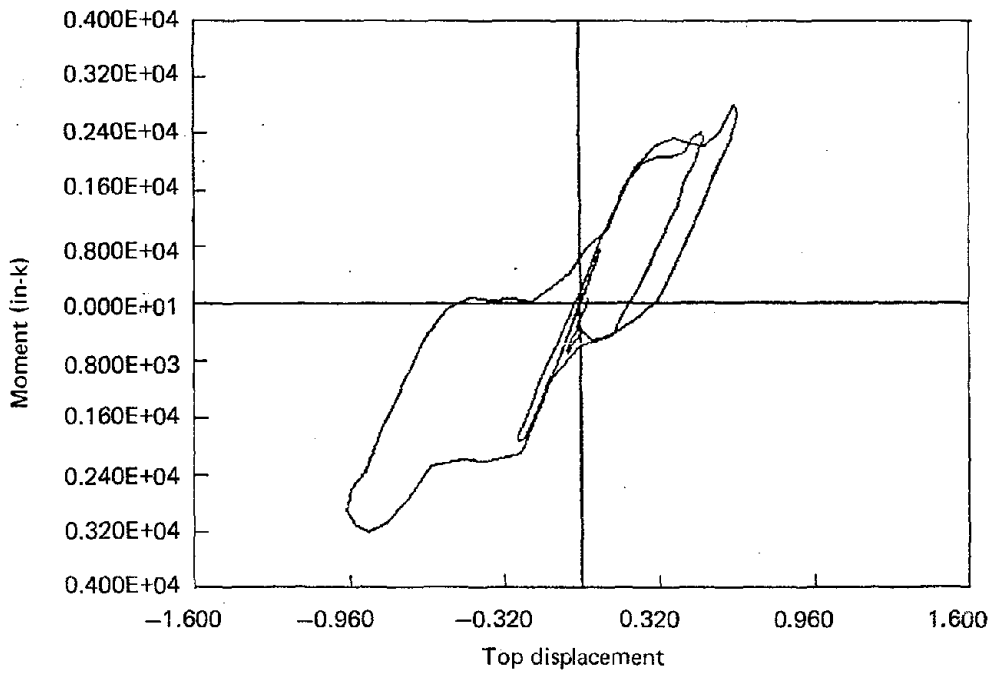
Fig. 5.4. Lower Joint, Moment Plotted with
Top Displacement for Model of Fig. 5.3.
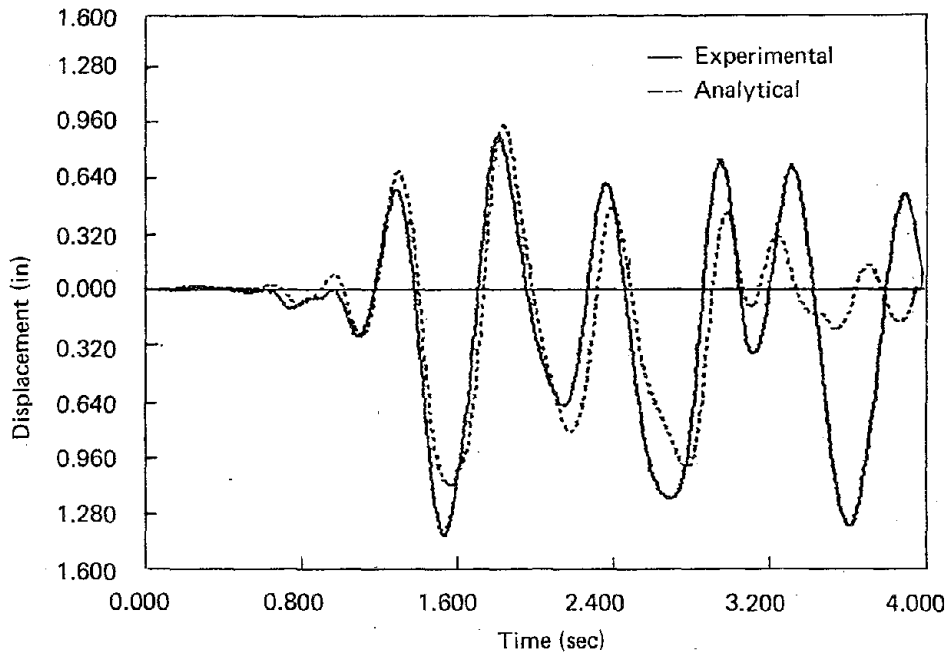
Fig. 5.5. Inelastic Response of Analytical Model When Steel
Rupturing and Gap Opening is Allowed
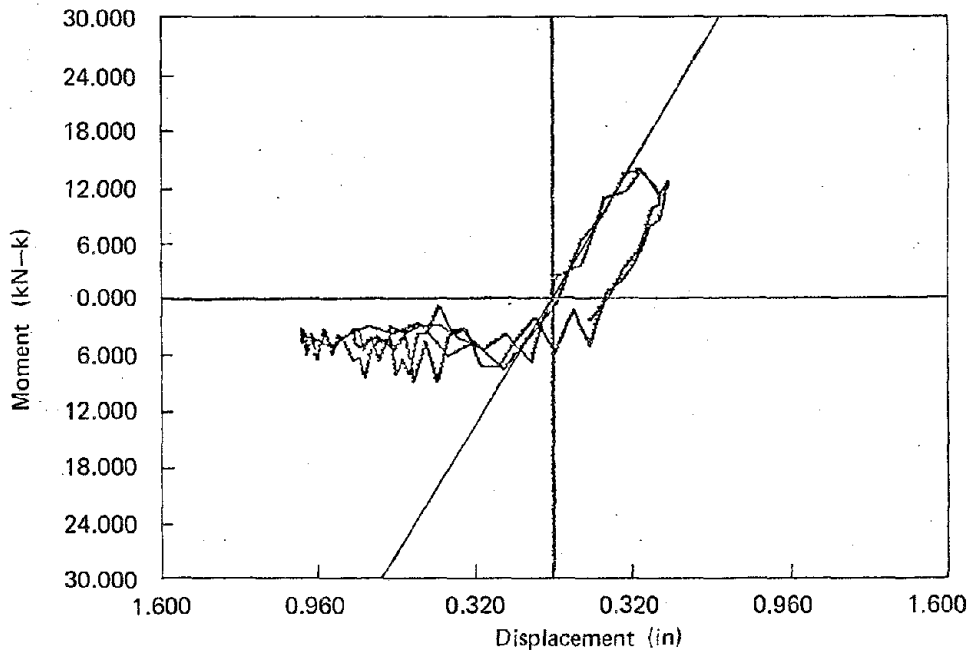
Fig. 5.6. Moment VS. Displacement Behaviour from Analytical
Model of Fig. 5.5. After Rupture Occurred
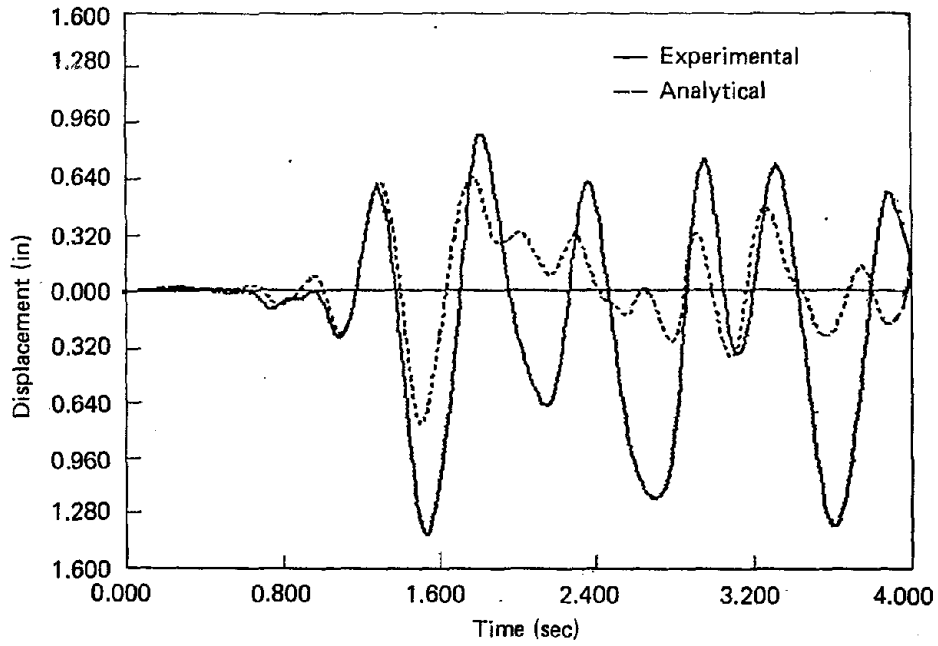
Fig. 5.7. Inelastic Response of Analytical Model when Plane
Section Deformation of Wall Panel is enforced
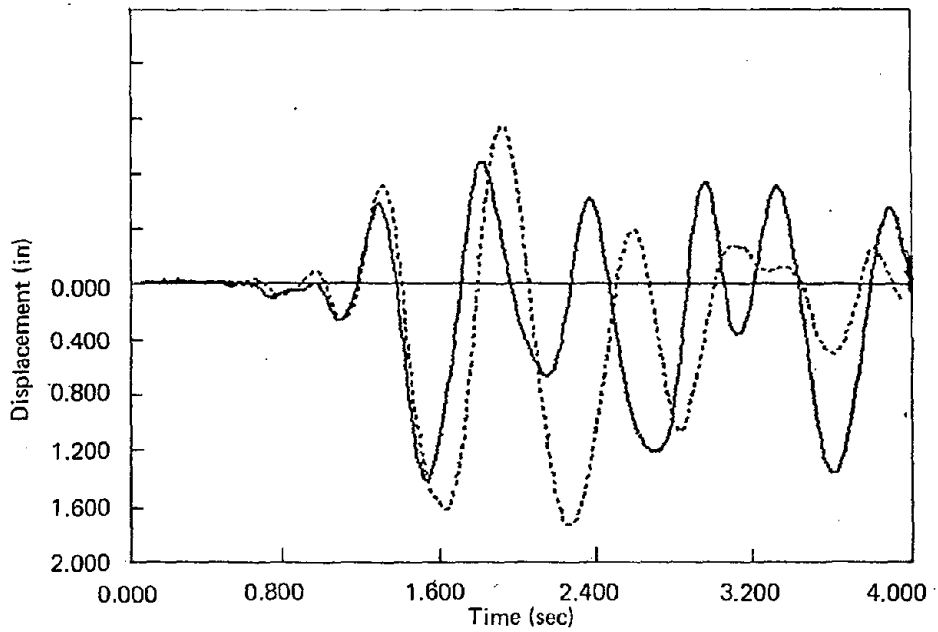
Fig. 5.8. Inelastic Response with Bauschinger Softening
in Joint Reinforcing
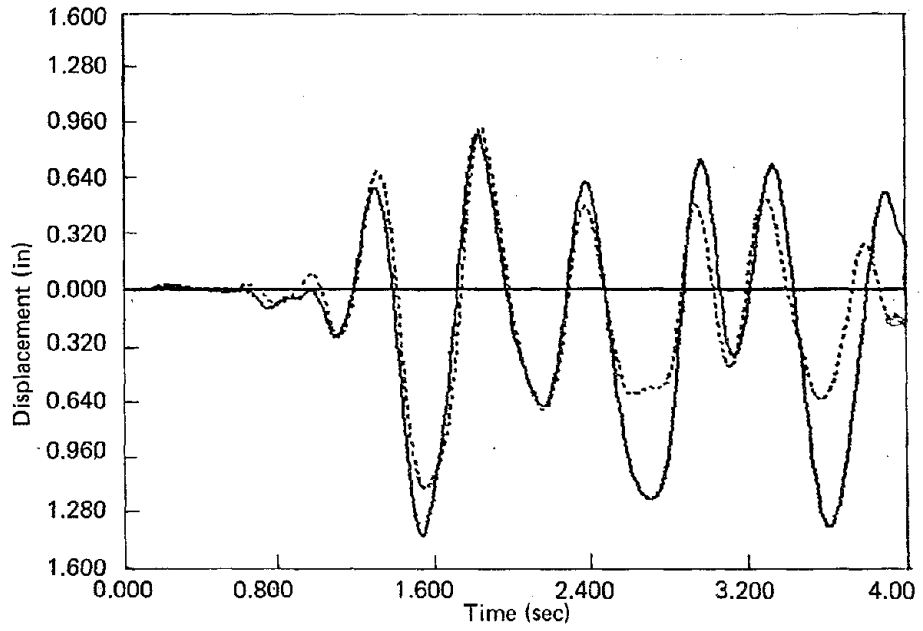
Fig. 5.9.   Inelastic Response of Analytical Model
Including Concrete Section Loss

6. CONCLUSIONS AND RECOMMENDATIONS

On the basis of the study presented in this report, it can generally be concluded that there is good correlation between the results of the shaking table and pseudostatic tests, which can be seen in the overall force capacity vs. displacement envelopes, in the similarity of the damage mechanisms and the good agreement between the other model response parameters.

Three substantial differences were apparent in the results from the test series under static load and dynamic load. (i) The energy dissipation exhibited within plots of base moment vs. top displacement was consistently higher in the static tests than in cycles of response of similar amplitude from the shaking table tests. It is believed that this is partially an effect caused by the horizontal orientation of the static specimens. (ii) The response of the flange walls was substantially different in the static and dynamic tests. The large slip in the static test occurred because several cycles of large applied top displacement created significant deterioration of the joints at the flanges and in the keys. The shaking table specimen only experienced one cycle of deformation at the maximum level of the static test and did not develop similar deterioration. (iii) A final minor difference always apparent in a comparison of the shaking table results and static test results was in the asymmetric character of damage from one end of the wall to the other in shaking the table tests. The controlled displacements of the static test invariably led to nearly symmetric damage at both ends of the wall. During shaking table tests once damage occurs at one location in a structural system the force which can be transferred through the damaged area is usually limited and the dynamic character of the system changes because of a lowered stiffness.

Very satisfactory agreement in results from the static and shaking table

tests occurred even though minor differences existed between the boundary con
ditions of the walls in the two tests, the ratios between shear, moment and
axial forces existing simultaneously, and the orientation of the specimens
during testing, as well as slight differences in the material strengths and
different means of applying the loads.

As to the correlation of the analytical results with the experimental ones
obtained by dynamic tests, it can be concluded that they agree quite well in
the case of elastic response, whereas the process of exact modelling of the
inelastic response must include other deformation and strength degradation
mechanisms such as Bauschinger softening in the remaining reinforcing and loss
of concrete cross section due to spalling and crushing.

On the basis of the above-mentioned facts, it can be concluded that
further investigation is necessary and should be directed towards: (i)
experimental testing of three-dimensional models on a seismic shaking table,
i.e., testing of a "box" system emphasizing the role of perpendicular walls and
of the considerably different effects in the elastic and inelastic phases of
structural behaviour; and (ii) analytical investigation of the inelastic
response of struc tures under strong motion and the corresponding modelling.

From the experimental investigations and the study on the large-panel
precast building system performance, it can generally be concluded that the RAD
panel system has a desirable balance of earthquake resistance capacity and
deformability which improves the survivability of the system when constructed
in areas of high seismicity.

REFERENCES

1. Oliva, M.G. and Clough, R.W., "Shaking Table Tests of Large-Panel Precast Concrete Building System Assemblages", UCB/EERC-83/14, University of California, Berkeley 1985.

2. Gavrilovic, P. and Velkov, M., "Experimental Testing of Three-Storey Models and Connection Systems of Large Panel Precast RAD System", Institute of Earthquake Engineering and Engineering Seismology, University "Kiril and Metodij", Skopje, 1982.

3. "Industrial Construction of Buildings in "RAD" System", Publication of the Construction Corporation "RAD" - Belgrade, Belgrade 1983.

4. Gavrilovic, P., Velkov, M., et al., "Experimental and Theoretical Investigation of the Precast Panel System "RAD" - Belgrade", IZIIS Report 82-44/1-8 (Vol. I, ...VIII), Skopje, 1982.

5. ACI Committee 318, Building Code Requirements for Reinforced Concrete, (ACI-318-77), Detroit, American Concrete Institute, 1977.

6. Clough, R.W., "Effect of Stiffness Degradation on Earthquake Ductility Requirements", Structures and Materials Research, Report 66-16, University of California, Berkeley 1966.

7. Baleh, C., "Analytical Correlation with the Results of Precast Wall Shaking Table Tests using Beam Analogy Technique", Master's Thesis, Dept. of Civil Engineering, Univ. of Wisconsin, Madison, 1987.

8. Belhadj, A., "Predicted Limit States of a 13-Story Precast Concrete Wall under Seismic Excitations", Master's Thesis, Dept. of Civil Engineering, Univ. of Wisconsin, Madison, 1988.

9. Malhas, F., "Seismic Response of Large Precast Panel Walls: Analytical
    Correlations with the Shaking Table Test Results", Ph.D. Thesis,
    Dept. of Civil Engineering, Univ. of Wisconsin, Madison, 1988.

10. Mahin, S., and Bertero, V., "RCCOLA: A Computer Program for Reinforced
    Concrete Column Analysis", Dept. of Civil Engineering, Univ. of
    California, Berkeley, 1977.

11. Swanson Analysis Systems, ANSYS PC/LINEAR, Rev. 4.2, Houston, 1988

12. Kanaan, A., and Powell, G., "DRAIN-2D: A General Purpose Computer
    Program for Dynamic Analysis of Inelastic Plane Structures",
    UCB/EERC-73/06 and 73/22, Earthquake Engineering Research Center,
    University of California, Berkeley, 1973.

13. Golafshani, A., DRAIN-2D - Mark II, Independent Study Report, SESM,
    University of California, Berkeley, 1981.

EARTHQUAKE ENGINEERING RESEARCH CENTER REPORT SERIES

EERC reports are available from the National Information Service for Earthquake Engineering(NISEE) and from the National Technical Information Service(NTIS). Numbers in parentheses are Accession Numbers assigned by the National Technical Information Service; these are followed by a price code. Contact NTIS, 5285 Port Royal Road, Springfield Virginia, 22161 for more information. Reports without Accession Numbers were not available from NTIS at the time of printing. For a current complete list of EERC reports (from EERC 67-1) and availablity information, please contact University of California, EERC, NISEE, 1301 South 46th Street, Richmond, California 94804.

UCB/EERC-80/01 "Earthquake Response of Concrete Gravity Dams Including Hydrodynamic and Foundation Interaction Effects," by Chopra, A.K., Chakrabarti, P. and Gupta, S., January 1980, (AD-A087297)A10.

UCB/EERC-80/02 "Rocking Response of Rigid Blocks to Earthquakes," by Yim, C.S., Chopra, A.K. and Penzien, J., January 1980, (PB80 166 002)A04.

UCB/EERC-80/03 "Optimum Inelastic Design of Seismic-Resistant Reinforced Concrete Frame Structures," by Zagajeski, S.W. and Bertero, V.V., January 1980, (PB80 164 635)A06.

UCB/EERC-80/04 "Effects of Amount and Arrangement of Wall-Panel Reinforcement on Hysteretic Behavior of Reinforced Concrete Walls," by Iliya, R. and Bertero, V.V., February 1980, (PB81 122 525)A09.

UCB/EERC-80/05 "Shaking Table Research on Concrete Dam Models," by Niwa, A. and Clough, R.W., September 1980, (PB81 122 368)A06.

UCB/EERC-80/06 "The Design of Steel Energy-Absorbing Restrainers and their Incorporation into Nuclear Power Plants for Enhanced Safety (Vol 1a): Piping with Energy Absorbing Restrainers: Parameter Study on Small Systems," by Powell, G.H., Oughourlian, C. and Simons, J., June 1980.

UCB/EERC-80/07 "Inelastic Torsional Response of Structures Subjected to Earthquake Ground Motions," by Yamazaki, Y., April 1980, (PB81 122 327)A08.

UCB/EERC-80/08 "Study of X-Braced Steel Frame Structures under Earthquake Simulation," by Ghanaat, Y., April 1980, (PB81 122 335)A11.

UCB/EERC-80/09 "Hybrid Modelling of Soil-Structure Interaction," by Gupta, S., Lin, T.W. and Penzien, J., May 1980, (PB81 122 319)A07.

UCB/EERC-80/10 "General Applicability of a Nonlinear Model of a One Story Steel Frame," by Sveinsson, B.I. and McNiven, H.D., May 1980, (PB81 124 877)A06.

UCB/EERC-80/11 "A Green-Function Method for Wave Interaction with a Submerged Body," by Kioka, W., April 1980, (PB81 122 269)A07.

UCB/EERC-80/12 "Hydrodynamic Pressure and Added Mass for Axisymmetric Bodies," by Nilrat, F., May 1980, (PB81 122 343)A08.

UCB/EERC-80/13 "Treatment of Non-Linear Drag Forces Acting on Offshore Platforms," by Dao, B.V. and Penzien, J., May 1980, (PB81 153 413)A07.

UCB/EERC-80/14 "2D Plane/Axisymmetric Solid Element (Type 3-Elastic or Elastic-Perfectly Plastic)for the ANSR-II Program," by Mondkar, D.P. and Powell, G.H., July 1980, (PB81 122 350)A03.

UCB/EERC-80/15 "A Response Spectrum Method for Random Vibrations," by Der Kiureghian, A., June 1981, (PB81 122 301)A03.

UCB/EERC-80/16 "Cyclic Inelastic Buckling of Tubular Steel Braces," by Zayas, V.A., Popov, E.P. and Mahin, S.A., June 1981, (PB81 124 885)A10.

UCB/EERC-80/17 "Dynamic Response of Simple Arch Dams Including Hydrodynamic Interaction," by Porter, C.S. and Chopra, A.K., July 1981, (PB81 124 000)A13.

UCB/EERC-80/18 "Experimental Testing of a Friction Damped Aseismic Base Isolation System with Fail-Safe Characteristics," by Kelly, J.M., Beucke, K.E. and Skinner, M.S., July 1980, (PB81 148 595)A04.

UCB/EERC-80/19 "The Design of Steel Energy-Absorbing Restrainers and their Incorporation into Nuclear Power Plants for Enhanced Safety (Vol.1B): Stochastic Seismic Analyses of Nuclear Power Plant Structures and Piping Systems Subjected to Multiple Supported Excitations," by Lee, M.C. and Penzien, J., June 1980, (PB82 201 872)A08.

UCB/EERC-80/20 "The Design of Steel Energy-Absorbing Restrainers and their Incorporation into Nuclear Power Plants for Enhanced Safety (Vol 1C): Numerical Method for Dynamic Substructure Analysis," by Dickens, J.M. and Wilson, E.L., June 1980.

UCB/EERC-80/21 "The Design of Steel Energy-Absorbing Restrainers and their Incorporation into Nuclear Power Plants for Enhanced Safety (Vol 2): Development and Testing of Restraints for Nuclear Piping Systems," by Kelly, J.M. and Skinner, M.S., June 1980.

UCB/EERC-80/22 "3D Solid Element (Type 4-Elastic or Elastic-Perfectly-Plastic) for the ANSR-II Program," by Mondkar, D.P. and Powell, G.H., July 1980, (PB81 123 242)A03.

UCB/EERC-80/23 "Gap-Friction Element (Type 5) for the Ansr-II Program," by Mondkar, D.P. and Powell, G.H., July 1980, (PB81 122 285)A03.

UCB/EERC-80/24 "U-Bar Restraint Element (Type 11) for the ANSR-II Program," by Oughourlian, C. and Powell, G.H., July 1980, (PB81 122 293)A03.

UCB/EERC-80/25 "Testing of a Natural Rubber Base Isolation System by an Explosively Simulated Earthquake," by Kelly, J.M., August 1980, (PB81 201 360)A04.

UCB/EERC-80/26 "Input Identification from Structural Vibrational Response," by Hu, Y., August 1980, (PB81 152 308)A05.

UCB/EERC-80/27 "Cyclic Inelastic Behavior of Steel Offshore Structures," by Zayas, V.A., Mahin, S.A. and Popov, E.P., August 1980, (PB81 196 180)A15.

UCB/EERC-80/28 "Shaking Table Testing of a Reinforced Concrete Frame with Biaxial Response," by Oliva, M.G., October 1980, (PB81 154 304)A10.

UCB/EERC-80/29 "Dynamic Properties of a Twelve-Story Prefabricated Panel Building," by Bouwkamp, J.G., Kollegger, J.P. and Stephen, R.M., October 1980, (PB82 138 777)A07.

UCB/EERC-80/30 "Dynamic Properties of an Eight-Story Prefabricated Panel Building," by Bouwkamp, J.G., Kollegger, J.P. and Stephen, R.M., October 1980, (PB81 200 313)A05.

UCB/EERC-80/31 "Predictive Dynamic Response of Panel Type Structures under Earthquakes," by Kollegger, J.P. and Bouwkamp, J.G., October 1980, (PB81 152 316)A04.

UCB/EERC-80/32 "The Design of Steel Energy-Absorbing Restrainers and their Incorporation into Nuclear Power Plants for Enhanced Safety (Vol 3): Testing of Commercial Steels in Low-Cycle Torsional Fatigue," by Spanner, P., Parker, E.R., Jongewaard, E. and Dory, M., 1980.

UCB/EERC-80/33   "The Design of Steel Energy-Absorbing Restrainers and their Incorporation into Nuclear Power Plants for Enhanced Safety (Vol 4): Shaking Table Tests of Piping Systems with Energy-Absorbing Restrainers," by Stiemer, S.F. and Godden, W.G., September 1980, (PB82 201 880)A05.

UCB/EERC-80/34   "The Design of Steel Energy-Absorbing Restrainers and their Incorporation into Nuclear Power Plants for Enhanced Safety (Vol 5): Summary Report," by Spencer, P., 1980.

UCB/EERC-80/35   "Experimental Testing of an Energy-Absorbing Base Isolation System," by Kelly, J.M., Skinner, M.S. and Beucke, K.E., October 1980, (PB81 154 072)A04.

UCB/EERC-80/36   "Simulating and Analyzing Artificial Non-Stationary Earth Ground Motions," by Nau, R.F., Oliver, R.M. and Pister, K.S., October 1980, (PB81 153 397)A04.

UCB/EERC-80/37   "Earthquake Engineering at Berkeley - 1980," by , September 1980, (PB81 205 674)A09.

UCB/EERC-80/38   "Inelastic Seismic Analysis of Large Panel Buildings," by Schricker, V. and Powell, G.H., September 1980, (PB81 154 338)A13.

UCB/EERC-80/39   "Dynamic Response of Embankment, Concrete-Gavity and Arch Dams Including Hydrodynamic Interation," by Hall, J.F. and Chopra, A.K., October 1980, (PB81 152 324)A11.

UCB/EERC-80/40   "Inelastic Buckling of Steel Struts under Cyclic Load Reversal.," by Black, R.G., Wenger, W.A. and Popov, E.P., October 1980, (PB81 154 312)A08.

UCB/EERC-80/41   "Influence of Site Characteristics on Buildings Damage during the October 3,1974 Lima Earthquake," by Repetto, P., Arango, I. and Seed, H.B., September 1980, (PB81 161 739)A05.

UCB/EERC-80/42   "Evaluation of a Shaking Table Test Program on Response Behavior of a Two Story Reinforced Concrete Frame," by Blondet, J.M., Clough, R.W. and Mahin, S.A., December 1980, (PB82 196 544)A11.

UCB/EERC-80/43   "Modelling of Soil-Structure Interaction by Finite and Infinite Elements," by Medina, F., December 1980, (PB81 229 270)A04.

UCB/EERC-81/01   "Control of Seismic Response of Piping Systems and Other Structures by Base Isolation," by Kelly, J.M., January 1981, (PB81 200 735)A05.

UCB/EERC-81/02   "OPTNSR- An Interactive Software System for Optimal Design of Statically and Dynamically Loaded Structures with Nonlinear Response," by Bhatti, M.A., Ciampi, V. and Pister, K.S., January 1981, (PB81 218 851)A09.

UCB/EERC-81/03   "Analysis of Local Variations in Free Field Seismic Ground Motions," by Chen, J.-C., Lysmer, J. and Seed, H.B., January 1981, (AD-A099508)A13.

UCB/EERC-81/04   "Inelastic Structural Modeling of Braced Offshore Platforms for Seismic Loading," by Zayas, V.A., Shing, P.-S.B., Mahin, S.A. and Popov, E.P., January 1981, (PB82 138 777)A07.

UCB/EERC-81/05   "Dynamic Response of Light Equipment in Structures," by Der Kiureghian, A., Sackman, J.L. and Nour-Omid, B., April 1981, (PB81 218 497)A04.

UCB/EERC-81/06   "Preliminary Experimental Investigation of a Broad Base Liquid Storage Tank," by Bouwkamp, J.G., Kollegger, J.P. and Stephen, R.M., May 1981, (PB82 140 385)A03.

UCB/EERC-81/07   "The Seismic Resistant Design of Reinforced Concrete Coupled Structural Walls," by Aktan, A.E. and Bertero, V.V., June 1981, (PB82 113 358)A11.

UCB/EERC-81/08   "Unassigned," by Unassigned, 1981.

UCB/EERC-81/09   "Experimental Behavior of a Spatial Piping System with Steel Energy Absorbers Subjected to a Simulated Differential Seismic Input," by Stiemer, S.F., Godden, W.G. and Kelly, J.M., July 1981, (PB82 201 898)A04.

UCB/EERC-81/10   "Evaluation of Seismic Design Provisions for Masonry in the United States," by Sveinsson, B.I., Mayes, R.L. and McNiven, H.D., August 1981, (PB82 166 075)A08.

UCB/EERC-81/11   "Two-Dimensional Hybrid Modelling of Soil-Structure Interaction," by Tzong, T.-J., Gupta, S. and Penzien, J., August 1981, (PB82 142 118)A04.

UCB/EERC-81/12   "Studies on Effects of Infills in Seismic Resistant R/C Construction," by Brokken, S. and Bertero, V.V., October 1981, (PB82 166 190)A09.

UCB/EERC-81/13   "Linear Models to Predict the Nonlinear Seismic Behavior of a One-Story Steel Frame," by Valdimarsson, H., Shah, A.H. and McNiven, H.D., September 1981, (PB82 138 793)A07.

UCB/EERC-81/14   "TLUSH: A Computer Program for the Three-Dimensional Dynamic Analysis of Earth Dams," by Kagawa, T., Mejia, L.H., Seed, H.B. and Lysmer, J., September 1981, (PB82 139 940)A06.

UCB/EERC-81/15   "Three Dimensional Dynamic Response Analysis of Earth Dams," by Mejia, L.H. and Seed, H.B., September 1981, (PB82 137 274)A12.

UCB/EERC-81/16   "Experimental Study of Lead and Elastomeric Dampers for Base Isolation Systems," by Kelly, J.M. and Hodder, S.B., October 1981, (PB82 166 182)A05.

UCB/EERC-81/17   "The Influence of Base Isolation on the Seismic Response of Light Secondary Equipment," by Kelly, J.M., April 1981, (PB82 255 266)A04.

UCB/EERC-81/18   "Studies on Evaluation of Shaking Table Response Analysis Procedures," by Blondet, J. M., November 1981, (PB82 197 278)A10.

UCB/EERC-81/19   "DELIGHT.STRUCT: A Computer-Aided Design Environment for Structural Engineering," by Balling, R.J., Pister, K.S. and Polak, E., December 1981, (PB82 218 496)A07.

UCB/EERC-81/20   "Optimal Design of Seismic-Resistant Planar Steel Frames," by Balling, R.J., Ciampi, V. and Pister, K.S., December 1981, (PB82 220 179)A07.

UCB/EERC-82/01   "Dynamic Behavior of Ground for Seismic Analysis of Lifeline Systems," by Sato, T. and Der Kiureghian, A., January 1982, (PB82 218 926)A05.

UCB/EERC-82/02   "Shaking Table Tests of a Tubular Steel Frame Model," by Ghanaat, Y. and Clough, R.W., January 1982, (PB82 220 161)A07.

UCB/EERC-82/03 "Behavior of a Piping System under Seismic Excitation: Experimental Investigations of a Spatial Piping System supported by Mechanical Shock Arrestors," by Schneider, S., Lee, H.-M. and Godden, W. G., May 1982, (PB83 172 544)A09.

UCB/EERC-82/04 "New Approaches for the Dynamic Analysis of Large Structural Systems," by Wilson, E.L., June 1982, (PB83 148 080)A05.

UCB/EERC-82/05 "Model Study of Effects of Damage on the Vibration Properties of Steel Offshore Platforms," by Shahrivar, F. and Bouwkamp, J.G., June 1982, (PB83 148 742)A10.

UCB/EERC-82/06 "States of the Art and Pratice in the Optimum Seismic Design and Analytical Response Prediction of R/C Frame Wall Structures," by Aktan, A.E. and Bertero, V.V., July 1982, (PB83 147 736)A05.

UCB/EERC-82/07 "Further Study of the Earthquake Response of a Broad Cylindrical Liquid-Storage Tank Model," by Manos, G.C. and Clough, R.W., July 1982, (PB83 147 744)A11.

UCB/EERC-82/08 "An Evaluation of the Design and Analytical Seismic Response of a Seven Story Reinforced Concrete Frame," by Charney, F.A. and Bertero, V.V., July 1982, (PB83 157 628)A09.

UCB/EERC-82/09 "Fluid-Structure Interactions: Added Mass Computations for Incompressible Fluid," by Kuo, J.S.-H., August 1982, (PB83 156 281)A07.

UCB/EERC-82/10 "Joint-Opening Nonlinear Mechanism: Interface Smeared Crack Model," by Kuo, J.S.-H., August 1982, (PB83 149 195)A05.

UCB/EERC-82/11 "Dynamic Response Analysis of Techi Dam," by Clough, R.W., Stephen, R.M. and Kuo, J.S.-H., August 1982, (PB83 147 496)A06.

UCB/EERC-82/12 "Prediction of the Seismic Response of R/C Frame-Coupled Wall Structures," by Aktan, A.E., Bertero, V.V. and Piazzo, M., August 1982, (PB83 149 203)A09.

UCB/EERC-82/13 "Preliminary Report on the Smart 1 Strong Motion Array in Taiwan," by Bolt, B.A., Loh, C.H., Penzien, J. and Tsai, Y.B., August 1982, (PB83 159 400)A10.

UCB/EERC-82/14 "Shaking-Table Studies of an Eccentrically X-Braced Steel Structure," by Yang, M.S., September 1982, (PB83 260 778)A12.

UCB/EERC-82/15 "The Performance of Stairways in Earthquakes," by Roha, C., Axley, J.W. and Bertero, V.V., September 1982, (PB83 157 693)A07.

UCB/EERC-82/16 "The Behavior of Submerged Multiple Bodies in Earthquakes," by Liao, W.-G., September 1982, (PB83 158 709)A07.

UCB/EERC-82/17 "Effects of Concrete Types and Loading Conditions on Local Bond-Slip Relationships," by Cowell, A.D., Popov, E.P. and Bertero, V.V., September 1982, (PB83 153 577)A04.

UCB/EERC-82/18 "Mechanical Behavior of Shear Wall Vertical Boundary Members: An Experimental Investigation," by Wagner, M.T. and Bertero, V.V., October 1982, (PB83 159 764)A05.

UCB/EERC-82/19 "Experimental Studies of Multi-support Seismic Loading on Piping Systems," by Kelly, J.M. and Cowell, A.D., November 1982.

UCB/EERC-82/20 "Generalized Plastic Hinge Concepts for 3D Beam-Column Elements," by Chen, P. F.-S. and Powell, G.H., November 1982, (PB83 247 981)A13.

UCB/EERC-82/21 "ANSR-II: General Computer Program for Nonlinear Structural Analysis," by Oughourlian, C.V. and Powell, G.H., November 1982, (PB83 251 330)A12.

UCB/EERC-82/22 "Solution Strategies for Statically Loaded Nonlinear Structures," by Simons, J.W. and Powell, G.H., November 1982, (PB83 197 970)A06.

UCB/EERC-82/23 "Analytical Model of Deformed Bar Anchorages under Generalized Excitations," by Ciampi, V., Eligehausen, R., Bertero, V.V. and Popov, E.P., November 1982, (PB83 169 532)A06.

UCB/EERC-82/24 "A Mathematical Model for the Response of Masonry Walls to Dynamic Excitations," by Sucuoglu, H., Mengi, Y. and McNiven, H.D., November 1982, (PB83 169 011)A07.

UCB/EERC-82/25 "Earthquake Response Considerations of Broad Liquid Storage Tanks," by Cambra, F.J., November 1982, (PB83 251 215)A09.

UCB/EERC-82/26 "Computational Models for Cyclic Plasticity, Rate Dependence and Creep," by Mosaddad, B. and Powell, G.H., November 1982, (PB83 245 829)A08.

UCB/EERC-82/27 "Inelastic Analysis of Piping and Tubular Structures," by Mahasuverachai, M. and Powell, G.H., November 1982, (PB83 249 987)A07.

UCB/EERC-83/01 "The Economic Feasibility of Seismic Rehabilitation of Buildings by Base Isolation," by Kelly, J.M., January 1983, (PB83 197 988)A05.

UCB/EERC-83/02 "Seismic Moment Connections for Moment-Resisting Steel Frames.," by Popov, E.P., January 1983, (PB83 195 412)A04.

UCB/EERC-83/03 "Design of Links and Beam-to-Column Connections for Eccentrically Braced Steel Frames," by Popov, E.P. and Malley, J.O., January 1983, (PB83 194 811)A04.

UCB/EERC-83/04 "Numerical Techniques for the Evaluation of Soil-Structure Interaction Effects in the Time Domain," by Bayo, E. and Wilson, E.L., February 1983, (PB83 245 605)A09.

UCB/EERC-83/05 "A Transducer for Measuring the Internal Forces in the Columns of a Frame-Wall Reinforced Concrete Structure," by Sause, R. and Bertero, V.V., May 1983, (PB84 119 494)A06.

UCB/EERC-83/06 "Dynamic Interactions Between Floating Ice and Offshore Structures," by Croteau, P., May 1983, (PB84 119 486)A16.

UCB/EERC-83/07 "Dynamic Analysis of Multiply Tuned and Arbitrarily Supported Secondary Systems," by Igusa, T. and Der Kiureghian, A., July 1983, (PB84 118 272)A11.

UCB/EERC-83/08 "A Laboratory Study of Submerged Multi-body Systems in Earthquakes," by Ansari, G.R., June 1983, (PB83 261 842)A17.

UCB/EERC-83/09 "Effects of Transient Foundation Uplift on Earthquake Response of Structures," by Yim, C.-S. and Chopra, A.K., June 1983, (PB83 261 396)A07.

UCB/EERC-83/10 "Optimal Design of Friction-Braced Frames under Seismic Loading," by Austin, M.A. and Pister, K.S., June 1983, (PB84 119 288)A06.

UCB/EERC-83/11 "Shaking Table Study of Single-Story Masonry Houses: Dynamic Performance under Three Component Seismic Input and Recommendations," by Manos, G.C., Clough, R.W. and Mayes, R.L., July 1983, (UCB/EERC-83/11)A08.

UCB/EERC-83/12 "Experimental Error Propagation in Pseudodynamic Testing," by Shiing, P.B. and Mahin, S.A., June 1983, (PB84 119 270)A09.

UCB/EERC-83/13 "Experimental and Analytical Predictions of the Mechanical Characteristics of a 1/5-scale Model of a 7-story R/C Frame-Wall Building Structure," by Aktan, A.E., Bertero, V.V., Chowdhury, A.A. and Nagashima, T., June 1983, (PB84 119 213)A07.

UCB/EERC-83/14 "Shaking Table Tests of Large-Panel Precast Concrete Building System Assemblages," by Oliva, M.G. and Clough, R.W., June 1983, (PB86 110 210/AS)A11.

UCB/EERC-83/15 "Seismic Behavior of Active Beam Links in Eccentrically Braced Frames," by Hjelmstad, K.D. and Popov, E.P., July 1983, (PB84 119 676)A09.

UCB/EERC-83/16 "System Identification of Structures with Joint Rotation," by Dimsdale, J.S., July 1983, (PB84 192 210)A06.

UCB/EERC-83/17 "Construction of Inelastic Response Spectra for Single-Degree-of-Freedom Systems," by Mahin, S. and Lin, J., June 1983, (PB84 208 834)A05.

UCB/EERC-83/18 "Interactive Computer Analysis Methods for Predicting the Inelastic Cyclic Behaviour of Structural Sections," by Kaba, S. and Mahin, S., July 1983, (PB84 192 012)A06.

UCB/EERC-83/19 "Effects of Bond Deterioration on Hysteretic Behavior of Reinforced Concrete Joints," by Filippou, F.C., Popov, E.P. and Bertero, V.V., August 1983, (PB84 192 020)A10.

UCB/EERC-83/20 "Correlation of Analytical and Experimental Response of Large-Panel Precast Building Systems," by Oliva, M.G., Clough, R.W., Velkov, M. and Gavrilovic, P., May 1988.

UCB/EERC-83/21 "Mechanical Characteristics of Materials Used in a 1/5 Scale Model of a 7-Story Reinforced Concrete Test Structure," by Bertero, V.V., Aktan, A.E., Harris, H.G. and Chowdhury, A.A., October 1983, (PB84 193 697)A05.

UCB/EERC-83/22 "Hybrid Modelling of Soil-Structure Interaction in Layered Media," by Tzong, T.-J. and Penzien, J., October 1983, (PB84 192 178)A08.

UCB/EERC-83/23 "Local Bond Stress-Slip Relationships of Deformed Bars under Generalized Excitations," by Eligehausen, R., Popov, E.P. and Bertero, V.V., October 1983, (PB84 192 848)A09.

UCB/EERC-83/24 "Design Considerations for Shear Links in Eccentrically Braced Frames," by Malley, J.O. and Popov, E.P., November 1983, (PB84 192 186)A07.

UCB/EERC-84/01 "Pseudodynamic Test Method for Seismic Performance Evaluation: Theory and Implementation," by Shing, P.-S.B. and Mahin, S.A., January 1984, (PB84 190 644)A08.

UCB/EERC-84/02 "Dynamic Response Behavior of Kiang Hong Dian Dam," by Clough, R.W., Chang, K.-T., Chen, H.-Q. and Stephen, R.M., April 1984, (PB84 209 402)A08.

UCB/EERC-84/03 "Refined Modelling of Reinforced Concrete Columns for Seismic Analysis," by Kaba, S.A. and Mahin, S.A., April 1984, (PB84 234 384)A06.

UCB/EERC-84/04 "A New Floor Response Spectrum Method for Seismic Analysis of Multiply Supported Secondary Systems," by Asfura, A. and Der Kiureghian, A., June 1984, (PB84 239 417)A06.

UCB/EERC-84/05 "Earthquake Simulation Tests and Associated Studies of a 1/5th-scale Model of a 7-Story R/C Frame-Wall Test Structure," by Bertero, V.V., Aktan, A.E., Charney, F.A. and Sause, R., June 1984, (PB84 239 409)A09.

UCB/EERC-84/06 "R/C Structural Walls: Seismic Design for Shear," by Aktan, A.E. and Bertero, V.V., 1984.

UCB/EERC-84/07 "Behavior of Interior and Exterior Flat-Plate Connections subjected to Inelastic Load Reversals," by Zee, H.L. and Moehle, J.P., August 1984, (PB86 117 629/AS)A07.

UCB/EERC-84/08 "Experimental Study of the Seismic Behavior of a Two-Story Flat-Plate Structure," by Moehle, J.P. and Diebold, J.W., August 1984, (PB86 122 553/AS)A12.

UCB/EERC-84/09 "Phenomenological Modeling of Steel Braces under Cyclic Loading," by Ikeda, K., Mahin, S.A. and Dermitzakis, S.N., May 1984, (PB86 132 198/AS)A08.

UCB/EERC-84/10 "Earthquake Analysis and Response of Concrete Gravity Dams," by Fenves, G. and Chopra, A.K., August 1984, (PB85 193 902/AS)A11.

UCB/EERC-84/11 "EAGD-84: A Computer Program for Earthquake Analysis of Concrete Gravity Dams," by Fenves, G. and Chopra, A.K., August 1984, (PB85 193 613/AS)A05.

UCB/EERC-84/12 "A Refined Physical Theory Model for Predicting the Seismic Behavior of Braced Steel Frames," by Ikeda, K. and Mahin, S.A., July 1984, (PB85 191 450/AS)A09.

UCB/EERC-84/13 "Earthquake Engineering Research at Berkeley - 1984," by , August 1984, (PB85 197 341/AS)A10.

UCB/EERC-84/14 "Moduli and Damping Factors for Dynamic Analyses of Cohesionless Soils," by Seed, H.B., Wong, R.T., Idriss, I.M. and Tokimatsu, K., September 1984, (PB85 191 468/AS)A04.

UCB/EERC-84/15 "The Influence of SPT Procedures in Soil Liquefaction Resistance Evaluations," by Seed, H.B., Tokimatsu, K., Harder, L.F. and Chung, R.M., October 1984, (PB85 191 732/AS)A04.

UCB/EERC-84/16 "Simplified Procedures for the Evaluation of Settlements in Sands Due to Earthquake Shaking," by Tokimatsu, K. and Seed, H.B., October 1984, (PB85 197 887/AS)A03.

UCB/EERC-84/17 "Evaluation of Energy Absorption Characteristics of Bridges under Seismic Conditions," by Imbsen, R.A. and Penzien, J., November 1984.

UCB/EERC-84/18 "Structure-Foundation Interactions under Dynamic Loads," by Liu, W.D. and Penzien, J., November 1984, (PB87 124 889/AS)A11.

UCB/EERC-84/19 "Seismic Modelling of Deep Foundations," by Chen, C.-H. and Penzien, J., November 1984, (PB87 124 798/AS)A07.

UCB/EERC-84/20 "Dynamic Response Behavior of Quan Shui Dam," by Clough, R.W., Chang, K.-T., Chen, H.-Q., Stephen, R.M., Ghanaat, Y. and Qi, J.-H., November 1984, (PB86 115177/AS)A07.

UCB/EERC-85/01 "Simplified Methods of Analysis for Earthquake Resistant Design of Buildings," by Cruz, E.F. and Chopra, A.K., February 1985, (PB86 112299/AS)A12.

UCB/EERC-85/02 "Estimation of Seismic Wave Coherency and Rupture Velocity using the SMART 1 Strong-Motion Array Recordings," by Abrahamson, N.A., March 1985, (PB86 214 343)A07.

UCB/EERC-85/03   "Dynamic Properties of a Thirty Story Condominium Tower Building," by Stephen, R.M., Wilson, E.L. and Stander, N., April 1985, (PB86 118965/AS)A06.

UCB/EERC-85/04   "Development of Substructuring Techniques for On-Line Computer Controlled Seismic Performance Testing," by Dermitzakis, S. and Mahin, S., February 1985, (PB86 132941/AS)A08.

UCB/EERC-85/05   "A Simple Model for Reinforcing Bar Anchorages under Cyclic Excitations," by Filippou, F.C., March 1985, (PB86 112 919/AS)A05.

UCB/EERC-85/06   "Racking Behavior of Wood-framed Gypsum Panels under Dynamic Load," by Oliva, M.G., June 1985.

UCB/EERC-85/07   "Earthquake Analysis and Response of Concrete Arch Dams," by Fok, K.-L. and Chopra, A.K., June 1985, (PB86 139672/AS)A10.

UCB/EERC-85/08   "Effect of Inelastic Behavior on the Analysis and Design of Earthquake Resistant Structures," by Lin, J.P. and Mahin, S.A., June 1985, (PB86 135340/AS)A08.

UCB/EERC-85/09   "Earthquake Simulator Testing of a Base-Isolated Bridge Deck," by Kelly, J.M., Buckle, I.G. and Tsai, H.-C., January 1986, (PB87 124 152/AS)A06.

UCB/EERC-85/10   "Simplified Analysis for Earthquake Resistant Design of Concrete Gravity Dams," by Fenves, G. and Chopra, A.K., June 1986, (PB87 124 160/AS)A08.

UCB/EERC-85/11   "Dynamic Interaction Effects in Arch Dams," by Clough, R.W., Chang, K.-T., Chen, H.-Q. and Ghanaat, Y., October 1985, (PB86 135027/AS)A05.

UCB/EERC-85/12   "Dynamic Response of Long Valley Dam in the Mammoth Lake Earthquake Series of May 25-27, 1980," by Lai, S. and Seed, H.B., November 1985, (PB86 142304/AS)A05.

UCB/EERC-85/13   "A Methodology for Computer-Aided Design of Earthquake-Resistant Steel Structures," by Austin, M.A., Pister, K.S. and Mahin, S.A., December 1985, (PB86 159480/AS)A10 .

UCB/EERC-85/14   "Response of Tension-Leg Platforms to Vertical Seismic Excitations," by Liou, G.-S., Penzien, J. and Yeung, R.W., December 1985, (PB87 124 871/AS)A08.

UCB/EERC-85/15   "Cyclic Loading Tests of Masonry Single Piers: Volume 4 - Additional Tests with Height to Width Ratio of 1," by Sveinsson, B., McNiven, H.D. and Sucuoglu, H., December 1985.

UCB/EERC-85/16   "An Experimental Program for Studying the Dynamic Response of a Steel Frame with a Variety of Infill Partitions," by Yanev, B. and McNiven, H.D., December 1985.

UCB/EERC-86/01   "A Study of Seismically Resistant Eccentrically Braced Steel Frame Systems," by Kasai, K. and Popov, E.P., January 1986, (PB87 124 178/AS)A14.

UCB/EERC-86/02   "Design Problems in Soil Liquefaction," by Seed, H.B., February 1986, (PB87 124 186/AS)A03.

UCB/EERC-86/03   "Implications of Recent Earthquakes and Research on Earthquake-Resistant Design and Construction of Buildings," by Bertero, V.V., March 1986, (PB87 124 194/AS)A05.

UCB/EERC-86/04   "The Use of Load Dependent Vectors for Dynamic and Earthquake Analyses," by Leger, P., Wilson, E.L. and Clough, R.W., March 1986, (PB87 124 202/AS)A12.

UCB/EERC-86/05   "Two Beam-To-Column Web Connections," by Tsai, K.-C. and Popov, E.P., April 1986, (PB87 124 301/AS)A04.

UCB/EERC-86/06   "Determination of Penetration Resistance for Coarse-Grained Soils using the Becker Hammer Drill," by Harder, L.F. and Seed, H.B., May 1986, (PB87 124 210/AS)A07.

UCB/EERC-86/07   "A Mathematical Model for Predicting the Nonlinear Response of Unreinforced Masonry Walls to In-Plane Earthquake Excitations," by Mengi, Y. and McNiven, H.D., May 1986, (PB87 124 780/AS)A06.

UCB/EERC-86/08   "The 19 September 1985 Mexico Earthquake: Building Behavior," by Bertero, V.V., July 1986.

UCB/EERC-86/09   "EACD-3D: A Computer Program for Three-Dimensional Earthquake Analysis of Concrete Dams," by Fok, K.-L., Hall, J.F. and Chopra, A.K., July 1986, (PB87 124 228/AS)A08.

UCB/EERC-86/10   "Earthquake Simulation Tests and Associated Studies of a 0.3-Scale Model of a Six-Story Concentrically Braced Steel Structure," by Uang, C.-M. and Bertero, V.V., December 1986, (PB87 163 564/AS)A17.

UCB/EERC-86/11   "Mechanical Characteristics of Base Isolation Bearings for a Bridge Deck Model Test," by Kelly, J.M., Buckle, I.G. and Koh, C.-G., 1987.

UCB/EERC-86/12   "Effects of Axial Load on Elastomeric Isolation Bearings," by Koh, C.-G. and Kelly, J.M., November 1987.

UCB/EERC-87/01   "The FPS Earthquake Resisting System: Experimental Report," by Zayas, V.A., Low, S.S. and Mahin, S.A., June 1987.

UCB/EERC-87/02   "Earthquake Simulator Tests and Associated Studies of a 0.3-Scale Model of a Six-Story Eccentrically Braced Steel Structure," by Whittaker, A., Uang, C.-M. and Bertero, V.V., July 1987.

UCB/EERC-87/03   "A Displacement Control and Uplift Restraint Device for Base-Isolated Structures," by Kelly, J.M., Griffith, M.C. and Aiken, I.D., April 1987.

UCB/EERC-87/04   "Earthquake Simulator Testing of a Combined Sliding Bearing and Rubber Bearing Isolation System," by Kelly, J.M. and Chalhoub, M.S., 1987.

UCB/EERC-87/05   "Three-Dimensional Inelastic Analysis of Reinforced Concrete Frame-Wall Structures," by Moazzami, S. and Bertero, V.V., May 1987.

UCB/EERC-87/06   "Experiments on Eccentrically Braced Frames with Composite Floors," by Ricles, J. and Popov, E., June 1987.

UCB/EERC-87/07   "Dynamic Analysis of Seismically Resistant Eccentrically Braced Frames," by Ricles, J. and Popov, E., June 1987.

UCB/EERC-87/08   "Undrained Cyclic Triaxial Testing of Gravels-The Effect of Membrane Compliance," by Evans, M.D. and Seed, H.B., July 1987.

UCB/EERC-87/09   "Hybrid Solution Techniques for Generalized Pseudo-Dynamic Testing," by Thewalt, C. and Mahin, S.A., July 1987.

UCB/EERC-87/10   "Ultimate Behavior of Butt Welded Splices in Heavy Rolled Steel Sections," by Bruneau, M., Mahin, S.A. and Popov, E.P., July 1987.

UCB/EERC-87/11   "Residual Strength of Sand from Dam Failures in the Chilean Earthquake of March 3, 1985," by De Alba, P., Seed, H.B., Retamal, E. and Seed, R.B., September 1987.

UCB/EERC-87/12   "Inelastic Seismic Response of Structures with Mass or Stiffness Eccentricities in Plan," by Bruneau, M. and Mahin, S.A., September 1987.

UCB/EERC-87/13   "CSTRUCT: An Interactive Computer Environment for the Design and Analysis of Earthquake Resistant Steel Structures," by Austin, M.A., Mahin, S.A. and Pister, K.S., September 1987.

UCB/EERC-87/14   "Experimental Study of Reinforced Concrete Columns Subjected to Multi-Axial Loading," by Low, S.S. and Moehle, J.P., September 1987.

UCB/EERC-87/15   "Relationships between Soil Conditions and Earthquake Ground Motions in Mexico City in the Earthquake of Sept. 19, 1985," by Seed, H.B., Romo, M.P., Sun, J., Jaime, A. and Lysmer, J., October 1987.

UCB/EERC-87/16   "Experimental Study of Seismic Response of R. C. Setback Buildings," by Shahrooz, B.M. and Moehle, J.P., October 1987.

UCB/EERC-87/17   "The Effect of Slabs on the Flexural Behavior of Beams," by Pantazopoulou, S.J. and Moehle, J.P., October 1987.

UCB/EERC-87/18   "Design Procedure for R-FBI Bearings," by Mostaghel, N. and Kelly, J.M., November 1987.

UCB/EERC-87/19   "Analytical Models for Predicting the Lateral Response of R C Shear Walls: Evaluation of their Reliability," by Vulcano, A. and Bertero, V.V., November 1987.

UCB/EERC-87/20   "Earthquake Response of Torsionally-Coupled Buildings," by Hejal, R. and Chopra, A.K., December 1987.

UCB/EERC-87/21   "Dynamic Reservoir Interaction with Monticello Dam," by Clough, R.W., Ghanaat, Y. and Qiu, X-F., December 1987.

UCB/EERC-87/22   "Strength Evaluation of Coarse-Grained Soils," by Siddiqi, F.H., Seed, R.B., Chan, C.K., Seed, H.B. and Pyke, R.M., December 1987.

UCB/EERC-88/01   "Seismic Behavior of Concentrically Braced Steel Frames," by Khatib, I., Mahin, S.A. and Pister, K.S., January 1988.

UCB/EERC-88/02   "Experimental Evaluation of Seismic Isolation of Medium-Rise Structures Subject to Uplift," by Griffith, M.C., Kelly, J.M., Coveney, V.A. and Koh, C.G., January 1988.

UCB/EERC-88/03   "Cyclic Behavior of Steel Double Angle Connections," by Astanch-Asl, A. and Nader, M.N., January 1988.

UCB/EERC-88/04   "Re-evaluation of the Slide in the Lower San Fernando Dam in the Earthquake of Feb. 9, 1971," by Seed, H.B., Seed, R.B., Harder, L.F. and Jong, H.-L., April 1988.

UCB/EERC-88/05   "Experimental Evaluation of Seismic Isolation of a Nine-Story Braced Steel Frame Subject to Uplift," by Griffith, M.C., Kelly, J.M. and Aiken, I.D., May 1988.

UCB/EERC-88/06   "DRAIN-2DX User Guide.," by Allahabadi, R. and Powell, G.H., March 1988.

UCB/EERC-88/07   "Cylindrical Fluid Containers in Base-Isolated Structures," by Chalhoub, M.S. and Kelly, J.M., April 1988.

UCB/EERC-88/08   "Analysis of Near-Source Waves: Separation of Wave Types using Strong Motion Array Recordings," by Darragh, R.B., June 1988.

UCB/EERC-88/09   "Alternatives to Standard Mode Superposition for Analysis of Non-Classically Damped Systems," by Kusainov, A.A. and Clough, R.W., June 1988.

UCB/EERC-88/10   "The Landslide at the Port of Nice on October 16, 1979," by Seed, H.B., Seed, R.B., Schlosser, F., Blondeau, F. and Juran, I., June 1988.

UCB/EERC-88/11   "Liquefaction Potential of Sand Deposits Under Low Levels of Excitation," by Carter, D.P. and Seed, H.B., August 1988.

UCB/EERC-88/12   "Nonlinear Analysis of Reinforced Concrete Frames Under Cyclic Load Reversals," by Filippou, F.C. and Issa, A., September 1988.

UCB/EERC-88/13   "Earthquake-Resistant Design of Building Structures: An Energy Approach," by Uang, C.-M. and Bertero, V.V., September 1988.

UCB/EERC-88/14   "An Experimental Study of the Behavior of Dual Steel Systems," by Whittaker, A.S., Uang, C.-M. and Bertero, V.V., September 1988.

UCB/EERC-88/15   "Dynamic Moduli and Damping Ratios for Cohesive Soils," by Sun, J.I., Golesorkhi, R. and Seed, H.B., August 1988.

UCB/EERC-88/16   "Reinforced Concrete Flat Plates Under Lateral Load: An Experimental Study Including Biaxial Effects," by Pan, A. and Moehle, J., November 1988.

UCB/EERC-88/17   "Earthquake Engineering Research at Berkeley - 1988," November 1988.

UCB/EERC-88/18   "Use of Energy as a Design Criterion in Earthquake-Resistant Design," by Uang, C.-M. and Bertero, V.V., November 1988.

UCB/EERC-88/19   "Steel Beam-Column Joints in Seismic Moment Resisting Frames," by Tsai, K.-C. and Popov, E.P., September 1988.

UCB/EERC-89/01   "Behavior of Long Links in Eccentrically Braced Frames," by Engelhardt, M.D. and Popov, E.P., January 1989.

UCB/EERC-89/02   "Earthquake Simulator Testing of Steel Plate Added Damping and Stiffness Elements," by Whittaker, A., Bertero, V., Alonso, J. and Thompson, C., January 1989.